

## Revision 2

# WinPyrox: A Windows program for pyroxene calculation classification and thermobarometry<sup>†</sup>

FUAT YAVUZ\*

Department of Geological Engineering, Istanbul Technical University, 34469 Maslak, Istanbul, Turkey

### ABSTRACT

A Microsoft® Visual Basic program, called WinPyrox, has been developed to calculate structural formulae of both wet-chemical and microprobe-derived pyroxene analyses. Based on the standard International Mineralogical Association (IMA-88) nomenclature scheme, WinPyrox primarily calculates and classifies pyroxene groups and then determines a specific pyroxene name with its possible modifiers. It is developed to predict cation site-allocations at the different structural positions, including *T*, *M1*, and *M2* sites, as well as to estimate end-members, molar fractions, end-member activities, components and activities, and single-clinopyroxene and two-pyroxene thermobarometers. The program allows the user editing and loading Microsoft® Excel files to calculate electron-microprobe pyroxene analyses for different ferric iron estimation methods and normalization schemes. This software generates and stores all the calculated results in the output of Microsoft® Excel file, which can be displayed and processed by any other software for verification, general data manipulation, and graphing purposes. The compiled program code is distributed as a self-extracting setup file, including a help file, test data files and related graphic files, which are designed to produce a high-quality printout from the Golden Software's Grapher™ software. The self-extracting setup file, which is approximately 11 Mb, may be downloaded from <http://code.google.com/p/winpyrox/> or can be obtained from author on request.

**Keywords:** International Mineralogical Association; pyroxene; classification; modifier; end-member; activity; thermobarometer; normalization; software

### INTRODUCTION

Pyroxenes are important rock-forming ferromagnesian silicates in igneous and metamorphic rocks. Although previous studies on pyroxenes were focused on petrographic and petrogenetic aims, today there is a wide range of research providing thermometry, barometry, and  $fO_2$

---

\* E-mail : [yavuz@itu.edu.tr](mailto:yavuz@itu.edu.tr)

<sup>†</sup> This paper is dedicated to the memory of my mother, Ayten Yavuz, who passed away in 2011.

34 conditions. The subcommittee on pyroxenes of the International Mineralogical Association  
35 (IMA) published a classification and nomenclature scheme of pyroxene group minerals via its  
36 Commission on New Minerals and Mineral Names (CNMMN) (Morimoto 1988). The proposed  
37 scheme is similar to that IMA's amphibole classification (e.g., Leake et al. 1997, 2004; Yavuz  
38 1999, 2007). Despite its incomplete and imprecise form (e.g., Rock 1990), the current IMA-88  
39 pyroxene classification scheme allows the derivation of a pyroxene formula from chemical  
40 analysis obtained from wet-chemical and electron-microprobe techniques.

41 Although several computer programs have been published for pyroxene calculation and  
42 classification in recent years, restricted attention was given to the estimation of end-members,  
43 which play an important role in thermodynamic and thermobarometric estimations. Petrakakis  
44 and Dietrich (1985) developed a FORTRAN-77 subroutine, called MINSORT, to calculate, sort,  
45 and create data files of microprobe analyses of silicate and oxide minerals. Using the MINSORT  
46 program, Dietrich and Petrakakis (1986) proposed a linear algebraic method for the sequence-  
47 independent calculation of eleven end-member components of pyroxene (i.e., Jd, Acm, Ur, TiTs,  
48 CaTs, FeTs, CrTs, Pm, Fs, En, and Wo; see Table 1) based on microprobe analyses. Lindsley  
49 (1986) criticized these eleven independent compositional variables and emphasized that in the  
50 absence of knowledge concerning the energetics of exchange reactions, there should be only  
51 nine parameters (i.e., Al<sup>IV</sup>, Al<sup>VI</sup>, Fe<sup>3+</sup>, Cr, Ti, Fe<sup>2+</sup>, Mn, Mg, and Ca). According to Lindsley (1986),  
52 a tenth independent parameter in pyroxene exists when tetrahedral Fe<sup>3+</sup> is required by  
53 stoichiometry or Mössbauer analysis. McHone (1987) developed a simple APL program, called  
54 PXC, for calculating pyroxene structural formulae and end-members in the sequence proposed  
55 by Cawthorn and Collerson (1974), which is modified from Kushiro (1962). Gómez (1990)

56 presented a compiled program, named PX, for pyroxene calculation, classification, and end-  
57 member components based on the procedure given by Cawthorn and Collerson (1974). Rock  
58 (1990) introduced a FORTRAN-77 program for pyroxenes, called PXTAB, discussed some poorly  
59 described statements in the report, and drew our attention to the lack of defined compositional  
60 boundaries for certain rare pyroxene species, further problems related to adjectival modifiers,  
61 and some incomplete, inexact and often ambiguous rules in computerization of the IMA-88  
62 nomenclature scheme. Yavuz (2001) developed a QUICKBASIC program, PYROX, providing the  
63 IMA-88 pyroxene calculation and classification together with Rock's (1990) suggestions for the  
64 Subcommittee on Pyroxenes. Sturm (2002) introduced a Microsoft® Excel spreadsheet which  
65 allows the user to calculate structural formulae of pyroxene analyses and to determine  
66 pyroxene names according to the IMA-88 pyroxene nomenclature scheme.

67 A Visual Basic program (i.e., WinPyrox) described in this paper is the revised and enhanced  
68 form of the earlier PYROX program (Yavuz 2001) for pyroxene analyses obtained both from wet-  
69 chemical and electron-microprobe techniques. WinPyrox is a compiled program that only runs  
70 on the Microsoft® Windows platform. The program recalculates multiple pyroxene chemical  
71 analyses into their structural formulae, partitions the recalculated anions into the *T*, *M1*, and  
72 *M2* sites, classifies and names pyroxene group minerals with modifiers based on the IMA-88  
73 nomenclature scheme, allocates iron from microprobe-derived analysis to Fe<sup>2+</sup> and Fe<sup>3+</sup> based  
74 on different procedures, estimates end-member components and activities, calculates single-  
75 clinopyroxene thermometers and barometers, provides various two-pyroxene thermometers  
76 and geobarometers, and plots recalculated analyses on various binary and ternary pyroxene  
77 classification and thermobarometer diagrams by using the Golden Software's Grapher™

78 program. All the calculated pyroxene data can be displayed in a single window and stored in a  
79 Microsoft® Excel file (i.e., output.xlsx) for further data manipulation and graphing purposes.  
80 WinPyrox is a user-friendly software that allows users to calculate pyroxene analyses assuming  
81 different normalization schemes, such as structural formulae with or without a total of four  
82 cations and presents a better user interface and interaction with its enhanced functionality and  
83 visual effects.

#### 84 **CALCULATION AND CLASSIFICATION PROCEDURE OF PYROXENE**

85 Pyroxene group minerals belong to the chain silicates with a general formula of  $M_2M_1T_2O_6$ .  
86 They are constructed of single chains of silicon tetrahedral (i.e.,  $T$ ) and two octahedral (i.e.,  $M_2$   
87 and  $M_1$ ) sites. The procedure of ideal site allocation of cations at  $T$ ,  $M_1$ , and  $M_2$  sites can be  
88 carried out by the following steps (see Morimoto et al. 1988):

- 89 1. Sum  $T$  to 2.00 using  $Si^{4+}$ , then  $Al^{3+}$ , then  $Fe^{3+}$ .
- 90 2. Sum  $M_1$  to 1.00 using any excess  $Al^{3+}$  and  $Fe^{3+}$  from (1). If there is insufficient  $Al^{3+}$  and  
91  $Fe^{3+}$  to sum to 1.00, then add  $Ti^{4+}$ ,  $Cr^{3+}$ ,  $V^{3+}$ ,  $Zr^{4+}$ ,  $Sc^{3+}$ ,  $Zn^{2+}$ , (if exists  $Ni^{2+}$ ,  $Co^{2+}$ ),  $Mg^{2+}$ ,  
92  $Fe^{2+}$  and finally,  $Mn^{2+}$  until the sum is 1.00.
- 93 3. Sum  $M_2$  to 1.00 using any excess  $Mg^{2+}$ ,  $Fe^{2+}$ ,  $Mn^{2+}$  from (2) and then add  $Li^+$ ,  $Ca^{2+}$ ,  
94  $Na^+$ , and  $K^+$  (if exists). If the sum of  $M_2$  is far from 1.00, then the analysis may be  
95 inaccurate.

96 Pyroxene group minerals are classified based on the occupancy of the  $M_2$  site (Nesse 2004).  
97 However, as the allocation of cations in the  $T$ ,  $M_1$ , and  $M_2$  sites is, in part, a function of

98 temperature, Morimoto et al. (1988) considered *M1* and *M2* sites as a single *M* site in order to  
99 avoid the difference between the real and ideal site occupancies. Twenty accepted and widely  
100 used pyroxene names by the IMA are listed in Table 1. The definition of pyroxene species in  
101 Table 1 is based on thirteen end-members or chemical components, including  $\text{Mg}_2\text{Si}_2\text{O}_6$   
102 (Enstatite (En)),  $\text{Fe}^{2+}_2\text{Si}_2\text{O}_6$  (Ferrosilite (Fs)),  $\text{MnMgSi}_2\text{O}_6$  (Konoite (Ka)),  $\text{CaMgSi}_2\text{O}_6$  (Diopside  
103 (Di)),  $\text{CaFe}^{2+}\text{Si}_2\text{O}_6$  (Hedenbergite (Hd)),  $\text{CaMnSi}_2\text{O}_6$  (Johannsenite (Jhn)),  $\text{CaZnSi}_2\text{O}_6$  (Petedunnite  
104 (Pe)),  $\text{CaFe}^{3+}\text{AlSiO}_6$  (Esseneite (Es)),  $\text{NaAlSi}_2\text{O}_6$  (Jadeite (Jd)),  $\text{NaFe}^{3+}\text{Si}_2\text{O}_6$  (Aegirine (Aeg)),  
105  $\text{NaCr}^{3+}\text{Si}_2\text{O}_6$  (Kosmochlor (Kos)),  $\text{NaSc}^{3+}\text{Si}_2\text{O}_6$  (Jervisite (Je)), and  $\text{LiAlSi}_2\text{O}_6$  (Spodumene (Spd)).

106 There is a wide variety of solid solutions in the Mg-Fe group pyroxenes and in some of the  
107 Ca pyroxenes (e.g., diopside and hedenbergite). These two groups cover the most common  
108 rock-forming pyroxenes. For an exact classification, Morimoto et al. (1988) proposed the  
109 following characteristics to divide all the pyroxenes into four chemical groups (see Table 2) :

- 110 1. Describe the Mg-Fe pyroxenes and Ca pyroxenes as the “Ca-Mg-Fe” or “quadrilateral”  
111 pyroxenes.
- 112 2. The “Na” pyroxenes show continuous solid-solution with the “quadrilateral”, resulting  
113 in the Na-Ca pyroxenes.
- 114 3. Owing to rare occurrence of some pyroxene minerals (e.g., donpeacorite and kanoite  
115 in the Mn-Mg pyroxene group; johannsenite, petedunnite, and esseneite in the Ca  
116 pyroxene group; and spodumene in the Li pyroxene group), they are all treated as the  
117 “other” pyroxenes.

118 The 20 mineral names recommended by IMA-88 thus can be divided into four chemical  
119 groups for the classification of pyroxenes, including “Ca-Mg-Fe” pyroxenes (i.e., “Quad” with  
120 eight names), “Ca-Na” pyroxenes (with two names), “Na” pyroxenes (with two names), and  
121 “other” pyroxenes (i.e., “Others”, with eight names). Pyroxene analyses obtained from both  
122 wet-chemical and electron-microprobe techniques are initially calculated based on six oxygens  
123 and then classified into four groups by using the *Q-J* diagram (see Fig. 1), where  $Q = \text{Ca} + \text{Mg} +$   
124  $\text{Fe}^{2+}$  (atoms per formula unit; *apfu*) and  $J = 2\text{Na}$  (*apfu*). The pyroxenes that plot in the “Quad”  
125 area of *Q-J* diagram are classified on the Wo-En-Fs ternary diagram (see Fig. 2) with normalized  
126 Ca-Mg-( $\text{Fe}_{\text{tot}} + \text{Mn}$ ) cations. The most common pyroxenes are those of the “Quad”, which is also  
127 called as the En ( $\text{Mg}_2\text{Si}_2\text{O}_6$ )-Fs ( $\text{Fe}^{2+}_2\text{Si}_2\text{O}_6$ )-Di ( $\text{CaMgSi}_2\text{O}_6$ )-Hd ( $\text{CaFe}^{2+}\text{Si}_2\text{O}_6$ ) quadrilateral. The  
128 pyroxenes that belong to the “Quad” cover clino- and orthopyroxenes with monoclinic and  
129 orthorhombic symmetry, respectively. When compared to the clinopyroxenes, the  
130 orthopyroxenes are characterized by enstatite and ferrosilite compositional end-members,  
131 ( $\text{Mg,Fe}$ ) $_2\text{Si}_2\text{O}_6$  solid solution series, and low wollastonite components ( $\leq 5\%$ ).

132 The classification of “Na” and “Ca-Na” pyroxenes are carried out on the Quad-Jd-Ac diagram  
133 (see Fig. 3) with the normalized *Q* (Wo+En+Fs), Jd ( $\text{NaAlSi}_2\text{O}_6$ ), and Ae ( $\text{NaFe}^{3+}\text{Si}_2\text{O}_6$ )  
134 components. In the Quad-Jd-Ac diagram, the division between the “Quad” pyroxenes and the  
135 “Ca-Na” pyroxenes is defined at the  $Q = 80$ , whereas the discrimination between the “Ca-Na”  
136 pyroxenes and the “Na” pyroxenes are established at the  $Q = 20$ . Subdivisions between the “Ca-  
137 Na” pyroxenes, including omphacite and aegirine-augite, and “Na” pyroxenes, consisting of  
138 jadeite and aegirine, are obtained by applying the 50 % rule (see Fig. 3).

139 Natural pyroxenes called as the “Others” in the *Q-J* classification diagram consist virtually of  
140 johannsenite ( $\text{CaMnSi}_2\text{O}_6$ ), petedunnite ( $\text{CaZnSi}_2\text{O}_6$ ), and spodumene ( $\text{LiAlSi}_2\text{O}_6$ ). No specific  
141 binary or ternary classification diagram was proposed by the IMA-88 for variety of other  
142 pyroxenes. However, Rock (1990) showed that some of Mn-bearing pyroxenes, including  
143 johannsenite, kanoite and its dimorph danpeacorite can be classified on the Ca-Mn-Mg ternary  
144 diagram. Several pyroxenes with an unusual chemical composition plot outside the area  
145 between the  $Q+J = 2.0$  and  $Q+J = 1.5$  lines in the *Q-J* classification diagram, because of some  
146 substitutions (e.g.,  $(\text{R}^+)\text{R}^{2+}_{0.5}(\text{R}^{4+}_{0.5})2\text{R}^{4+}$ ,  $\text{R}^{2+}(\text{R}^{3+})(\text{R}^{3+})\text{R}^{4+}$ , and  $\text{R}^{2+}\text{R}^{2+}_{0.5}(\text{R}^{4+}_{0.5})(\text{R}^{3+})\text{R}^{4+}$ ). These  
147 types of chemical constituents do not belong to the specific pyroxene groups proposed by  
148 Morimoto et al. (1988) and, thus can be divided into two groups, including Ca-rich pyroxenes  
149 (e.g.,  $\text{CaR}^{3+}\text{AlSiO}_6$  and  $\text{CaR}^{2+}_{0.5}\text{Ti}^{4+}_{0.5}\text{AlSiO}_6$ ) and Na-rich pyroxenes (e.g.,  $\text{NaR}^{2+}_{0.5}\text{Ti}^{4+}_{0.5}\text{Si}_2\text{O}_6$ ).  
150 According to Morimoto et al. (1988), these unusual pyroxenes can be classified with the  
151 accepted pyroxene names and adjectival modifiers (see Table 3).

152 The adjectival modifiers, in general, are used to describe the mineral with an uncommon  
153 amount of any chemical component. Although the prefix is an essential part of a mineral name,  
154 it is not considered in the current IMA-88 pyroxene classification scheme. The modifier  
155 generally defines a subsidiary substitution and is optional. All modifiers have an “-ian” or “-  
156 oan” ending. The suffix “-ian” is commonly used for the higher valence state (except for lithian)  
157 and the suffix of “-oan” is always applied for the lower valence state of element (Nickel and  
158 Mandarino 1987). In the current IMA-88 pyroxene nomenclature scheme, there are no rules for  
159 the  $\text{Sc}^{3+}$ -,  $\text{V}^{3+}$ - and  $\text{Zr}^{4+}$ -bearing pyroxenes. However, Rock (1990) defined the “scandian”,

160 “vanadoan”, and “zirconian” to cover pyroxenes with  $Sc^{3+}$ ,  $V^{3+}$ , or  $Zr^{4+} > 0.01$  apfu, respectively  
161 (see rows 17 to 19 in Table 3).

## 162 PYROXENE THERMOMETERS AND BAROMETERS

163 Thermometry and barometry, also called thermobarometry, are the estimation of  
164 temperature ( $T$ , °C) and pressure ( $P$ , kbar) conditions of metamorphic and igneous rocks based  
165 on the presence and compositions of liquid and mineral components. Over the past 40 years,  
166 the application of mineral–pair thermobarometers to ultramafic rocks played an important role  
167 in understanding the thermal structure and history of the Earth’s upper mantle (Taylor 1998). A  
168 practical good thermometer is based on chemical reactions with low volume ( $\Delta V_r$ ) and high  
169 entropy ( $\Delta S_r$ ) and enthalpy ( $\Delta H_r$ ) (Powell 1985; Ravna and Paquin 2003). These reactions are  
170 extremely  $T$  dependent and show steep slopes in the  $P$ - $T$  diagrams. According to Essene (1982),  
171 a good thermometer with  $\Delta S_r \geq 4.0$  J/mole.K and  $\Delta V_r \geq 0.2$  J/bar is essential for the  
172 metamorphic systems, and these limits may also be used for the igneous systems (e.g., Putirka  
173 2008). Similarly, a good geobarometer can be obtained by mineral reactions with high  $\Delta V_r$  and  
174 low to moderate  $\Delta S_r$  and  $\Delta H_r$  (Wood and Fraser 1978; Ravna and Paquin 2003). These reactions  
175 are substantially dependent on variations in  $P$  and to a lesser extent on  $T$ , and thus producing  
176 gentle slopes in the  $P$ - $T$  diagrams. Although some thermobarometers are developed from  
177 volumetric and calorimetric data, most practical ones are based on the regression analysis  
178 obtained from experimental data, where the equilibrium constant ( $K_{eq}$ ),  $P$ , and  $T$  are all known  
179 (Putirka 2008).

180 Davis and Boyd (1966) presented the first two-pyroxene thermometer for the join  $Mg_2Si_2O_6$ -  
181  $CaMgSi_2O_6$  at a pressure of 30 kbar, and numerous pyroxene thermobarometers have been



182 published since then. The two-pyroxene thermometer, however, received much more attention  
183 than the single-pyroxene approach. The lesser amount of both clino- and orthopyroxene  
184 phenocrysts in volcanic rocks than in mafic-ultramafic rocks limited the application of two-  
185 pyroxene thermobarometers in volcanic systems, and thus thermobarometers were produced  
186 based on single-clinopyroxene compositions (e.g., Nimis 1995, 1999; Nimis and Ulmer 1998;  
187 Nimis and Taylor 2000) or clinopyroxene-liquid equilibria (e.g., Putirka et al. 1996, 2003; Putirka  
188 2008).

### 189 **Single-clinopyroxene barometers**

190 Recent studies on clinopyroxenes have shown that crystal-chemical variations, as well as the  
191 *P-T* conditions, play an important role in the composition of clinopyroxenes crystallized from  
192 magmas (e.g., Dal Negro et al. 1985; Malgarotto et al. 1993; Pasqual et al. 1995; Nazzareni et al.  
193 1998; Bindi et al. 1999; Aydin et al. 2009). Clinopyroxene in basic magmas has received  
194 particular interest because its stability is a strong function of pressure. Crystal-structure  
195 modeling is an important technique to estimate structural changes in *C2/c* pyroxenes. Dal  
196 Negro et al. (1989) showed that the structural parameters of natural pyroxenes can be used as  
197 the applicable petrogenetic markers. As the alumina content of parental basalt is a sensitive  
198 factor for clinopyroxene, Nimis (1995) proposed a clinopyroxene geobarometer based on the  
199 crystal-structure, which is applicable only to *C2/c* clinopyroxenes that crystallized from  
200 anhydrous melts of basaltic composition (i.e.,  $\text{Mg}/(\text{Mg}+\text{Fe}^{2+})_{\text{Cpx}} = 0.7\text{-}0.9$ ), excluding high-  
201 alumina basalts (i.e.,  $\text{Al}_2\text{O}_3 \geq 18$  wt%), and experimental conditions between 0 and 24 kbar:

$$202 \quad PN_{95\text{-BS-Cpx}} (\pm 2, \text{ kbar}) = 698.443 - 1.15378 * V_{\text{Cell}} (\text{\AA}^3) - 16.1598 * V_{M1} (\text{\AA}^3) \quad (1)$$

203 where  $PN_{95-BS-Cpx}$  denotes the Nimis (1995) geobarometer for basaltic systems and  $V_{Cell}$  and  $V_{M1}$   
204 are the unit cell volume and  $M1$ -site volume, respectively.

205 The  $V_{Cell}$  and  $V_{M1}$  volumes at room conditions (i.e.,  $P_0 = 1$  atm and  $T_0 = 25$  °C) can be either  
206 measured by the X-ray diffraction analysis or calculated by the following equations using  
207 recalculated cations (*apfu*) at different sites:

$$\begin{aligned} 208 \quad V_{Cell} = & 11.864 * Fe_{M1}^{2+} + 9.107 * Fe^{3+} - 18.375 * Al_{M1} + 11.794 * Ti - 1.4925 * Cr + 439.97 * Ca + \\ 209 \quad & 419.68 * Na + 431.72 * Mg_{M2} + 432.56 * Fe_{M2}^{2+} + 428.03 * Mn - 28.652 * (Mg_{M2})^2 - \\ 210 \quad & 12.741 * (Fe_{M2}^{2+})^2 \end{aligned} \quad (2)$$

$$\begin{aligned} 211 \quad V_{M1} = & -0.3085 * Al_T + 0.8130 * Fe_{M1}^{2+} - 0.4173 * Fe^{3+} - 2.029 * Al_{M1} - 1.0864 * Ti - 0.8001 * Cr + \\ 212 \quad & 11.931 * Ca + 11.288 * Na + 11.432 * Mg_{M2} + 11.885 * Fe_{M2}^{2+} + 12.038 * Mn + \\ 213 \quad & 2.4335 * (Mg_{M2})^2 - 1.1661 * (Fe_{M2}^{2+})^2 \end{aligned} \quad (3)$$

214 In the absence of X-ray diffraction data, Eq. 4 is useful for the geobarometric condition of  
215 clinopyroxenes:

$$\begin{aligned} 216 \quad P (\pm 2, \text{ kbar}) = & 698.443 + 4.985 * Al_T - 26.826 * Fe_{M1}^{2+} - 3.764 * Fe^{3+} + 53.989 * Al_{M1} + 3.948 * Ti + \\ 217 \quad & 24.651 * Cr - 700.431 * Ca - 666.629 * Na - 682.848 * Mg_{M2} - 691.138 * Fe_{M2}^{2+} - \\ 218 \quad & 688.384 * Mn - 6.267 * (Mg_{M2})^2 - 4.144 * (Fe_{M2}^{2+})^2 \end{aligned} \quad (4)$$

219 In these equations, the elements with no sites show the total amount of that element in the  
220 formula (*apfu*).

221 The Nimis (1995) geobarometer can be used for many natural clinopyroxenes occurring both  
222 as phenocrysts and megacrysts or forming well-preserved cumulate pyroxenites. Alternatively,  
223 cell volume ( $V_{Cell}$ ) vs.  $M1$ -site volume ( $V_{M1}$ ) plot may also be used to determine the pressure  
224 conditions of clinopyroxene during the magma crystallization. According to Putirka (2008),  
225 geobarometers based on co-existing clinopyroxene and liquid compositions proposed by

226 Putirka et al. (1996, 2003) are the highest precision and have the least systematic error for  
227 anhydrous and hydrous systems, when compared to the Nimis (1995) model. Nimis and Ulmer  
228 (1998) produced a new calibration of the geobarometer, which is valid for only clinopyroxenes  
229 with  $(Ca+Na) > 0.5$  (*apfu*),  $Mg/(Mg+Fe^{2+}) > 0.7$ , and  $Al_2O_3/SiO_2$  (wt%)  $< 0.375$  (i.e.,  $Al_2O_3 < 18$   
230 wt%) based on the crystal-structure modeling of Ca-rich clinopyroxenes coexisting with  
231 anhydrous, basic, and ultrabasic melts at pressure conditions corresponding Earth's crust and  
232 uppermost mantle (i.e.,  $P = 0-24$  kbar):

$$233 \quad PNU_{98-BA-Cpx} (\pm 1.75, \text{ kbar}) = 771.48 - 1.323 * V_{Cell} (\text{\AA}^3) - 16.064 * V_{M1} (\text{\AA}^3) \quad (5)$$

234 where  $PNU_{98-BA-Cpx}$  denotes the Nimis and Ulmer (1998) geobarometer and  $V_{Cell}$  and  $V_{M1}$  show  
235 the cell volume and  $M1$ -site volume, respectively.

236 In the absence of X-ray diffraction data, the pressure value can be estimated from Eq. 6 for the  
237 geobarometric formulation of clinopyroxenes (Nimis and Ulmer 1998):

$$238 \quad P (\pm 1.75, \text{ kbar}) = 771.48 + 4.956 * Al_T - 26.756 * Fe_{M1}^{2+} - 5.345 * Fe^{3+} + 56.904 * Al_{M1} + 1.848 * Ti + \\ 239 \quad 14.827 * Cr - 773.74 * Ca - 736.57 * Na - 754.81 * Mg_{M2} - 763.20 * Fe_{M2}^{2+} - 759.66 * Mn \\ 240 \quad - 1.185 * (Mg_{M2})^2 - 1.876 * (Fe_{M2}^{2+})^2 \quad (6)$$

241 According to Nimis and Ulmer (1998), the revised clinopyroxene geobarometer has smaller  
242 residuals (i.e.,  $P_{Cal} - P_{Exp}$ ) and data show similar values for  $P < 10$  kbar, but slightly higher values  
243 for  $P > 10$  kbar, when compared with the earlier version of Nimis (1995) model (i.e.,  $P_{95-BS-Cpx}$  in  
244 Eq. 1). The  $V_{Cell}$  and  $V_{M1}$  may not reflect the true unit-cell and site volumes of the  
245 clinopyroxenes during the  $P$ - $T$  conditions of crystallization, and thus needs a correction for

246 thermal expansivity and compressibility. For that reason Eq. 7, which is the corrected  
247 clinopyroxene structural geobarometer, is used for anhydrous and hydrous basic magmas:

$$248 \quad P_{N98\text{cor-BH-Cpx}} (\pm 1.70, \text{ kbar}) = 654.47 - 1.186 * V_{\text{Cell}}^{\text{corr}} (\text{\AA}^3) - 9.140 * V_{M1}^{\text{corr}} (\text{\AA}^3) \quad (7)$$

249 where  $P_{98\text{cor-BH-Cpx}}$  denotes the corrected Nimis and Ulmer (1998) geobarometer and  $V_{\text{Cell}}^{\text{corr}}$  and  
250  $V_{M1}^{\text{corr}}$  show the corrected cell volume and  $M1$ -site volume, respectively.

251 Nimis and Ulmer (1998) suggest that this geobarometer is applicable to a wide range of natural  
252 clinopyroxenes in basic and ultrabasic rocks, as well as the mantle equilibrium partial-melting  
253 residua, if they are unable to re-equilibrate after the melt extraction. The  $V_{\text{Cell}}^{\text{corr}}$  vs.  $V_{M1}^{\text{corr}}$  plot  
254 can also be used to understand the pressure conditions of crystallization. The simple  
255 geobarometric formula proposed by Nimis and Ulmer (1998) showed that clinopyroxene molar-  
256 volume variations and structural balance play a major role in the regulation of  
257 clinopyroxene/liquid equilibria at different pressure conditions.

258 This approach for clinopyroxenes was later extended by Nimis (1999) for a wide range of  
259 magmatic compositions, including basic to acidic and from tholeiitic subalkaline (i.e., Eq. 8,  $P$  =  
260 0-18 kbar) to be mildly alkaline (i.e., Eq. 9,  $P$  = 0-24 kbar) magmas, as well as the shoshonitic  
261 series:

$$262 \quad P_{N99\text{-TH-Cpx}} (\pm 1.00, \text{ kbar}) = 537.003 - 1.017 * V_{\text{Cell}}^{P,T} - 5.663 * V_{M1}^{P,T} - 2.722 * mg \quad (8)$$

$$263 \quad P_{N99\text{-MA-Cpx}} (\pm 1.10, \text{ kbar}) = 621.151 - 1.220 * V_{\text{Cell}}^{P,T} - 4.620 * V_{M1}^{P,T} - 7.773 * mg \quad (9)$$

264 where  $P_{N99\text{-TH-Cpx}}$  and  $P_{N99\text{-MA-Cpx}}$  denote the Nimis (1999) geobarometers. In these equations  
265 (i.e., Eq. 8 and Eq. 9), the  $mg = \text{Mg}/(\text{Mg}+\text{Fe}^{2+})^{\text{Cpx}}$  and  $V_{\text{Cell}}^{P,T}$  and  $V_{M1}^{P,T}$  show volumes corrected

266 for thermal expansivity and compressibility at valid  $P$ - $T$  conditions. The  $mg$  term, which is not  
267 considered in previous (e.g., Nimis 1995; Nimis and Ulmer 1998) models should be required,  
268 especially for clinopyroxenes coexisting with the fractionated melts. Ignoring this term in  
269 equations 8 and 9 may result in lower pressure estimation for iron-rich clinopyroxenes (Nimis  
270 1999). At higher pressures, the  $TH$ -formulation in Eq. 8 may give lower pressure values than the  
271  $MA$ -formulation in Eq. 9. Accordingly, pressures exceeding 15 kbar estimated by using the  
272  $TH$ -formulation should be regarded with caution. The Nimis (1999) model can be applied to  
273 basic through intermediate-acid magmatic rocks. According to Nimis (1999), an attempt to  
274 extend this approach to clinopyroxenes from calc-alkaline melts for the  $MA$ - and  $TH$ -  
275 formulations, either in combination or separately, may give unsatisfactory results, and they  
276 must be used with caution.

277 Nimis and Taylor (2000) used the CMS (CaO-MgO-SiO<sub>2</sub>) and CMAS-Cr (CaO-MgO-Al<sub>2</sub>O<sub>3</sub>-SiO<sub>2</sub>)  
278 systems at 850-1500 °C and 0-60 kbar experimental conditions to calibrate a Cr-in-Cpx  
279 barometer and enstatite-in-Cpx thermometer for Cr-diopsides from garnet peridotites. The Cr-  
280 in-Cpx barometer is based on the Cr exchange between clinopyroxene and garnet and, thus can  
281 be used as an alternative to the Al-in-Opx barometer to determine the pressure conditions of  
282 equilibration of natural garnet lherzolites. It is formulated as a function of  $T$  (K) and  
283 clinopyroxene composition:

$$284 \quad PNT_{00-Cpx} \text{ (kbar)} = \frac{T(^{\circ}\text{K})}{126.9} * \ln \left[ a_{CaCrTs}^{Cpx} \right] + 15.483 * \ln \left( \frac{Cr\#^{Cpx}}{T(^{\circ}\text{K})} \right) + \frac{T(^{\circ}\text{K})}{71.38} + 107.8 \quad (10)$$

285 where  $a_{CaCrTs}^{Cpx} = Cr - 0.81 * Cr\# * (Na+K)$  and  $Cr\# = (Cr / (Cr+Al))$ .

286 Putirka (2008) recalibrated using experiment conditions from 0.001 to 80 kbar and proposed  
287 three new barometers for clinopyroxene composition (i.e., Eq. 32a in Putirka 2008) and  
288 pyroxene-liquid components (i.e., Eq. 32b and 32c in Putirka 2008) based on the Nimis (1995)  
289 model. The current WinPyrox program allows the user to estimate the  $P$ - $T$  conditions only for  
290 clinopyroxene-orthopyroxene analyses, but not pyroxene-liquid components. Geobarometer  
291 proposed by Putirka (2008) for clinopyroxene composition is calculated by WinPyrox program  
292 as follows:

$$293 \quad PP_{08-Cpx} \text{ (Eq. 32a)} \text{ (kbar)} = 3205 + 0.384 * T \text{ (K)} - 518 * \ln(T \text{ (K)}) - 5.62 * (X_{Mg}^{Cpx}) + 83.2 * (X_{Na}^{Cpx}) \\ + 68.2 * (X_{DiHd}^{Cpx}) + 2.52 * \ln(X_{Al^{VI}}^{Cpx}) - 51.1 * (X_{DiHd}^{Cpx})^2 + 34.8 * (X_{EnFs}^{Cpx})^2 \quad (11)$$

294 where  $X_{DiHd}^{Cpx} = Ca - CaTs - CaTi - CrCaTs$  and  $X_{EnFs}^{Cpx} = ((Fe_{tot} + Mg) - (Ca - CaTi - CaTs - CrCaTs))/2$ .

295 Although Eq. 11, improves the precision of the Nimis (1995) model (i.e., Eq. 1), it still contains  
296 systematic errors due to the hydrous experiments (Putirka 2008).

### 297 **Single-clinopyroxene thermometers**

298 Compared to the two-pyroxene thermometer formulations, studies on single-pyroxene  
299 thermometers, either in clinopyroxene or orthopyroxene, are scarce. Bertrand and Mercier  
300 (1985/1986) provided a reliable method to estimate an equilibrium temperature for natural  
301 lherzolites. They gave a simplified thermometer based only on the clinopyroxene solvus, which  
302 is calibrated for potential applications in a single clinopyroxene phase, provided that the  
303 clinopyroxene was once in equilibrium with the orthopyroxene (e.g., xenocrysts, intensely  
304 altered lherzolites):

$$305 \quad TBM_{85/86-Cpx} (^{\circ}K) = \frac{33696 + 454.5 * P \text{ (GPa)}}{17.61 - 8.314 * \ln\left(\frac{1 - X_{Ca}^{M2}}{0.95}\right) - 12.13 * (X_{Ca}^{M2})^2} \quad (12)$$

306 Pyroxene thermometry is a powerful tool for the estimation of the equilibration temperature  
 307 of natural lherzolites. Temperature calculation methods for single-pyroxene, either in clino- or  
 308 orthopyroxene, are commonly based on Ca-Mg equilibria. Taking into account that  $a_{en}^{Cpx}$  is  
 309 close to unity in natural peridotitic rocks, Nimis and Taylor (2000) formulated Brey and Köhler's  
 310 (1990) two-pyroxene thermometry as a single-clinopyroxene thermometer:

$$311 \quad TNT_{00-Cpx} (^{\circ}K) = \frac{23166 + 39.28 * P \text{ (kbar)}}{13.25 + 15.35 * Ti + 4.5 * Fe - 1.55 * (Al + Cr - Na - K) + (\ln a_{en}^{Cpx})^2} \quad (13)$$

312 where all cations in (*apfu*) and  $a_{en}^{Cpx} = (1 - Ca - Na - K) * (1 - 0.5 * (Al + Cr + Na + K))$ . The enstatite-in-Cpx  
 313 thermometer (Eq. 13) and Cr-in-Cpx barometer (Eq. 10), can be used to estimate the *P-T*  
 314 conditions of equilibration of Cr-diopside alone, and thus allowing application to partly altered  
 315 xenoliths, inclusions in diamonds, and loose grains from sediments. This thermobarometer is a  
 316 powerful tool in diamond exploration.

317 Using Nimis and Taylor's (2000) activity model, Putirka (2008) produced a new and more  
 318 precise thermometer:

$$319 \quad TP_{08-Cpx} (^{\circ}K) = \frac{93100 + 544 * P \text{ (kbar)}}{61.1 + 36.6 * (X_{Ti}^{Cpx}) + 10.9 * (X_{Fe}^{Cpx}) - 0.95 * (X_{Al_{tot}}^{Cpx} + X_{Cr}^{Cpx} - X_{Na}^{Cpx} - X_{K}^{Cpx}) + 0.395 * [\ln(a_{En}^{Cpx})]^2} \quad (14)$$

320 where  $a_{En}^{Cpx} = (1 - X_{Ca}^{Cpx} - X_{Na}^{Cpx} - X_{K}^{Cpx}) * (1 - 0.5 * (X_{Al_{tot}}^{Cpx} + X_{Cr}^{Cpx} + X_{Na}^{Cpx} + X_{K}^{Cpx}))$ .

321 An application of intracrystalline Fe<sup>2+</sup>-Mg partitioning in clinopyroxene can be used to  
 322 estimate the closure or equilibration (i.e., quench) temperatures based on the exchange

323 reaction between the *M2* and *M1* sites. However, the Fe-Mg ordering in clinopyroxene is  
324 dependent not only on temperature, but also on the intracrystalline polyhedral configuration.  
325 Dal Negro et al. (1982) showed that the *M2* site configuration is mainly controlled by the Ca and  
326 Na cations, whereas the *M1* site configuration is intensely affected by the  $R^{3+}$  trivalent cations,  
327 including  $Al^{VI}$ ,  $Fe^{3+}$ , and  $Cr^{3+}$ , as well as  $Ti^{4+}$ . Based on data for Ca-rich clinopyroxenes from  
328 McCallister et al. (1976), the following equation was proposed by Dal Negro et al. (1982) to  
329 determine the temperature of intracrystalline equilibrium:

$$330 \quad T_{DN_{82-Cpx}} (^{\circ}K) = \left[ 1000 * \frac{5.465 * (R^{3+}) + 7.324 * Ca'' - 3.039}{-\ln K_D + 4.032 * (R^{3+}) + 5.383 * Ca'' - 3.767} \right] \quad (15)$$

331 where  $Ca'' = (Ca+Na+Mn)$ ,  $R^{3+} = (Al^{VI}+Fe^{3+}+Cr+Ti^{4+})$ , and  $K_D = (Fe_{M1} * Mg_{M2}) / (Fe_{M2} * Mg_{M1})$ . An  
332 application of Eq. 15 to basaltic pyroxenes, in some cases, may give poor results (Molin and  
333 Zanazzi 1991). Assuming  $-\ln K_D = -1.75 + 4449.5 * 1/T$ , Molin and Zanazzi (1991) revised Eq. 15 and  
334 proposed a similar expression for the closure temperature of a typical augitic composition:

$$335 \quad T_{MZ_{91-Cpx}} (^{\circ}K) = \left[ 1000 * \frac{1.188 * [5.465 * (R^{3+}) + 7.324 * Ca'' - 3.039]}{-\ln K_D + 4.032 * (R^{3+}) + 5.383 * Ca'' - 3.767} \right] \quad (16)$$

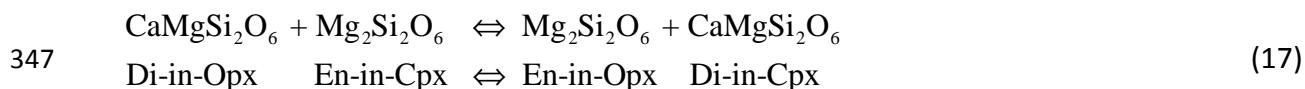
336 This thermometer yields reliable results only for augites of comparable chemical composition,  
337 as the equilibrium temperature is dependent primarily on the site configuration, which is  
338 controlled to the content of Ca and trivalent cations in the *M2* and *M1* sites. Both Dal Negro et  
339 al. (1982) and Molin and Zanazzi (1991) methods are therefore, capable of giving useful  
340 information on the cooling history of magmatic rocks containing only clinopyroxene.

341

## Two-pyroxene thermometers



342 The mutual solubility of clinopyroxene coexisting with orthopyroxene established that the  
343 relationship between the enstatite and diopside components is temperature controlled, and  
344 thus can be used as a thermometer (Ravna and Paquin 2003 and references therein). The two-  
345 pyroxene solvus in the simple CMS system is controlled by the following Ca-Mg exchange in the  
346 *M2* site reaction.



348 Over twenty different calibrations of two-pyroxene thermometers were proposed and most of  
349 the widely used ones are incorporated into the WinPyrox software. Davis and Boyd (1966)  
350 studied the phase relations for the join  $\text{Mg}_2\text{Si}_2\text{O}_6$ - $\text{CaMgSi}_2\text{O}_6$  at a pressure of 30 kb with its  
351 application to Fe- and Al-poor pyroxenes from kimberlites and introduced the concept of the  
352 two-pyroxene thermometer. Since then, numerous two-pyroxene thermometers, commonly  
353 based on the enstatite-diopside partitioning, have been published to estimate the equilibration  
354 temperature of magmatic rocks (e.g., Wood and Banno 1973; Wells 1977; Nickel and Brey 1984;  
355 Nickel et al. 1985; Bertrand and Mercier 1985/1986; Carlson and Lindsley 1988; Sen and Jones  
356 1989; Brey and Köhler 1990; Taylor 1998; Putirka, 2008).

357 Because of the potential usefulness of Davis and Boyd's (1966) thermometer, Wood and  
358 Banno (1973) attempted to apply the same simple approach to the iron-bearing compositions  
359 and obtained the following expression for equilibration temperature ( $T$ , °K):

$$TWB_{73\text{-Opx-Cpx}} (^{\circ}\text{K}) = \frac{-10202}{\ln\left(\frac{a_{\text{Mg}_2\text{Si}_2\text{O}_6}^{\text{Cpx}}}{a_{\text{Mg}_2\text{Si}_2\text{O}_6}^{\text{Opx}}}\right) - 7.65 * X_{\text{Fe}}^{\text{Opx}} + 3.88 * (X_{\text{Fe}}^{\text{Opx}})^2 - 4.6} \quad (18)$$

361 where  $a_{\text{Mg}_2\text{Si}_2\text{O}_6} = \left( \frac{\text{Mg}^{2+}}{\text{Ca}^{2+} + \text{Mg}^{2+} + \text{Fe}^{2+} + \text{Mn}^{2+} + \text{Na}^+} \right)_{M2} * \left( \frac{\text{Mg}^{2+}}{\text{Fe}^{3+} + \text{Fe}^{2+} + \text{Al}^{3+} + \text{Ti}^{4+} + \text{Cr}^{3+} + \text{Mg}^{2+}} \right)_{M1}$  and

362  $X_{\text{Fe}}^{\text{Opx}} = \left( \frac{\text{Fe}^{2+}}{\text{Fe}^{2+} + \text{Mg}^{2+}} \right)$ . In Eq. 18, the activity of the enstatite component in both the clino- and

363 orthopyroxene is calculated using the same formula. In most cases, the model reproduces

364 calculated temperatures within 70 °C. In calculating temperature from microprobe analyses,

365 Wood and Banno (1973) did not consider the possible ferric iron contents in the pyroxenes, and

366 thus all iron is assumed as  $\text{Fe}^{2+}$ . However, if  $\text{Fe}^{3+}$  content is taken into account, then the

367 calculated equilibration temperature from Eq. 18 is increased due to the decreased  $X_{\text{Fe}}^{\text{Opx}}$

368 value. Compared to the optical or X-ray diffraction analyses, the Wood and Banno (1973) model

369 gives inconsistent values, particularly at low temperatures with experimental data obtained by

370 microprobe techniques.

371 Wells (1977) applied simple mixing models to two-pyroxene solid solutions and obtained a

372 semi-empirical equation for the diopside-enstatite miscibility gap for a temperature range of

373 800 °C to 1700 °C by using the Wood and Banno's (1973) activity formula:

374 
$$TW_{77\text{-Opx-Cpx}} (^{\circ}\text{K}) = \frac{7341}{3.355 + 2.44 * X_{\text{Fe}}^{\text{Opx}} - \ln K} \quad (19)$$

375 where  $K = \frac{a_{\text{Mg}_2\text{Si}_2\text{O}_6}^{\text{Cpx}}}{a_{\text{Mg}_2\text{Si}_2\text{O}_6}^{\text{Opx}}}$  and  $X_{\text{Fe}}^{\text{Opx}} = \left( \frac{\text{Fe}^{2+}}{\text{Fe}^{2+} + \text{Mg}^{2+}} \right)$ . The Wells (1977) model reproduces most

376 of the experimental data within 70 °C and thus is applicable to aluminous pyroxenes in the

377 CMAS system. The Wells (1977) thermometer is similar to the Wood and Banno (1973) model,

378 but deviates significantly for naturally equilibrated Mg-rich, two-pyroxenes due to the large

379 inaccuracies in the thermometer of Wood and Banno (1973) for Mg-rich compositions. At  
380 higher temperatures, the Wells (1977) model gives low temperature values as it inconsiderate  
381 both an observed non-ideality and pressure-dependency situations.

382 The Nickel and Brey (1984) model yields two equilibration temperatures for subsolidus  
383 orthopyroxene and clinopyroxene in the CMS system over a large range of temperature (i.e.,  
384 850 °C to 1500 °C) and pressure (i.e., 2 kbar to 60 kbar) conditions:

$$385 \quad TNB(A)_{84\text{-Opx-Cpx}} (^{\circ}\text{K}) = \frac{(-7 - P \text{ (kbar)} * 0.06188 + 34 * (X_{\text{Di}}^{\text{Opx}})^2 - (21.905 - P \text{ (kbar)} * 0.05229 * (X_{\text{Di}}^{\text{Cpx}})^2)}{(0.0083143 * \ln K_D(A) + 0.004431 * (X_{\text{Di}}^{\text{Cpx}})^2 - 0.00397)} \quad (20)$$

$$386 \quad TNB(B)_{84\text{-Opx-Cpx}} (^{\circ}\text{K}) = \frac{(12.909 + P \text{ (kbar)} * 0.1633 + 34 * (X_{\text{En}}^{\text{Opx}})^2 - (21.905 - P \text{ (kbar)} * 0.05229 * (X_{\text{En}}^{\text{Cpx}})^2)}{(0.0083143 * \ln K_D(B) + 0.004431 * (X_{\text{En}}^{\text{Cpx}})^2 + 0.0085)} \quad (21)$$

387 where  $K_D(A) = \frac{X_{\text{En}}^{\text{Cpx}}}{X_{\text{En}}^{\text{Opx}}}$  and  $K_D(B) = \frac{X_{\text{Di}}^{\text{Cpx}}}{X_{\text{Di}}^{\text{Opx}}}$ . The model is qualitatively in agreement with  
388 observed stability regions for iron-free and low-calcium pyroxenes, including pigeonite.  
389 However, this model predicts that pigeonite is not stable at high pressures. According to Nickel  
390 and Brey (1984), application of these equations to the experimental data showed that the  
391 reproduction of temperatures obtained by the Eq. 20 is better than the Eq. 21, because of the  
392  $K_D(B)$  is very sensitive to small changes in  $X_{\text{Di}}^{\text{Opx}}$ . Accordingly, Eq. 21 gives larger deviations (i.e.,  
393 over- or underestimations), especially at temperatures < 1000 °C, and hence is not useful for  
394 thermometric studies at relatively low temperatures. These formulations, however, should not  
395 be applied directly to pyroxene analyses from more complex systems (i.e., CMAS).

396 Nickel et al. (1985) proposed a thermometer for coexisting ortho- and clinopyroxene in the  
397 CMAS system at 1000 °C - 1670 °C and 30 kbar - 50 kbar conditions:

398  $TN_{85\text{-Opx-Cpx}} (^{\circ}\text{C}) = 1616.67 + 287.935 * \ln K_D + 2.933 * P \text{ (kbar)}$  (22)

399 where  $K_D = \left( \frac{(1 - \frac{\text{Al}}{2}) * (1 - \text{Ca})^{\text{Cpx}}}{(1 - \frac{\text{Al}}{2}) * (1 - \text{Ca})^{\text{Opx}}} \right)$  and all cations are in (*apfu*). Although this simple

400 empirical thermometer is valid for CMS and CMAS systems in the *P-T* range of the experiments  
 401 and gives an idea of formation conditions, it should not be used for natural rocks (e.g., Nickel et  
 402 al. 1985).

403 Bertrand and Mercier (1985/1986) provided a reliable method to calculate the equilibration  
 404 temperature of natural Iherzolite based on coexisting ortho- and clinopyroxene, the latter  
 405 represented as calcic diopside, in the simple (i.e., CMS, MAS) and more complex (i.e., CMAS,  
 406 CFMS, CFMAS where F = FeO) systems. The proposed two-pyroxene thermometer is given by:

408  $TBM_{85/86\text{-Opx-Cpx}} (^{\circ}\text{K}) = \frac{(36273 + 399 * P \text{ (GPa)})}{[19.31 - 8.314 * \ln K - 12.15 * (\text{Ca}_{\text{Cpx}}^*)^2]}$  (23)

410 where  $K = \frac{1 - \text{Ca}_{\text{Cpx}}^*}{1 - \text{Ca}_{\text{Opx}}^*}$ ,  $\text{Ca}_{\text{Cpx}}^* = \frac{X_{\text{Ca}}^{\text{M2}}}{1 - X_{\text{Na}}^{\text{M2}}} + (-0.77 + 10^{-3} * T) * \left[ \frac{\text{Fe}}{\text{Fe} + \text{Mg}} \right]$ , and  $\text{Ca}_{\text{Opx}}^* = \frac{X_{\text{Ca}}^{\text{M2}}}{1 - X_{\text{Na}}^{\text{M2}}}$

411 According to Bertrand and Mercier (1985/1986), the advantage of this thermometer is that it is  
 412 tested against the natural pyroxene analyses from reequilibration experiments in the range of  
 413 950 °C-1500 °C and 30 to 44 kbar, and thus can be applied to realistic equilibrium conditions.

414 Carlson and Lindsley (1988) studied the thermochemistry of pyroxenes on the join  $\text{Mg}_2\text{Si}_2\text{O}_6$ -  
 415  $\text{CaMgSi}_2\text{O}_6$  and proposed two-pyroxene thermometers based on experiments ranging in

416 temperature from 850 °C to 1500 °C and pressure from 1 bar to 60 kbar. The temperatures of  
 417 equilibration are obtained by the thermodynamic formulations A and B (see Carlson and  
 418 Lindsley 1988) and given in the following equations:

$$419 \quad T_{CL(A)}_{88-Opx-Cpx} (^{\circ}C) = -273.15 + \frac{4.261 + 0.059 * P + W_{G1}^{Cpx} * (X_2^{Cpx})^2 * (1 - 2 * X_1^{Cpx}) + 2 * W_{G2}^{Cpx} * (X_1^{Cpx}) * (X_2^{Cpx})^2 - W_G^{Oen} * (X_2^{Oen})^2}{0.002721 - 0.0083143 * \ln\left(\frac{X_1^{Cpx}}{X_1^{Oen}}\right)} \quad (24)$$

$$420 \quad T_{CL(B)}_{88-Opx-Cpx} (^{\circ}C) = -273.15 + \frac{-35.92 - 1.753 * P + W_{G2}^{Cpx} * (X_1^{Cpx})^2 * (1 - 2 * X_2^{Cpx}) + 2 * W_{G1}^{Cpx} * (X_2^{Cpx}) * (X_1^{Cpx})^2 - W_G^{Oen} * (X_1^{Oen})^2}{0.002721 - 0.0083143 * \ln\left(\frac{X_2^{Cpx}}{X_2^{Oen}}\right)} \quad (25)$$

421 where  $W_{G1}^{Cpx} = 26.23 - 0.02229 * P$  (kbar),  $W_{G2}^{Cpx} = 32.44 - 0.08646 * P$  (kbar),  $W_G^{Oen} = 28.60 -$   
 422  $1.749 * P$  (kbar), and  $X_i^{Cpx}$  refers to the mole fraction of component  $i$  (i.e.,  $X_1^{Cpx}$  = enstatite and  
 423  $X_2^{Cpx}$  = diopside) in clinopyroxene. The advantage of these thermometers is their application to  
 424 the wide range of temperature and pressure conditions of rocks containing two pyroxenes.

425 Sen and Jones (1989) carried out pyroxene equilibration experiments in the multivariate  
 426 systems (CMS and CMAS) at 925 °C to 1150 °C and 10 kbar to 15 kbar conditions and proposed  
 427 two thermometric equations :

$$428 \quad TSJ(1)_{89-Opx-Cpx} (^{\circ}K) = \frac{4900}{[1.807 - \ln K_D(1)]} \quad (26)$$

$$429 \quad TSJ(2)_{89-Opx-Cpx} (^{\circ}K) = \frac{7045}{[2.47 - \ln K_D(2)]} \quad (27)$$

$$430 \quad \text{where } K_D(1) = \frac{[X_{En}]^{Cpx}}{[X_{En}]^{Opx}} \text{ and } K_D(2) = \frac{[X_{Di}]^{Opx}}{[X_{Di}]^{Cpx}} .$$

431 Compared to Sen and Jones (1989) models, the previous Wells (1977) and Nickel et al. (1985)  
432 thermometers give consistently higher temperatures. According to Sen and Jones (1989),  
433 thermometer of Bertrand and Mercier (1985/1986) gives a temperature range that is the  
434 closest to the Eq. 26 and Eq. 27. These thermometers are found to be useful in estimating  
435 temperatures of natural spinel peridotites to within  $\pm 50$  °C.

436 Taking into account the Ca- and Na-partitioning between orthopyroxene and clinopyroxene,  
437 Brey and Köhler (1990) formulated two-pyroxene thermometers based on reversed  
438 experiments, which can be applied both to the CMS and the CMAS systems:

$$439 \quad TBK_{90\text{-Ca-in-Opx-Cpx}} (^{\circ}\text{K}) = \frac{23664 + (24.9 + 126.3 * X_{\text{Fe}}^{\text{Cpx}}) * P(\text{kbar})}{13.38 + (\ln K_D^*)^2 + 11.59 * X_{\text{Fe}}^{\text{Opx}}} \quad (28)$$

$$440 \quad TBK_{90\text{-Na-in-Opx-Cpx}} (^{\circ}\text{K}) = \frac{35000 + 61.5 * P(\text{kbar})}{(\ln D_{\text{Na}})^2 + 19.8} \quad (29)$$

$$441 \quad \text{where } K_D^* = \frac{(1 - \text{Ca}^*)_{\text{Cpx}}}{(1 - \text{Ca}^*)_{\text{Opx}}}, \text{ Ca}^* = \frac{\text{Ca}^{M2}}{(1 - \text{Na}^{M2})}, X_{\text{Fe}}^{\text{Cpx or Opx}} = \frac{\text{Fe}^{2+}}{\text{Fe}^{2+} + \text{Mg}}, \text{ and } D_{\text{Na}} = \frac{\text{Na}^{\text{Opx}}}{\text{Na}^{\text{Cpx}}}.$$

442 Considering the suggestion that Ca-in-orthopyroxene, which is in equilibrium with  
443 clinopyroxene can be used as a thermometer by Sachtleben and Seck (1981), Brey and Köhler  
444 (1990) fitted the reversed experiments in the CMS system, given by Nickel and Brey (1984), as a  
445 function of  $P$  and reciprocal  $T$  and derived an equation for temperature that may be calculated  
446 from the Ca content (*apfu*) of orthopyroxene:

$$447 \quad TBK_{90\text{-Ca-in-Opx}} (^{\circ}\text{K}) = \frac{6425 + 26.4 * P(\text{kbar})}{-\ln \text{Ca}^{\text{Opx}} + 1.843} \quad (30)$$

448 Equation 30 can be applied both to the CMS and the natural systems, but is not as good as the  
449 Ca-in-Opx-Cpx thermometer (i.e., Eq. 28). In natural systems, the Ca content in orthopyroxene  
450 is lowered in the presence of Al and a variable amount of Na in the *M2* site. In this case, the Ca-  
451 in-Opx thermometer may be used to understand the closure temperature of the Ca-Mg  
452 exchange. However, the Ca-in-Opx thermometer (i.e., Eq. 30) may provide a potential  
453 alternative to the solvus two-pyroxene thermometers, especially for ultramafic rocks. Among  
454 two-pyroxene thermometers, the Brey and Köhler (1990) models (e.g., Eq. 28) have been used  
455 widely in mantle systems. The Bertrand and Mercier (1985/1986) model, which is fundamental  
456 to Brey and Köhler's (1990) Ca-in-Opx-Cpx thermometer, somewhat underestimates the  
457 temperatures, possibly because of the Fe correction of Ca in clinopyroxene and the narrow  
458 temperature calibration range (e.g., 800 °C – 1000 °C) of the experiments. Brey and Köhler's  
459 (1990) formulation showed that if a correction factor of -0.77 in  $Ca_{cpx}^*$  (see Eq. 23) is replaced  
460 by -0.97, the Bertrand and Mercier (1985/1986) model reproduces results obtained with their  
461 thermometer for natural rocks and can be applied to equilibration temperatures > 750 °C.

462 Taylor (1998) carried out an experimental study of upper mantle peridotites, produced a  
463 new two-pyroxene thermometer, discussed some of the existing thermobarometers in terms of  
464 which thermobarometers are the most applicable to fertile lherzolite and websterite, and  
465 proposed modifications or new calibrations for inadequate geobarometers. The Taylor (1998)  
466 thermometer is a modified form of the Brey and Köhler (1990) model, which is based on  
467 mineral chemical data from a series of high *P-T*, *fO<sub>2</sub>*-controlled, fluid-saturated experiments in  
468 the range of *P* = 1.0 to 3.5 GPa and *T* = 1050 to 1260 °C:

$$469 \quad TT_{98\text{-Opx-Cpx}} (^{\circ}\text{K}) = \frac{24787 + 678 * P \text{ (GPa)}}{15.67 + 14.37 * Ti^{Cpx} + 3.69 * Fe^{Cpx} - 3.25 * X_{ts} + (\ln K_d)^2} \quad (31)$$

470 where  $X_{ts} = (Al+Cr-Na)^{Cpx}$ ,  $\ln K_d = \ln [a(En)^{Cpx}] - \ln [a(En)^{Opx}]$ ,

$$471 \quad a(En)^{Cpx \text{ or } Opx} = (1 - Ca - Na) * (1 - Al^{VI} - Cr - Ti) * \left(1 - \frac{Al^{IV}}{2}\right)^2, \quad Al^{IV} = \left(\frac{Al}{2} + \frac{Cr}{2} + Ti - \frac{Na}{2}\right)^{\text{for Cpx and Opx}},$$

$$472 \quad Al^{VI} = \left(\frac{Al}{2} - \frac{Cr}{2} - Ti + \frac{Na}{2}\right)^{\text{for Cpx and Opx}}, \quad \text{and all in cations (apfu).}$$

473 This model is applicable to a wide range of fertile peridotite compositions, including spinel,  
 474 garnet and pyroxene, with a high  $P$  range (i.e., 1.0 to 3.5 GPa). Taylor (1998) also established  
 475 that the Brey and Köhler (1990) formulations (e.g., Eq. 28 and Eq. 29), which are accepted as a  
 476 standard model in mantle studies, tend to overestimate the  $T$  of fertile peridotite compositions.

477 Putirka (2008) introduced two two-pyroxene thermometers, one for mafic systems (i.e.,  
 478  $Mg\#^{Cpx} > 0.75$ ) and the other only for experiments with high  $Mg\#$  compositions ( $Mg\#^{Cpx} > 0.75$ )  
 479 based on the partitioning of enstatite+ferrosilite between ortho- and clinopyroxene by using a  
 480 new global regression model:

$$481 \quad TP(1)_{08\text{-Opx-Cpx}} = \frac{10000}{11.2 - 1.96 * \ln \left( \frac{X_{EnFs}^{Cpx}}{X_{EnFs}^{Opx}} \right) - 3.3 * (X_{Ca}^{Cpx}) - 25.8 * (X_{CrCaTs}^{Cpx}) + 33.2 * (X_{Mn}^{Opx}) - 23.6 * (X_{Na}^{Opx}) - 2.08 * (X_{En}^{Opx}) - 8.33 * (X_{Di}^{Opx}) - 0.05 * P \text{ (kbar)}} \quad (32)$$

$$482 \quad TP(2)_{08\text{-Opx-Cpx}} = \frac{10000}{13.4 - 3.4 * \ln \left( \frac{X_{EnFs}^{Cpx}}{X_{EnFs}^{Opx}} \right) + 5.59 * (X_{Mg}^{Cpx}) - 8.8 * (Mg \#^{Cpx}) + 23.85 * (X_{Mn}^{Opx}) + 6.48 * (X_{FmAl_2SiO_6}^{Opx}) - 2.38 * (X_{Di}^{Cpx}) - 0.044 * P \text{ (kbar)}} \quad (33)$$



483 where  $X_{En}^{Opx} = \left[ \frac{X_{Mg}^{Opx}}{X_{Mg}^{Opx} + X_{Fe}^{Opx} + X_{Mn}^{Opx}} \right] * (X_{Fm_2Si_2O_6}^{Opx})$  and  $X_{Di}^{Opx} = \left[ \frac{X_{Mg}^{Opx}}{X_{Mg}^{Opx} + X_{Fe}^{Opx} + X_{Mn}^{Opx}} \right] * (X_{CaFmSi_2O_6}^{Opx})$

484 In these equations, the  $X_{EnFs}^{Cpx}$ ,  $X_{EnFs}^{Opx}$ ,  $X_{Di}^{Cpx}$ ,  $X_{Di}^{Opx}$ ,  $X_{En}^{Opx}$ , and  $X_{FmAl_2SiO_6}^{Opx}$  show the  
485 components of clino- and orthopyroxene given by formulations in the “Two-pyroxene.xls” Excel  
486 spreadsheet developed by Putirka (2008). Two-pyroxene thermometers (i.e., Eq. 32 and Eq. 33)  
487 and the other most commonly used formulations can be calculated and compared in an Excel  
488 workbook (i.e., “[Two-pyroxene.xls](#)”) published by Putirka (2008).

489 According to Nimis and Grütter (2010), the Taylor (1989) model for two-pyroxene and the  
490 Nimis and Taylor (2000) model for single-clinopyroxene thermometers give the most reliable  
491 temperatures in variety of simple and natural peridotitic systems. However, the temperature  
492 estimation methods based on two-pyroxene thermometers for garnet peridotites and  
493 pyroxenites show that the models are not internally consistent and in some cases the  
494 difference between formulations exceeds 200 °C in a well-equilibrated mantle xenoliths (e.g.,  
495 Nimis and Grütter 2010). In order to improve the internal consistency between two-pyroxene  
496 and Ca-in-Opx models of Brey and Köhler (1990) for temperatures of mantle-derived rocks,  
497 Nimis and Grütter (2010) proposed the following empirical correction:

498  $TNT_{10-Ca-in-Opx} (^{\circ}C) = -628.7 + 2.0690 * TBKN_{90-Ca-in-Opx} - 4.530 * 10^{-4} * (TBKN_{90-Ca-in-Opx})^2$  (34)

499 where  $TBKN_{90-Ca-in-Opx}$  is the Ca-in-Opx thermometer (i.e., Eq. 30) of Brey and Köhler (1990).

500

### Two-pyroxene barometers

501 Mercier et al. (1984) proposed two empirical  $P$  formulations to estimate the equilibrium  
502 conditions of ophiolitic lherzolites:

$$503 \quad PM(1)_{84\text{-Opx-Cpx}} \text{ (GPa)} = \frac{1.279}{(K_f + 0.0006) - 2.29} \quad (35)$$

$$504 \quad PM(2)_{84\text{-Opx-Cpx}} \text{ (GPa)} = \frac{1.073}{(K_f + 0.028) - 1.65} \quad (36)$$

505 where  $K_f = \frac{[Ca^*]_{\text{Opx}}}{\{1 - [Ca^*]_{\text{Cpx}}\}}$ . In this equation, the  $[Ca^*]_{\text{Opx}}$  and  $[Ca^*]_{\text{Cpx}}$  are the Ca (*apfu*) contents

506 of ortho- and clinopyroxene, respectively. Equation 35 is used for all available CMS and CMAS  
 507 systems, whereas Eq. 36 is considered when discarding the questionable data points in the data  
 508 set used for calibration at or below 0.5 GPa.

509 Putirka (2008), with a similar limitation on high Mg# composition (i.e., Mg# > 0.75),  
 510 calibrated Mercier et al.'s (1984) *P* model by applying a new global regression approach:

$$511 \quad PP(1)_{08\text{-Opx-Cpx}} \text{ (kbar)} = -279.8 + 293*(X_{\text{Al}^{\text{VI}}}^{\text{Opx}}) + 455*(X_{\text{Na}}^{\text{Opx}}) + 229*(X_{\text{Cr}}^{\text{Opx}}) + 519*(X_{\text{Fm}_2\text{Si}_2\text{O}_6}^{\text{Opx}}) \\ - 563*(X_{\text{En}}^{\text{Opx}}) + 371*(X_{\text{Di}}^{\text{Opx}}) + 327*(a_{\text{En}}^{\text{Opx}}) + \frac{1.19}{K_f} \quad (37)$$

$$512 \quad PP(2)_{08\text{-Opx-Cpx}} \text{ (kbar)} = -94.25 + 0.045*T(^{\circ}\text{C}) + 187.7*(X_{\text{Al}^{\text{VI}}}^{\text{Opx}}) + 246.8*(X_{\text{Fm}_2\text{Si}_2\text{O}_6}^{\text{Opx}}) - 212.5*(X_{\text{En}}^{\text{Opx}}) \\ + 127.5*(a_{\text{En}}^{\text{Opx}}) - \frac{1.66}{K_f} - 69.4*(X_{\text{EnFs}}^{\text{Cpx}}) - 133.9*(a_{\text{Di}}^{\text{Cpx}}) \quad (38)$$

$$513 \quad \text{where } X_{\text{En}}^{\text{Opx}} = (X_{\text{Fm}_2\text{Si}_2\text{O}_6}^{\text{Opx}})*\left(\frac{X_{\text{Mg}}^{\text{Opx}}}{[X_{\text{Mg}}^{\text{Opx}} + X_{\text{Mn}}^{\text{Opx}} + X_{\text{Fe}}^{\text{Opx}}]}\right), \quad X_{\text{Di}}^{\text{Opx}} = (X_{\text{CaFmSi}_2\text{O}_6}^{\text{Opx}})*\left(\frac{X_{\text{Mg}}^{\text{Opx}}}{[X_{\text{Mg}}^{\text{Opx}} + X_{\text{Mn}}^{\text{Opx}} + X_{\text{Fe}}^{\text{Opx}}]}\right),$$

$$514 \quad a_{\text{En}}^{\text{Opx}} = \left(\frac{0.5*X_{\text{Mg}}^{\text{Opx}}}{X_{\text{Ca}}^{\text{Opx}} + 0.5*X_{\text{Mg}}^{\text{Opx}} + 0.5*X_{\text{Fe}^{2+}}^{\text{Opx}} + X_{\text{Mn}}^{\text{Opx}} + X_{\text{Na}}^{\text{Opx}}}\right)*\left(\frac{0.5*X_{\text{Mg}}^{\text{Opx}}}{0.5*X_{\text{Fe}^{2+}}^{\text{Opx}} + 0.5*X_{\text{Fe}^{3+}}^{\text{Opx}} + X_{\text{Al}^{\text{VI}}}^{\text{Opx}} + X_{\text{Ti}}^{\text{Opx}} + X_{\text{Cr}}^{\text{Opx}} + 0.5*X_{\text{Mg}}^{\text{Opx}}}\right),$$

$$515 \quad \text{and } a_{\text{Di}}^{\text{Cpx}} = \frac{(X_{\text{Ca}}^{\text{Cpx}})}{(X_{\text{Ca}}^{\text{Cpx}} + 0.5*X_{\text{Mg}}^{\text{Cpx}} + 0.5*X_{\text{Fe}^{2+}}^{\text{Cpx}} + X_{\text{Mn}}^{\text{Cpx}} + X_{\text{Na}}^{\text{Cpx}})}. \text{ In these equations, the } K_f \text{ ratio}$$

516 (see Eq. 35 and Eq. 36) is the same as in Mercier et al. (1984) and  $X_{\text{element}}^{\text{Pyx}}$  refers to the cations  
517 (*apfu*). In contrast to *T*-independent Eq. 37, the temperature-dependent pressure formulation  
518 recovers *P* to  $\pm 2.8$  kbar and thus the precision is increased when *T* is used as an input in Eq. 38  
519 (Putirka 2008).

## 520 **DESCRIPTION OF PROGRAM**

521 WinPyrox is a compiled program developed for running in the Microsoft® Windows platform.  
522 The program is designed to calculate and classify electron-microprobe and wet-chemical  
523 pyroxene analyses. WinPyrox also calculates the most widely used single-clinopyroxene and  
524 two-pyroxene thermobarometers, which allows the user to make an extensive comparison of  
525 different calibrations using their own pyroxene analyses. The program comes up with a self-  
526 extracting setup file ( $\approx 11$  Mb), which is created by the Inno Setup Compiler (i.e., version 5.5.2)  
527 developed by Jordan Russell (<http://www.jrsoftware.org/isdl.php>). The program runs as a single  
528 executable file, WinPyrox.exe (4.6 Mb), provided that the Microsoft® Visual Studio package is  
529 installed. However, with the help of necessary .ocx and .dll support files in the self-extracting  
530 setup file, the users of this program can execute WinPyrox without requiring the Microsoft®  
531 Visual Studio package. Upon successful installation of the WinPyrox program, the start-up  
532 screen with various pull-down menus and shortcuts appears. Execution of WinPyrox may also  
533 be started by clicking the program icon from *All Programs* options.

## 534 **Data entry**

535 The users of this program can edit pyroxene analyses obtained from wet-chemical or  
536 electron-microprobe techniques by clicking the *New* icon on the tool bar, by selecting *New File*

537 from the pull-down menu of *File* option or pressing the *Ctrl + N* keys. The standard 19 variables  
538 are defined by the program for calculation and classification of pyroxene analysis in the  
539 following order:

540 Sample No, SiO<sub>2</sub>, TiO<sub>2</sub>, Al<sub>2</sub>O<sub>3</sub>, V<sub>2</sub>O<sub>3</sub>, Cr<sub>2</sub>O<sub>3</sub>, Fe<sub>2</sub>O<sub>3</sub>, FeO, MnO, NiO, CoO, ZnO, MgO, CaO, Na<sub>2</sub>O,  
541 K<sub>2</sub>O, ZrO<sub>2</sub>, Sc<sub>2</sub>O<sub>3</sub>, and Li<sub>2</sub>O.

542 In data entry section, the program thus permits the user to enter a total of 40 variables,  
543 including oxides (wt%) both for clino- and orthopyroxenes, *P* (kbar), and *T* (°C). *P-T* values  
544 entered by users are used by the program for estimation of thermobarometric conditions.  
545 Pyroxene analyses typed in Excel files with the extension of “.xls” and “.xlsx” in the above order,  
546 can be loaded into the program’s data entry section by clicking the *Open Excel File* option from  
547 the pull-down menu of *File*. For example, two representative pyroxene Excel data files  
548 (WinPyrox\_Rock and WinPyrox\_Putirka) in the folder (C:\Program Files\WinPyrox\Open Excel  
549 Files) can be used for this purpose by the user. However, using the copy-paste options, one can  
550 incorporate pyroxene data from a Microsoft® Excel spreadsheet into the data entry section of  
551 the program more quickly. By selecting the *Edit Excel File* option from the pull-down menu of  
552 *File*, pyroxene analyses can be typed in a blank Excel file (i.e., WinPyrox) in the (C:\Program  
553 Files\WinPyrox>Edit Excel File) folder, stored in a different file name with the extension of “.xls”  
554 or “.xlsx”, and then loaded into the program’s data entry section by clicking the *Open Excel File*  
555 option from the pull-down menu of *File* for further calculation. Once the pyroxene analyses in  
556 an Excel file are displayed on the screen by using the *Open Excel File* option, they can be stored  
557 with the extension of “.pyx” by clicking the *Save As* option from the pull-down menu of *File*.

558 Additional information about data entry or similar topics can be accessed by pressing the F1  
559 function key to display the WinPyrox.hlp file on the screen. For example, by selecting the *Data*  
560 *Entry* section from the index of WinPyrox.chm file, it displays the necessary documents  
561 concerning the pyroxene *Data Entry* section on the screen.

## 562 **Normalization**

563 WinPyrox calculates pyroxene analyses with cations estimated based on 6 oxygens in the  
564 formula. Once the program is executed, the program begins with to calculate pyroxene data  
565 based on the structural formulae with a total of 4 cations. However, by clicking *structural*  
566 *formulae* option from the pull-down menu of *Normalization*, the program allows the user two  
567 types of the cation normalization schemes, such as i) *structural formulae with a total of 4*  
568 *cations* and ii) *structural formulae without a total of 4 cations*. In most of the pyroxene chemical  
569 studies, cations are used with normalization to a total of 4, whereas some authors (e.g., Putirka  
570 2008) prefer to use cations without normalization to 4, especially for thermobarometric  
571 estimations. WinPyrox, providing these two options in the *Normalization* menu, thus enables  
572 the user the opportunity to calculate pyroxene analyses for different total cation procedures.

## 573 **Ferric iron estimation**

574 Pyroxene analyses with measured Fe<sub>2</sub>O<sub>3</sub> (wt%) and FeO (wt%) contents (e.g., wet-chemical)  
575 are calculated by program as Fe<sup>+3</sup> (*apfu*) and Fe<sup>2+</sup> (*apfu*) separately. If pyroxene analyses are  
576 given as Fe<sub>2</sub>O<sub>3</sub> (wt%) = 0 and FeO (wt%) > 0, then the program assumes FeO (wt%) content as  
577 FeO<sub>total</sub> (wt%) and estimates the ferric and ferrous iron stoichiometrically. The ferric iron  
578 estimation (Fe<sup>3+</sup>, *apfu*) from a total iron content (FeO<sub>total</sub>, wt%) of electron-microprobe

579 pyroxene analysis is carried out by different empirical equations in WinPyrox (e.g., Droop 1987;  
580 Papike et al. 1974). The program begins with to estimate the  $\text{Fe}^{3+}$  content based on method  
581 proposed by Droop (1987) as follows:

$$582 \quad \text{Fe}^{3+} = 12 * \left( 1 - \frac{4}{S} \right) \quad (39)$$

583 where  $S$  shows the observed cation total per 6 oxygens calculated assuming all iron to be  
584 ferrous iron. However, WinPyrox also allows the user to select the second procedure proposed  
585 by Papike et al. (1974) from the pull-down menu of *the Ferric iron estimation* options in  
586 estimating the  $\text{Fe}^{3+}$  content from a total iron content of pyroxene analysis.

$$587 \quad \text{Fe}^{3+} = \text{Al}^{\text{IV}} + \text{Na} - \text{Al}^{\text{VI}} - \text{Cr} - 2 * \text{Ti} \quad (40)$$

588 In most case, an empirical ferric iron content estimation of electron-microprobe pyroxene  
589 analysis between the Droop (1987) and Papike et al. (1974) models can be represented by the  
590 following equation:

$$591 \quad \text{Fe}^{3+}_{\text{D87}} = \frac{3}{2} * \text{Fe}^{3+}_{\text{P74}} \quad (41)$$

592 where  $\text{Fe}^{3+}_{\text{D87}}$  and  $\text{Fe}^{3+}_{\text{P74}}$  denotes the  $\text{Fe}^{3+}$  contents by Droop (1987) and Papike et al. (1974),  
593 respectively. Ferric iron estimation based on the Droop (1987) method produces the maximum  
594  $\text{Fe}^{3+}$  content, whereas Papike et al.'s (1974) approach gives the minimum  $\text{Fe}^{3+}$  content.  
595 Alternatively, an average  $\text{Fe}^{3+}$  content based on the Droop (1987) and Papike et al. (1974)  
596 formulations can be estimated as follows:

$$597 \quad \text{Fe}^{3+}_{\text{TS}} = \frac{(\text{Fe}^{3+}_{\text{D87}} + \text{Fe}^{3+}_{\text{P74}})}{2} \quad (42)$$

598 where TS denotes this study. WinPyrox allows the user to estimate an average Fe<sup>3+</sup> content of  
599 electron-microprobe pyroxene analyses by selecting “Fe3+ estimation (This study)” from the  
600 pull-down menu of *Ferric iron estimation* option.

601

## WORKED EXAMPLES

602 The following examples show how WinPyrox can be used for a variety of calculations and  
603 classifications of pyroxenes. Table 4 lists the specific calculation steps in the *Calculation Screen*  
604 of the program. Validity of program outputs has been tested for numerous data sets, and  
605 results are given in Tables 5–8.

606

### Classification of pyroxenes

607 Once the pyroxene analyses are processed by clicking the *Calculate* icon (i.e.,  $\Sigma$ ) in the *Data*  
608 *Entry Section* of the program (Fig. 4a), all estimation parameters both for clinopyroxene and  
609 orthopyroxene are displayed in columns 1-130 and 131-211 (see Table 4) of the *Calculation*  
610 *Screen* (Fig. 4b), respectively. Pressing the *Ctrl + F* keys or clicking the *Open File to Calculate*  
611 option from the *Calculate* menu also executes the data processing for a selected data file with  
612 the extension of “.pyx”. Representative pyroxene analyses with their estimations based on six  
613 oxygen by the program are given in Table 5.

614 WinPyrox distributes the recalculated cations into the *T*, *M1*, and *M2* sites (see rows 3 and  
615 15 in Table 4). The program first calculates the structural formulae (see rows 19-36 in Table 5)  
616 and then defines pyroxene groups (row 39 in Table 5) in the *Q* vs. *J* classification diagram (see  
617 Fig. 1) taking into account the *Q* and *J* values (rows 37 and 38 in Table 5). Following the group  
618 name separation, WinPyrox specifies pyroxene names (see row 40 in Table 5) with possible

619 adjectival modifiers (see row 41 in Table 5). The IMA-88 list comprises fifteen adjectival  
620 modifiers (see rows 1 to 15 in Table 3), but exclude some of the elements, including  $V^{3+}$ ,  $Zr^{4+}$ ,  
621 and  $Sc^{3+}$ . WinPyrox considers these elements and determines adjectival modifiers as vanadoan,  
622 zirconian, and scandian, respectively (see rows 17 to 19 in Table 3). The software also identifies  
623 the cobaltian adjectival modifier provided that the  $Co^{2+} > 0.01$  (see row 16 in Table 3).  
624 WinPyrox classifies all IMA-88 proposed pyroxene groups with their mineral subdivisions (see  
625 Table 2).

626 The program, cannot distinguish enstatite/ferrosilite from clinoenstatite/clinoferrosilite and  
627 produces two names, such as enstatite/clinoenstatite (e.g., see the sample S1 in row 40 in Table  
628 5) and ferrosilite/clinoferrosilite because the identification of the orthorhombic and  
629 monoclinic varieties are insensitive to chemical parameters and are commonly identified by  
630 their optical properties. There is no distinctive classification procedure for all the other  
631 pyroxene group minerals in the IMA-88 nomenclature scheme. WinPyrox, thus names other  
632 pyroxene group minerals (see Table 2) based on the criteria given by Rock (1990) such as  
633 donpeacorite/kanoite (rare Mn-Mg pyroxene), johannsenite-petedunnite-esseneite (rare Ca  
634 pyroxene), spodumene (rare Li-Al pyroxene), kosmochlor (rare-Na-Cr<sup>3+</sup> pyroxene), and jervisite  
635 (rare-Na pyroxene) (e.g., see rows 39 and 40 in Table 5).

636 WinPyrox allows the user to produce eighteen pyroxene-related plots in the pull-down menu  
637 of *Graph*, which are grouped as i) *Classification Diagrams* (including six diagrams), ii) *Graphical*  
638 *Two-Pyroxene Thermometry* (including four diagrams), and iii) *Miscellaneous Plots* (including  
639 eight diagrams). For example, by clicking the *Classification Diagram* option and selecting Wo-



640 En-Fs and Q-Jd-Ae ternary diagrams from the pull-down menu of *Graph* in the *Calculation*  
641 *Screen*, the program enables the user to display each sample in the specific IMA pyroxene  
642 classification plots (Morimoto et al. 1988) (see Fig.2a and Fig. 3a) and on plots suggested by  
643 Rock (1990) for the Subcommittee on Pyroxenes (see Fig. 2b and Fig. 3b), provided that the  
644 Golden Software's Grapher™ is installed on the computer. Clinopyroxenes, in the four  
645 component system (i.e.,  $\text{CaMgSi}_2\text{O}_6$ - $\text{CaFeSi}_2\text{O}_6$ - $\text{Mg}_2\text{Si}_2\text{O}_6$ - $\text{Fe}_2\text{Si}_2\text{O}_6$ ), can be classified on  
646 Poldervaart and Hess's (1951) ternary  $\text{CaSiO}_3$  (wollastonite)- $\text{MgSiO}_3$  (clinoenstatite)- $\text{FeSiO}_3$   
647 (clinoferrosilite) diagram (Fig. 5a). Pyroxenes within different compositions may be displayed on  
648 the Papike et al.'s (1974) ternary Ti-Na- $\text{Al}^{\text{IV}}$  diagram (Fig. 5b) with variable solid solution  
649 components. All pyroxene analyses belonging to Ca-Mg-Fe, Ca-Na, and Na groups are  
650 automatically selected and plotted in each classification diagram by WinPyrox.

#### 651 **End-members, molar fractions and end-member activities**

652 A number of calculation schemes has been proposed for the estimation of pyroxene end-  
653 member components (e.g., Yoder and Tilley 1962; Cawthorn and Collerson 1974; Dietrich and  
654 Petrakakis 1986; Harlow 1997). Although the order of recalculation of end-members is  
655 arbitrary, a scheme of end-member calculation should contain a minimum of uncertainties and  
656 errors. However, most calculation schemes are sequential and lead to an overestimation of the  
657 component that is calculated first.

658 The calculation procedure for pyroxene end-members by Yoder and Tilley (1962) starts with  
659 acmite, and thus may cause an overestimation of the acmite and the Ca-Tschermak's  
660 component when compared to the jadeite and ferri-Tschermak's components (e.g., see rows

661 58-62 in Table 5). On the other hand, the end-member calculation scheme proposed by  
662 Cawthorn and Collerson (1974) starts with jadeite and in this case, the jadeite and ferri-  
663 Tschermak's components may show higher values than the acmite and Ca-Tschermak's  
664 component (e.g., see rows 63-71 in Table 5). The end-member method based on a linear  
665 algebraic model by Dietrich and Petrakakis (1986) calculates 11 linearly independent  
666 components, including jadeite (Jd), acmite (Acm), Ureyite (Ur), Ti-Tschermakite (TiTs), Ca-  
667 Tschermakite (CaTs), Fe-Tschermakite (FeTs), Cr-Tschermakite (CrTs), pyroxmangite (Pm),  
668 ferrosilite (Fs), enstatite (En), and wollastonite (Wo). In these methods (e.g., Yoder and Tilley  
669 1962; Cawthorn and Collerson 1974; Dietrich and Petrakakis 1986), acmite or jadeite is  
670 calculated first and may give an overestimation of that component. One attempt to solve this  
671 problem was proposed by Harlow (1997) that starts with the Ca-Tschermak's component (see  
672 rows 72-79 in Table 5). Except for the Dietrich and Petrakakis (1986) model, WinPyrox  
673 estimates all these end-member components (see rows 42-79 in Table 5) in the *Calculation*  
674 *Screen* window for pyroxenes (columns from 48 to 78). The program also gives end-members  
675 (e.g., Wo-En-Fs, Q-Jd-Aeg, Wo-Hyp-Jd, and Aug-Jd-Aeg in %) using the simple formula compiled  
676 by Soto and Soto (1995) in columns of 48-59 (see rows 42-57 in Table 5).

677 Estimation of molar fractions at different sites (e.g.,  $X_{M1}^{Fe^{2+}}$ ,  $X_{M1}^{Fe^{2+}}$ ), end-members and their  
678 activities (e.g.,  $a_{En}$ ,  $a_{Di}$ ) from microanalysis of rock-forming minerals are important parameters.  
679 These parameters are used in thermometric formulations for estimating the  $P$ - $T$  conditions of  
680 magmatic and metamorphic rocks. WinPyrox calculates seven molar fractions (see rows 86-92  
681 in Table 5) and seven end-member activities (see rows 93-99 in Table 5) of pyroxenes taking  
682 into account the formulations compiled by Soto and Soto (1995; see references therein). The

683 program calculates molar fractions and end-member activities of clinopyroxenes in the  
684 *Calculation Screen* window between the column numbers of 85-91 and 96-102, respectively.  
685 End-member activities such as  $a_{En}$  and  $a_{Di}$  given in the *Calculation Screen* window, at columns  
686 111-112 and 185-186 for clino- and orthopyroxenes, respectively, are estimations following  
687 Wood and Banno (1973), which are used in some of the two-pyroxene thermometers (e.g.,  
688 Wood and Banno 1973; Carlson and Lindsley 1988; Sen and Jones 1989).

### 689 **Thermobarometry**

690 The main aim of this study is to recalculate and classify pyroxene analyses according to the  
691 current IMA-88 nomenclature scheme, as well as enable the user to estimate widely used  
692 pyroxene thermobarometers. The current program ignores in estimation of clino- and  
693 orthopyroxene-liquid thermobarometers (e.g., Putirka et al. 1996; Putirka 1999; Putirka et al.  
694 2003), but performs calculations for thirty five single-clinopyroxene, two-pyroxene, and Ca-in-  
695 orthopyroxene thermobarometers. In order to test the program output, twenty four pyroxene  
696 analyses were used from Putirka's (2008) Excel spreadsheet (i.e., Two-pyroxene *P-T*) and  
697 selected clino- and orthopyroxenes are given in Table 6 and Table 7, respectively, with their  
698 calculation/classification parameters and thermobarometers. In both Nimis' (1995, 1999) and  
699 Putirka et al.'s (1996, 2003) models, clinopyroxene components are estimated based on the  
700 numbers of cations on 6 six oxygen basis. In contrast to the Putirka et al.'s (1996, 2003)  
701 models, the Nimis' (1995, 1999) model assumes cation fractions normalized to 4. Taking into  
702 account Putirka's (2008) approach, pyroxene analyses in Table 6 and Table 7 are calculated  
703 using the WinPyrox program by clicking *structural formulae* option from the pull-down menu of  
704 *Normalization* and selecting *structural formulae without a total of 4 cations* option. Single-

705 clinopyroxene barometers in Table 6 (rows 42-48) are obtained by using the different  
706 calibrations proposed by Nimis (1995; see Eq. 1), Nimis and Ulmer (1998; see Eq. 5 and Eq. 7),  
707 Nimis (1999; see Eqs. 8 and 9), Nimis and Taylor (2000; see Eq. 10), and Putirka (2008; see Eq.  
708 11).

709 Nimis (2000) presented an Excel spreadsheet (i.e., CpxBar) for quantitative pressure  
710 estimations of magmatic systems using clinopyroxene compositions. The spreadsheet considers  
711 cation fractions that are normalized to 4 and presents four different pressure (kbar) calibrations  
712 for: i) anhydrous melts from basalt to low alkali nephelinites (i.e., PBA; see Eq. 5), ii) hydrous  
713 melts from basalt to low alkali nephelinites (i.e., PBH; see Eq. 7), iii) the tholeiitic series from  
714 basalt to dacite (i.e., PTH; see Eq. 8), and iv) the mildly alkaline series from basalt to dacite (i.e.,  
715 PMA; see Eq. 9) which requires  $T$  ( $^{\circ}\text{C}$ ) as an input value. Using Putirka's (2008) clinopyroxene  
716 data for different normalization and ferric iron estimation methods, the comparison of CpxBar  
717 (see rows 2-5 in Table 8) those with the WinPyrox's outputs (see rows 6-21 in Table 8) are given  
718 in Table 8. This table shows that for the selected clinopyroxene data set there is no distinctive  $P$   
719 (kbar) variation between normalization procedures and ferric iron estimation methods.  
720 Correlation coefficients ( $r$ ) for pressures from CpxBar vs. WinPyrox range from 0.99 to 0.86 (see  
721 Fig. 6).

722 Clinopyroxene barometers for magmatic rocks based on the crystal-structure modeling (e.g.,  
723 Nimis 1995, 1999; Nimis and Ulmer 1998) can be plotted in several  $V_{\text{Cell}}$  vs.  $V_{M1}$  diagrams. These  
724 plots are displayed by WinPyrox from the pull-down menu of *Graph* in the *Calculation Screen*.  
725 The user, for example, can display six different barometer plots for clinopyroxenes based on the

726 empirical expressions by clicking first *Miscellaneous Plots* and then selecting one of six Vcell-  
727 VM1 diagrams. The  $Al^{VI}/Al^{IV}$  ratio in clinopyroxenes from a variety of petrological environments  
728 increases with increasing pressure values (Bondi et al. 2002). Accordingly, aluminium content  
729 in the  $Al^{VI}$  vs.  $Al^{IV}$  diagram (after Aoki and Shiba 1973) can be used to estimate qualitatively the  
730 pressure condition of crystallization. WinPyrox allows the user to display this plot from the  
731 pull-down menu of *Graph* in the *Calculation Screen* by clicking first *Miscellaneous Plots* and  
732 then selecting the Al(VI)-Al(IV) Diagram option.

733 Following Putirka's (2008) approach, including ferric iron estimation based on Papike et al.  
734 (1974) and total cations without normalization to 4, a comparison of two-pyroxene  
735 thermobarometry is given in Table 7 (see rows 42-64 and 67-86). Except for a few data points in  
736 some of the two-pyroxene thermometers, all lie in a straight line with the high correlation  
737 coefficients ( $r \geq 0.96$ ). This is evidence of the good relationship between the Putirka's (2008)  
738 model and WinPyrox's outputs. Using different ferric iron estimation methods (e.g., Papike et  
739 al. 1974; Droop 1987) and normalization procedures (e.g., cations total to 4 and without  
740 normalization to 4) by WinPyrox program for Putirka's (2008) model together with selected  
741 pyroxene data display a slight difference, but not an important variation in  $P$  (kbar) and  $T$  ( $^{\circ}C$ )  
742 values. In this study, a calibrated and improved formulation of the Nimis (1995) model  
743 proposed by Putirka (2008; i.e., Eq. 32a) is also tested against Nimis (1995), Nimis and Ulmer  
744 (1998), and Nimis (1999) models. High correlation coefficients between  $PN_{95-BS-Cpx}$  and  $PP_{08-}$   
745  $Cpx(Eq. 32a)$  and  $PNU_{98-BA-Cpx}$  and  $PP_{08-Cpx(Eq. 32a)}$  ( $r = 0.94$ ) decrease to  $r = 0.59$  for the  $PNU_{98-Cor-BH-}$   
746  $Cpx$  vs.  $PP_{08-Cpx(Eq. 32a)}$  relationship. Although Putirka's (2008; see Eq. 11) model improves the  
747 precision of Nimis (1995) model and yields a high correlation coefficient ( $r = 0.94$ ) through the

748 Nimis and Ulmer (1998; see Eq. 5) method for anhydrous melts from basalt to low-alkali  
749 nephelinites, it still preserves the systematic error with respect to hydrous experiments. The  
750 low correlation coefficient (i.e.,  $r = 0.59$ ) between the Putirka (2008; i.e., Eq. 32a) and Nimis and  
751 Ulmer (1998; see Eq. 7) models for hydrous melts from basalt to low-alkali nephelinites, thus is  
752 consistent with the anhydrous to hydrous components.

### 753 **Graphical two-pyroxene thermometry**

754 Lindsley and Andersen (1983) and Lindsley (1983) proposed graphical, two-pyroxene  
755 thermometers based on experimentally determined Ca-Mg-Fe pyroxene phase relations at 800  
756 °C-1200 °C and 1 atm to 15 kbar for the Di-En and Hd-Fs joins. The diagrams should be applied  
757 to nearly pure quadrilateral pyroxenes (e.g.,  $Wo+En+Fs > 98\%$ ). The graphical two-pyroxene  
758 thermometers are commonly used for the augite-orthopyroxene, augite-pigeonite, and  
759 pigeonite-orthopyroxene pairs. The graphical two-pyroxene thermometers also give a minimum  
760  $T$  (°C) for the formation of single pyroxenes. From the pull-down menu of *Graphical pyroxene*  
761 *thermometry* in the *Data Entry Screen* of WinPyrox, the program allows the user to select an  
762 option of clinopyroxene components for augite and pigeonite. Clinopyroxene components in  
763 the Di-Hd-En-Fs quadrilateral can also be displayed by selecting options of Wo-En-Fs end-  
764 members from the pull-down menu of *Graphical pyroxene thermometry* in the *Data Entry*  
765 *Screen*. If any of these options from the menu of *Graphical pyroxene thermometry* is not  
766 selected by the user, the program automatically calculates the clinopyroxene components  
767 based on the augite option according to the estimation procedures proposed by Lindsley  
768 (1983). WinPyrox, thus allows the user to display graphical two-pyroxene thermometers from

769 the pull-down menu of *Graph* in the *Calculation Screen* by clicking first *Graphical Two-Pyroxene*  
770 *Thermometry* and then selecting one of four Di-Hd-En-Fs Quadrilateral diagrams.

## 771 **SUMMARY AND AVAILABILITY OF THE PROGRAM**

772 WinPyrox is a user-friendly package for pyroxene analyses, which is developed for personal  
773 computers running in the Windows operating system. The program calculates structural  
774 formulae of multiple clino- and orthopyroxene analyses, obtained both from wet-chemical and  
775 electron-microprobe techniques, using different normalization and ferric iron estimation  
776 methods. Calculation and classification of each pyroxene analysis are carried out according to  
777 the IMA-88 nomenclature. The program generates two main windows. The first window (i.e.,  
778 *Data Entry Screen*) appears on the screen with several pull-down menus and equivalent  
779 shortcuts. By selecting options or clicking buttons on the start-up screen, the user can  
780 enter/load pyroxene analyses into the data entry section and make necessary arrangements for  
781 a desired calculation scheme. The second window (i.e., *Calculation Screen*) allows the user to  
782 display the structural formulae in the *T*, *M1*, and *M2* sites with pyroxene classification  
783 parameters, including groups, names and modifiers. In the *Calculation Screen*, the program also  
784 gives end-member calculations, Fe<sup>2+</sup>-Mg partitioning, molar fractions, end-member activities,  
785 component activities, and single-clinopyroxene and two-pyroxene thermobarometers. All the  
786 estimated pyroxene data in the *Calculation Screen* can be sent to a Microsoft® Excel file (i.e.,  
787 output.xlsx) and then this file can be used for further data manipulation and graphing purposes.

788 When compared to the earlier published DOS-based PYROX (Yavuz 2001) program, the  
789 present software has additional features, including a better graphical user interface and

790 interaction for the visual programming environment. WinPyrox classifies recalculated pyroxene  
791 analyses in six binary and ternary pyroxene classification diagrams, which can be viewed and  
792 printed by the commercial program, Grapher™, available from Golden software. These plots  
793 appear on the screen by clicking *Classification Diagrams* option from the pull-down menu of  
794 *Graph* in the *Calculation Screen*. The program also allows the user to display four quadrilateral  
795 graphical two-pyroxene thermometers and eight binary barometer diagrams based on  
796 clinopyroxene data, by clicking *Graphical Two-Pyroxene Thermometry* and *Miscellaneous Plots*  
797 options from the pull-down menu of *Graph*, respectively.

798 WinPyrox is a compiled program that consists of a self-extracting setup file. If the Microsoft®  
799 Visual Studio package is not installed on the computer, all the necessary support files used by  
800 program are added to the installation file. The program and its associated files are installed  
801 into the directory of “C:\Program Files\WinPyrox” during the installation process. The self-  
802 extracting setup file is approximately 11 Mb and may be downloaded from  
803 <http://code.google.com/p/winpyrox/> or can be obtained from author on request.

804

805

806

## 807 **Acknowledgements**

808 I am grateful for constructive reviews and comments from Keith D. Putirka on an earlier draft,  
809 which improved the overall quality and clarity of the paper. I would like to thank anonymous  
810 reviewers and the expert editorial handling of the manuscript by Don R. Baker for his careful  
811 and insightful reviews.



## 812 **References**

- 813 Aoki, K. and Shiba, I. (1973) Pyroxenes from Iherzolite inclusions of Itinome-gata, Japan. *Lithos*,  
814 6, 41–51.  
815
- 816 Aydin, F., Thompson, R. M., Karsli, O. Uchida, H., Burt, J. B., and Downs, R.T. (2009) C2/c  
817 pyroxene phenocrysts from three potassic series in the Neogene alkaline volcanics, NE  
818 Turkey: their crystal chemistry with petrogenetic significance as an indicator of P–T  
819 conditions. *Contributions to Mineralogy and Petrology*, 158, 131-146.  
820
- 821 Bertrand, P., and Mercier, J.-C.C. (1985/1986) The mutual solubility of coexisting ortho- and  
822 clinopyroxene: toward an absolute geothermometer for the natural system? *Earth and*  
823 *Planetary Science Letters*, 76, 109-122.
- 824 Bindi, L., Cellai, D., Melluso, L., Conticelli, S., Morra, V., and Menchetti, S. (1999) Crystal  
825 chemistry of clinopyroxenes from alkaline undersaturated rocks of the Monte Vulture  
826 Volcano, Italy. *Lithos*, 46, 259-274.
- 827 Brey, G.P., and Köhler, T. (1990) Geothermobarometry in four-phase Iherzolites II. New  
828 thermobarometers, and practical assessment of existing thermobarometers. *Journal of*  
829 *Petrology*, 31, 1353-1378.
- 830 Bondi, M., Morten, L., Nimis, P., Rossi, P.L., and Tranne, C.A. (2002) Megacrysts and mafic-  
831 ultramafic xenolith-bearing ignimbrites from Sirwa Volcano, Morocco: Phase petrology and  
832 thermobarometry. *Mineralogy and Petrology*, 75, 203–221.
- 833 Carlson, W.D., and Lindsley, D.H. (1988) Thermochemistry of pyroxenes on the join  $Mg_2Si_2O_6$ -  
834  $CaMgSi_2O_6$ . *American Mineralogist*, 73, 242-252.
- 835 Cawthorn, R.G., and Collerson, K.D. (1974) The recalculation of pyroxene end-member  
836 parameters and the estimation of ferrous and ferric iron content from electron microprobe  
837 analyses. *American Mineralogist*, 59, 1203-1208.
- 838 Dal Negro, A., Carbonin, S., Molin, G.M., Cundari, A., and Piccirillo, E.M. (1982) Intracrystalline  
839 cation distribution in natural clinopyroxenes of tholeiitic, transitional, and alkaline basaltic  
840 rocks. In S.K. Saxena, Eds., *Advances in Physical Geochemistry*, 2, p. 117-150, Springer-  
841 Verlag, New York.
- 842 Dal Negro, A., Carbonin, S., Salviulo, G., Piccirillo, E.M., and Cundari, A. (1985) Crystal chemistry  
843 and site configuration of the clinopyroxene from leucite-bearing rocks and related genetic  
844 significance: the Sabatini lavas, Roman Region, Italy. *Journal of Petrology*, 26, 1027-1040.

- 845 Dal Negro, A., Molin, G.M., Salviulo, G., Secco, L., Cundari, A., and Piccirillo, E.M. (1989) Crystal  
846 chemistry of clinopyroxene and its petrogenetic significance: A new approach. In A. Boriani,  
847 M. Bonafede, G.B. Piccardo, and G.B. Vai, Eds., The lithosphere in Italy: Advances in earth  
848 science research. Acc Naz Lincei, Atti Convegni Lincei, 80, p. 105-121.
- 849 Davis, B.T.C., and Boyd, E.R. (1966) The join  $Mg_2Si_2O_6$ - $CaMgSi_2O_6$  at 30 kilobars pressure and its  
850 application to pyroxenes from kimberlites. Journal of Geophysical Research, 71, 3567-3576.
- 851 Dietrich, H., and Petrakakis, K. (1986) A linear algebraic method for the calculation of pyroxene  
852 endmember components. Tschermaks Mineralogische und Petrographische Mitteilungen,  
853 35, 275-282.
- 854 Droop, G.T.R. (1987) A general equation for estimating  $Fe^{3+}$  concentrations in ferromagnesian  
855 silicates and oxides from microprobe analyses, using stoichiometric criteria. Mineralogical  
856 Magazine, 51, 431-435.
- 857 Essene, E.J. (1982) Geologic thermometry and barometry. In J.M. Ferry, Ed. Characterization of  
858 Metamorphism through Mineral Equilibria, 10, p. 153-206. Reviews in Mineralogy and  
859 Petrology, Mineralogical Society of America.
- 860 Gómez, J.M.C. (1990) PX: a program for pyroxene classification and calculation of end-  
861 members. American Mineralogist, 75, 1426-1427.
- 862 Harlow, G.E. (1997) K in clinopyroxene at high pressure and temperature: An experimental  
863 study. American Mineralogist, 82, 259-269.
- 864 Kushiro, I. (1962) Clinopyroxene solid solutions. Part 1. The  $CaAl_2SiO_6$  component. Japanese  
865 Journal of Geology and Geography, 33, 213-220.
- 866 Leake, B. E., et al. (1997) Nomenclature of amphiboles: Report of the subcommittee on  
867 amphiboles of the International Mineralogical Association, commission on new minerals  
868 and mineral names. Canadian Mineralogist, 35, 219-246.  
869
- 870 Leake, B. E., et al. (2004) Nomenclature of amphiboles: Additions and revisions to the  
871 International Mineralogical Association's amphibole nomenclature. European Journal of  
872 Mineralogy, 16, 191-196.  
873
- 874 Lindsley, D.H. (1983) Pyroxene thermometry. American Mineralogist, 68, 477-493.  
875
- 876 Lindsley, D.H. (1986) Discussion of "A linear algebraic method for the calculation of pyroxene  
877 endmember components" by Dietrich and Petrakakis (Tschermaks Mineralogische und  
878 Petrographische Mitteilungen, 35, 275-282, 1986), Tschermaks Mineralogische und  
879 Petrographische Mitteilungen, 35, 283-285.

- 880 Lindsley, D.H., and Andersen, D.J. (1983) A two-pyroxene thermometer. *Journal of Geophysical*  
881 *Research*, 88, A887-A906.  
882
- 883 Malgarotto, C., Molin, G., and Zanazzi, P.F. (1993) Crystal chemistry of clinopyroxenes from  
884 Filicudi and Salina (Aeolian Islands, Italy). *Geothermometry and barometry. European*  
885 *Journal of Mineralogy*, 5, 915-923.  
886
- 887 McCallister, R.H., Finger, L.W., and Ohashi, Y. (1976) Intracrystalline Fe<sup>2+</sup>-Mg equilibria in three  
888 natural Ca-rich clinopyroxenes. *American Mineralogist*, 61, 671-676.  
889
- 890 McHone, J.G. (1987) PXC: an APL program for calculating pyroxene structural formulae and end  
891 members. *Computers & Geosciences*, 13, 89-91.
- 892 Mercier, J.-C.C., Benoit, V., and Girardeau, J. (1984) Equilibrium state of diopside-bearing  
893 harzburgites from ophiolites: geobarometric and geodynamic implications. *Contributions to*  
894 *Mineralogy and Petrology*, 85, 391-403.  
895
- 896 Molin, G., and Zanazzi, F. (1991) Intracrystalline Fe<sup>2+</sup>-Mg ordering in augite: Experimental study  
897 and geothermometric applications. *European Journal of Mineralogy*, 3, 863-875.  
898
- 899 Morimoto, N., Fabries, J., Ferguson, A.K., Ginzburg, I.V., Ross, M., Seifert, F.A., Zussman, J., Aoki,  
900 K., and Gottardi, G. (1988) Nomenclature of pyroxenes. *American Mineralogist*, 73, 1123-  
901 1133.
- 902 Nazzareni, S., Molin, G., Peccerillo, A., and Zanazzi, P.F. (1998) Structural and chemical  
903 variations in clinopyroxenes from the island of Alicudi (Aeolian arc) and their implications  
904 for conditions of crystallization. *European Journal of Mineralogy*, 10, 291-300.
- 905 Nickel, K.G., and Brey, G. (1984) Subsolidus orthopyroxene-clinopyroxene systematics in the  
906 system CaO-MgO-SiO<sub>2</sub> to 60 kb: a reevaluation of the regular solution model. *Contributions*  
907 *to Mineralogy and Petrology*, 87, 35-42.
- 908 Nickel, K.G., Brey, G.P., and Kogarko, L. (1985) Orthopyroxene-clinopyroxene equilibria in the  
909 system CaO-MgO-Al<sub>2</sub>O<sub>3</sub>-SiO<sub>2</sub> (CMAS): new experimental results and implications for two-  
910 pyroxene thermometry. *Contributions to Mineralogy and Petrology*, 91, 44-53.
- 911 Nickel, E.H., and Mandarino, J.A. (1987) Procedures involving the IMA Commission on New  
912 Minerals and Mineral Names, and guidelines on mineral nomenclature. *Canadian*  
913 *Mineralogist*, 25, 353-377.
- 914 Nimis, P. (1995) A clinopyroxene geobarometer for basaltic systems based on crystal-structure  
915 modeling. *Contributions to Mineralogy and Petrology*, 121, 44-125.

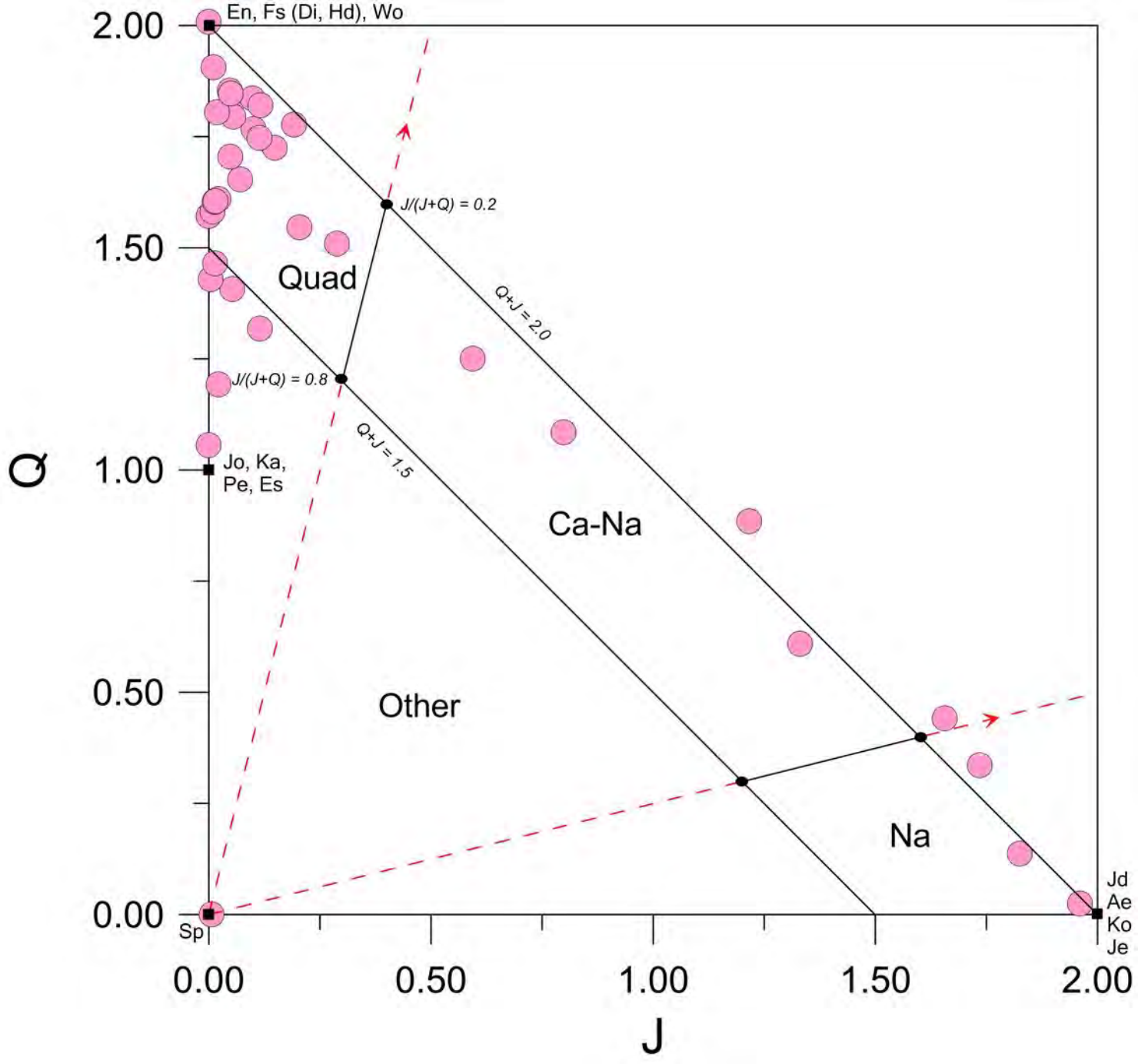
- 916 Nimis, P. (1999) Clinopyroxene geobarometry of magmatic rocks. Part 2. Structural  
917 geobarometers for basic to acid, tholeiitic and mildly alkaline magmatic systems,  
918 Contributions to Mineralogy and Petrology, 135, 62-74.
- 919 Nimis, P. (2000) CpxBar-Excel program: Clinopyroxene geobarometers for magmatic systems:  
920 Loadable from <http://www.dmp.unipd.it/Nimis/cpxbar3ex.zip>
- 921 Nimis, P, and Grütter, H. (2010) Internally consistent geothermobarometers for garnet  
922 peridotites and pyroxenites. Contributions to Mineralogy and Petrology, 159, 411-427.
- 923 Nimis, P., and Ulmer, P. (1998), Clinopyroxene geobarometry of magmatic rocks Part 1: An  
924 expanded structural geobarometer for anhydrous and hydrous, basic and ultrabasic  
925 systems. Contributions to Mineralogy and Petrology, 133, 122-135.
- 926 Nimis, P., and Taylor, W.R. (2000) Single clinopyroxene thermobarometry for garnet peridotites.  
927 Part I. Calibration and testing of a Cr-in-Cpx barometer and an enstatite-in-Cpx  
928 thermometer. Contributions to Mineralogy and Petrology, 139, 541-554.
- 929 Papike, J.J., Cameron, K.L., and Baldwin, K. (1974) Amphiboles and pyroxenes: characterization  
930 of other than quadrilateral components and estimates of ferric iron from microprobe data,  
931 Geological Society of America Abstract Program, 6, p. 1053-1054.  
932
- 933 Pasqual, D., Molin, G., and Zanazzi, P.F. (1995) Crystal chemistry of Stromboli clinopyroxene: a  
934 comparison with analogues from other Aeolian Islands (Italy). European Journal of  
935 Mineralogy, 7, 369-378.  
936
- 937 Petrakakis, K., and Dietrich, H. (1985) MINSORT: A program for the processing and archivation  
938 of microprobe analyses of silicate and oxide minerals. Neues Jahrbuch für Mineralogie, 74,  
939 379-384.
- 940 Poldervaart, A., and Hess, H.H. (1951) Pyroxenes in the crystallization of basaltic magmas.  
941 Journal of Geology, 59, 472-489.
- 942 Powel, R. (1985) Regression diagnostics and robust regression in  
943 geothermometer/geobarometer calibration: the garnet-clinopyroxene geothermometer  
944 revisited. Journal of Metamorphic Geology, 3, 231-243.
- 945 Putirka, K. (1999) Clinopyroxene + liquid equilibria to 100 kbar and 2450 K. Contributions to  
946 Mineralogy and Petrology, 135, 151-163.
- 947 Putirka, K.D. (2008) Thermometers and Barometers for volcanic systems. In K.D. Putirka, and  
948 F.J., Tepley III, Eds. Minerals, inclusions and volcanic processes, 69, p. 61-142. Reviews in  
949 Mineralogy and Petrology, Mineralogical Society of America, Chantilly, Virginia.

- 950 Putirka, K., Johnson, M., Kinzler, R., Longhi, J., and Walker, D. (1996) Thermobarometry of mafic  
951 igneous rocks based on clinopyroxene-liquid equilibria, 0-30 kbar. Contributions to  
952 Mineralogy and Petrology, 123, 92-108.
- 953 Putirka, K.D., Mikaelian, H., Ryerson, F., and Shaw, H. (2003) New clinopyroxene-liquid  
954 thermobarometers for mafic, evolved, and volatile-bearing lava compositions, with  
955 applications to lavas from Tibet and Snake River Plain, Idaho. American Mineralogist, 88,  
956 1542-1554.
- 957 Ravna, E.J.K., and Paquin, J. (2003) Thermobarometric methodologies applicable to eclogites  
958 and garnet ultrabasites. EMU Notes in Mineralogy, 8, 229-259.
- 959 Rock, N.M.S. (1990) The International Mineralogical Association (IMA/CNMMN) pyroxene  
960 nomenclature scheme: computerization and its consequences. Mineralogy and Petrology,  
961 43, 99-119.  
962
- 963 Russell, J. (2012) Inno Setup program: Loadable from <http://www.jrsoftware.org/isdl.php>.
- 964
- 965 Sachtleben, T., and Seck, H.A. (1981) Chemical control on of Al-solubility in orthopyroxene and  
966 its implications for pyroxene geothermometry. Contributions to Mineralogy and Petrology,  
967 78, 157-165.
- 968 Sen, G., and Jones, R. (1989) Experimental equilibration of multicomponent pyroxenes in the  
969 spinel peridotite field: implications for practical thermometers and a possible barometer.  
970 Journal of Geophysical Research, 94, 17871-17880.  
971
- 972 Siivola, J., and Schmid, R. (2007) List of mineral abbreviations, Recommendations by the IUGS  
973 Subcommittee on the systematics of metamorphic rocks, Web version 01.02.07,  
974 [www.bgs.ac.uk/scmr/home.html](http://www.bgs.ac.uk/scmr/home.html).
- 975 Soto, J.I., and Soto, V.M. (1995) Ptmafic: Software package for thermometry, barometry, and  
976 activity calculations in mafic rocks using an IBM-compatible computer. Computers &  
977 Geosciences, 21, 619-652.
- 978 Sturm, R. (2002) PX-NOM- an interactive spreadsheet program for the computation of pyroxene  
979 analyses derived from the electron microprobe. Computers & Geosciences, 28, 473-483.
- 980 Taylor, W.R. (1998) An experimental test of some geothermometer and geobarometer  
981 formulations for upper mantle peridotites with application to the thermobarometry of  
982 fertile lherzolite and garnet websterite. Neues Jahrbuch für Mineralogie- Abhandlungen,  
983 172, 381-408.

- 984 Yavuz, F. (1999) A revised program for microprobe-derived amphibole analyses using the IMA  
985 rules. *Computers & Geosciences*, 25, 909–927.
- 986 Yavuz, F. (2001) PYROX: A computer program for the IMA pyroxene classification and  
987 calculation scheme. *Computers & Geosciences*, 27, 97-107.
- 988 Yavuz, F. (2007) WinAmphcal: A Windows program for the IMA-04 amphibole classification.  
989 *Geochemistry Geophysics Geosystems*, 8, 1-12.
- 990 Yoder, H.S., Jr., and Tilley, C.E. (1962) Origin of basalt magmas: An experimental study of  
991 natural and synthetic rock systems. *Journal of Petrology*, 3, 342-532.
- 992 Wells, P.R.A. (1977) Pyroxene thermometry in simple and complex systems, *Contributions to*  
993 *Mineralogy and Petrology*, 62, 129-139.
- 994 Whitney, D.L., and Evans, B.W. (2010) Abbreviations for names of rock-forming minerals.  
995 *American Mineralogist*, 95, 185-187.
- 996 Wood, B.J., and S. Banno (1973) Garnet-orthopyroxene and orthopyroxene-clinopyroxene  
997 relationships in simple and complex systems. *Contributions to Mineralogy and Petrology*, 42,  
998 109-124.
- 999 Wood, B.J., and Fraser, D.G. (1978) *Elementary thermodynamics for geologists*, Oxford  
1000 University Press, 303p., Oxford.
- 1001
- 1002
- 1003
- 1004
- 1005
- 1006
- 1007
- 1008
- 1009
- 1010

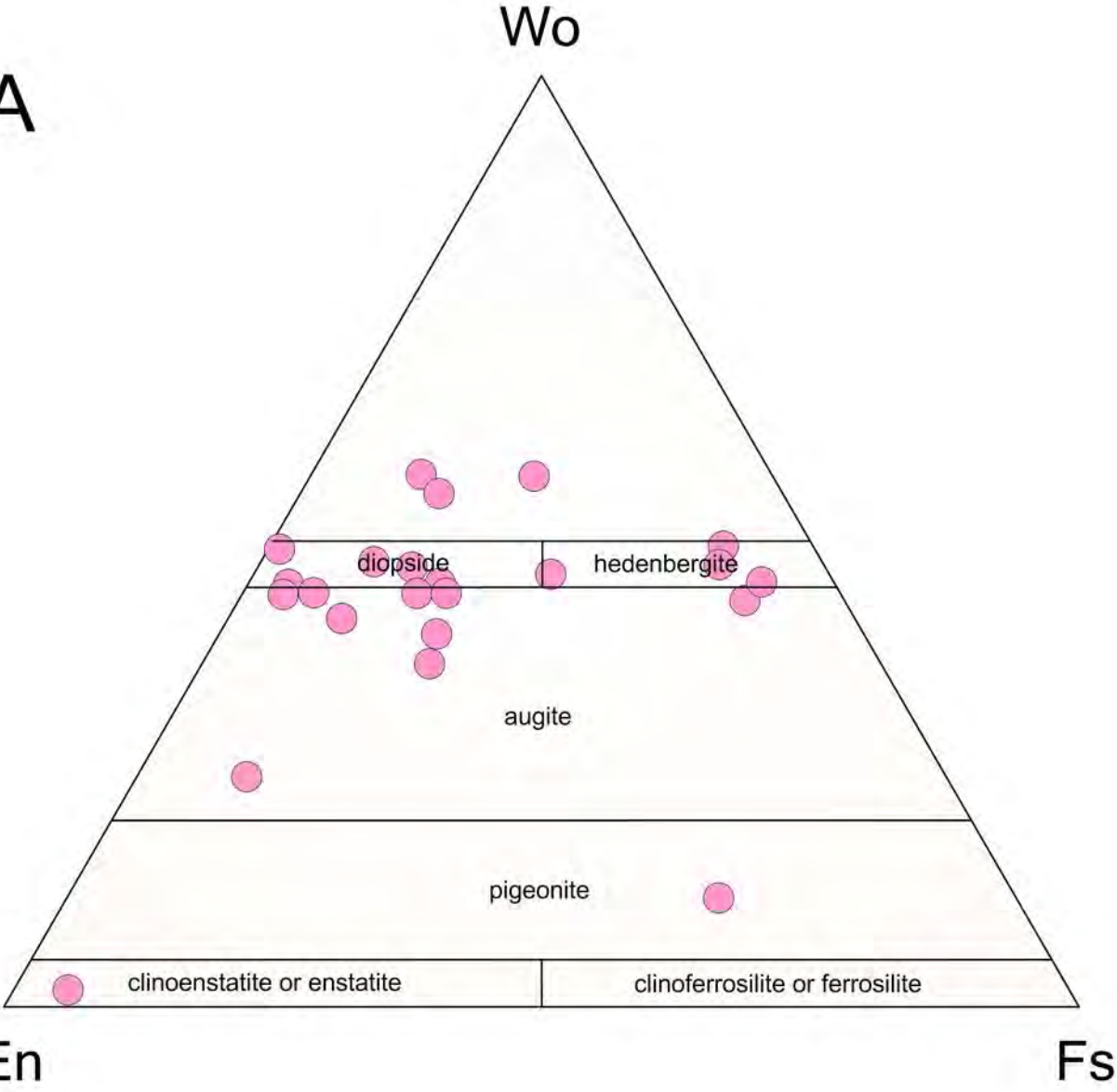
1011 **Figure List**

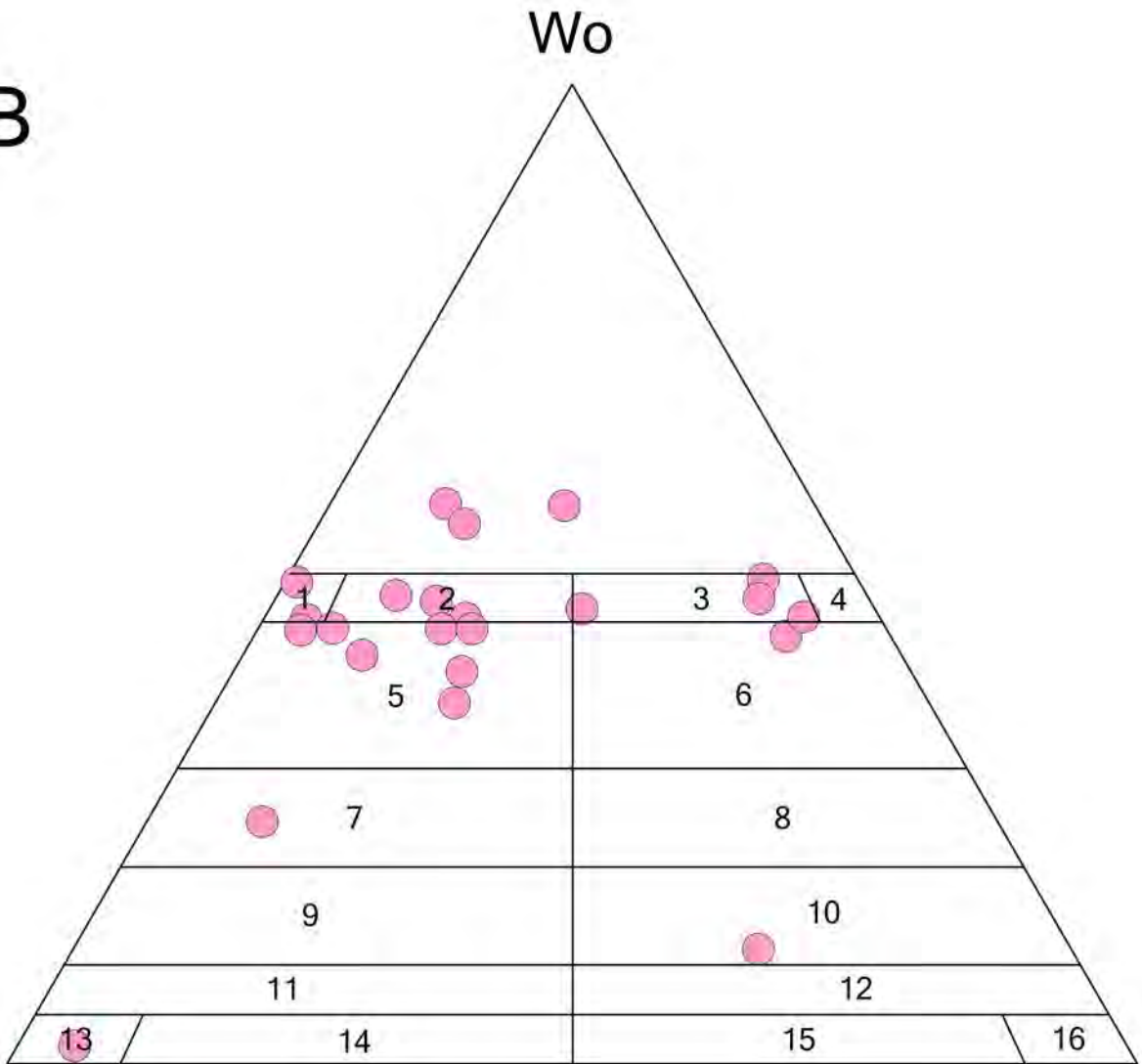
- 1012 Figure 1. The *Q-J* diagram used for classification of pyroxenes (after Morimoto et al. 1988).  
1013 Data used in this figure are taken from Rock (1990).
- 1014 Figure 2. (a) Plot of Ca-Mg-Fe pyroxenes in the Wo-En-Fs ternary diagram (after Morimoto et  
1015 al. 1988). (b) Classification of Ca-Mg-Fe pyroxenes in the Wo-En-Fs ternary diagram  
1016 (after Rock 1990). Data used in these figures are taken from Rock (1990).
- 1017 Figure 3. (a) Plot of Ca-Na and Na pyroxenes in the Q-Jd-Ae ternary diagram [after Morimoto  
1018 et al. 1988]. (b) Classification of Ca-Na and Na pyroxenes in the Q-Jd-Ae ternary  
1019 diagram (after Rock 1990). Data used in these figures are taken from Rock (1990).
- 1020 Figure 4. (a) Screenshot of the WinPyrox *Data Entry Screen* showing data edits of pyroxene  
1021 analyses. (b) *Calculation Screen* window for WinPyrox program displaying results of  
1022 estimated pyroxene analyses.
- 1023 Figure 5. (a) Classification of clinopyroxenes in the system  $\text{CaMgSi}_2\text{O}_6$ - $\text{CaFeSi}_2\text{O}_6$ - $\text{Mg}_2\text{Si}_2\text{O}_6$ -  
1024  $\text{Fe}_2\text{Si}_2\text{O}_6$  (after Poldervaart and Hess 1951). (b) Plot of clinopyroxenes in the Ti-Na-  
1025  $\text{Al}^{\text{IV}}$  (*apfu*) ternary diagram (after Papike et al. 1974). Data used in these figures are  
1026 taken from Putirka (2008).
- 1027 Figure 6. Comparison of single-clinopyroxene barometers (kbar) of (a) BA = anhydrous melts  
1028 from basalt through trachybasalt, basanite, tephrite to low-alkali nephelinites (after  
1029 Nimis and Ulmer 1998), (b) BH = hydrous melts from basalt through trachybasalt,  
1030 basanite, tephrite to low-alkali nephelinites (after Nimis and Ulmer 1998), (c) TH =  
1031 tholeiitic series from basalt to dacite (after Nimis 1999), (d) MA = mildly alkaline  
1032 series from alkali basalt to trachyandesite, including mildly alkaline and transitional  
1033 melts of the shoshonitic series (after Nimis 1999). Data used in these figures are  
1034 taken from Putirka (2008).
- 1035
- 1036





A



**B****En****Fs**

- |                                       |  |
|---------------------------------------|--|
| 1 = Diopside                          | 9 = Calcian (magnesium-rich) Pigeonite |
| 2 = Ferroan diopside                  | 10 = Calcian (iron-rich) Pigeonite     |
| 3 = Magnesian hedenbergite            | 11 = (Magnesium-rich) Pigeonite        |
| 4 = Hedenbergite                      | 12 = (Iron-rich) Pigeonite             |
| 5 = [Magnesium-rich] Augite           | 13 = (Clino) Enstatite                 |
| 6 = [Iron-rich] Augite                | 14 = Ferroan (Clino) Enstatite         |
| 7 = [Subcalcic magnesium-rich] Augite | 15 = Magnesian Clino (Ferrosilite)     |
| 8 = [Subcalcic iron-rich] Augite      | 16 = (Clino) Ferrosilite               |

A

Q

Quad

omphacite

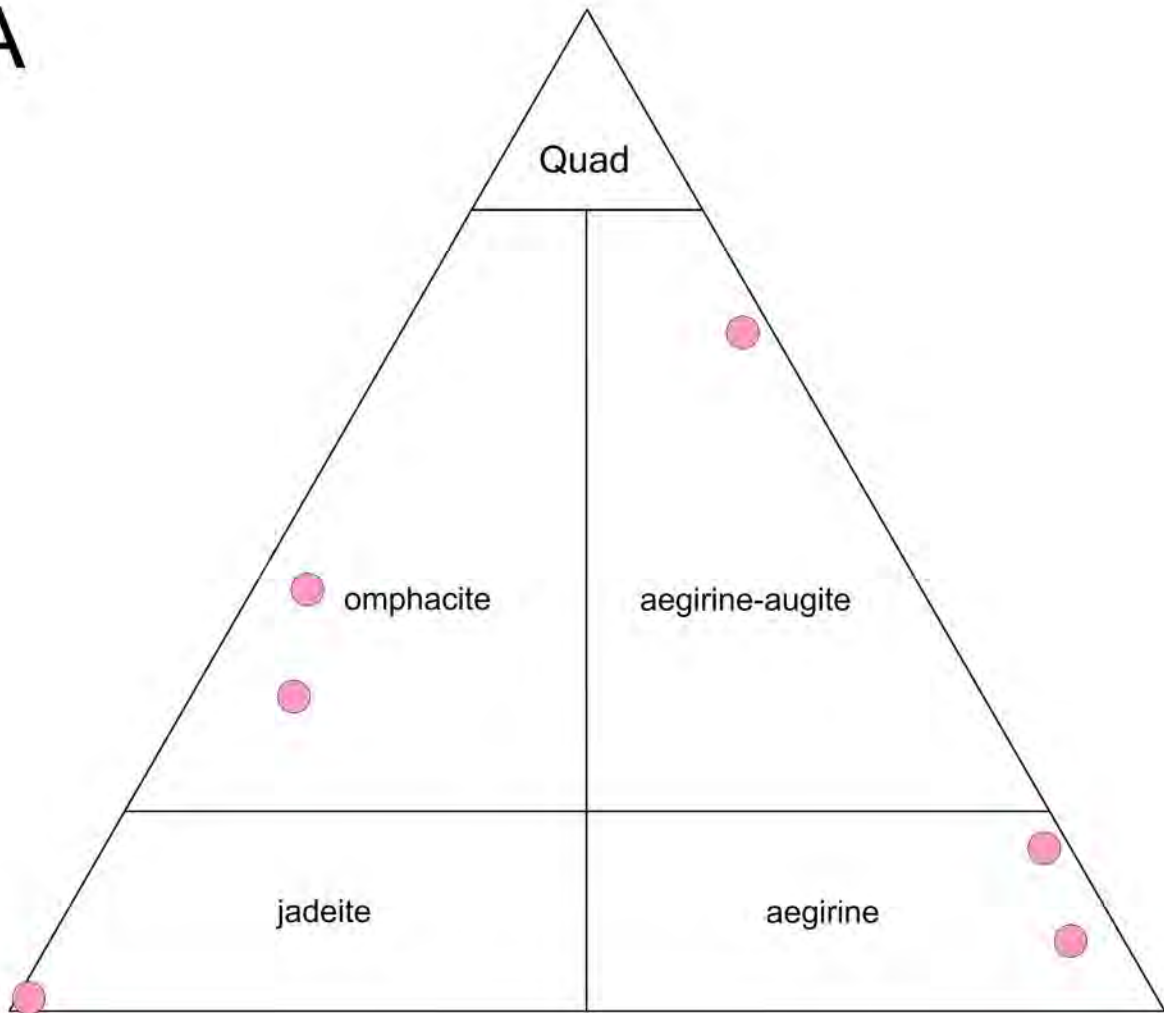
aegirine-augite

jadeite

aegirine

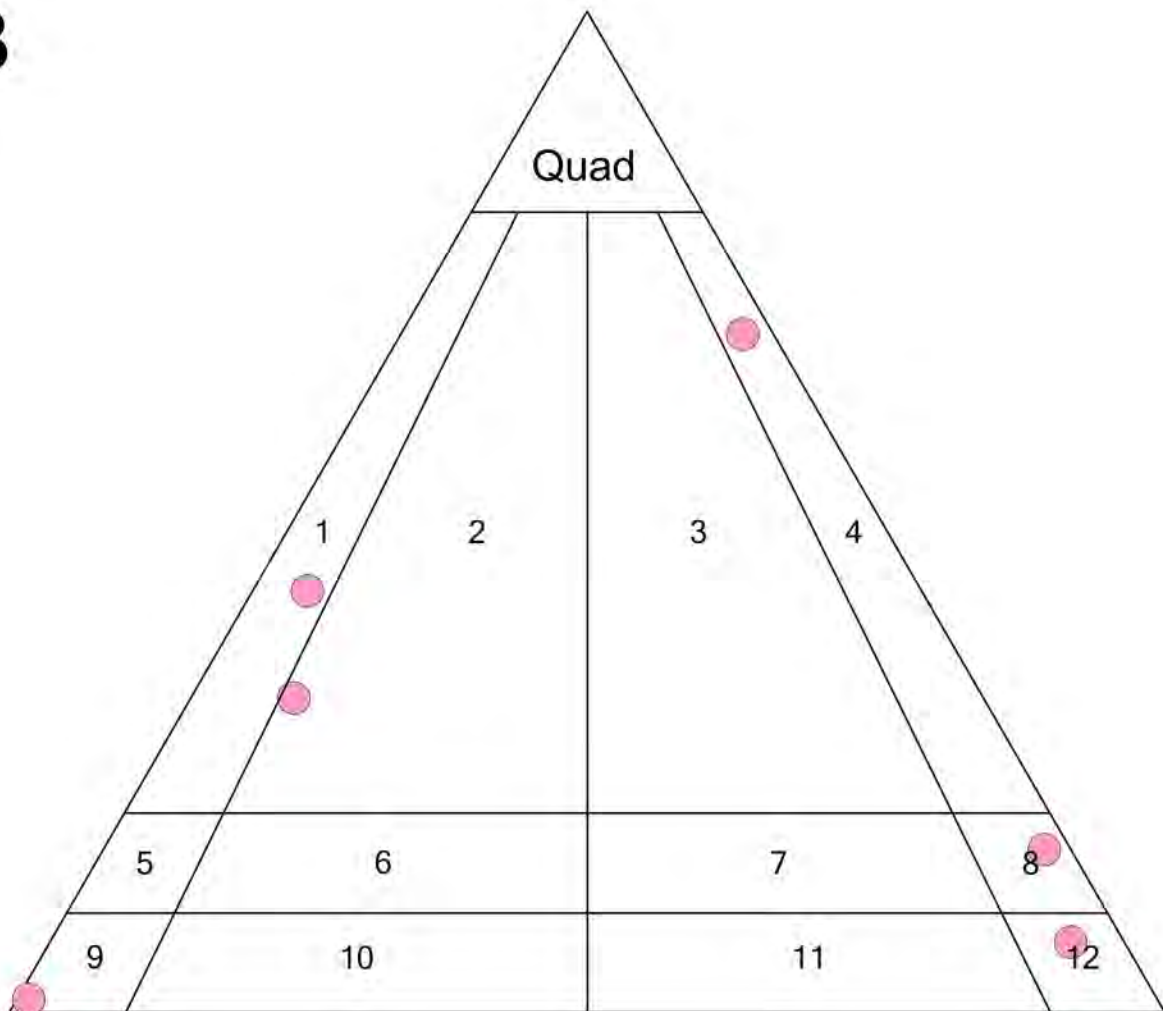
Jd

Ae



**B****Q**

Quad

**Jd****Ae**

- |                               |                                |
|-------------------------------|--------------------------------|
| 1 = Omphacite                 | 7 = Calcian aluminian aegirine |
| 2 = Ferrian omphacite         | 8 = Calcian aegirine           |
| 3 = Aluminian aegirine-augite | 9 = Jadeite                    |
| 4 = Aegirine-augite           | 10 = Ferrian jadeite           |
| 5 = Calcian jadeite           | 11 = Aluminian aegirine        |
| 6 = Calcian ferrian jadeite   | 12 = Aegirine                  |





A

*A Windows Program for Pyroxene Calculation Classification (IMA-1988) and Thermobarometry*

*Data Entry Screen*

Row No	Sample	SiO2 [c]	TiO2 [c]	Al2O3 [c]	V2O3 [c]	Cr2O3 [c]	Fe2O3 [c]	FeO [c]	MnO [c]	NiO [c]	CoO [c]	ZnO [c]	MgO [c]	CaO [c]	Na2O [c]	K2O [c]	ZrO2 [c]	Sc2O3 [c]	Li2O [c]		
1	clino1	52.3	0.7	3		0.58		5.1	0.11				16.6	21.5	0.33						
2	clino2	51.7	0.28	8.38		0.05		6.69	0.15				21.4	11.7	0.64						
3	clino3	51.5	0.45	8.1		0.09		6.96	0.17				20.3	12.6	0.56						
4	clino4	51.06	0.62	3.16		0.01		6.18	0.12				15.78	20.82	0.27						
5	clino5	53.32	0.48	2.25		0.12		5.92	0.15				16.91	20.73	0.28						
6	clino6	51.58		7.28		1.2		3.75					19.55	15.94	0.7						
7	clino7	51.12	0.1	8.07		1.16		3.57					17.95	17.26	0.77						
8	clino8	52.5		5.19		1.45		4.12					21.28	15.45							
9	clino9	51.8	0.17	5.1		1.58		4.6	0.19				21.5	14.9	0.21						
10	clino10	51.67	0.16	5.62		1.56		4.45	0.16				21.82	14.34	0.22						
11	clino11	53	0.11	4.5		1.5		5.1	0.2				24.7	10.9	0.16						
12	clino12	51.64	0.38	8.16		0.75		3.97					19.66	14.85	0.66						
13	clino13	51.3	0.19	7.2		0.5		3.9	0.09				17.6	19.1	0.5						
14	clino14	52.4	0.14	6		0.9		4.1	0.08				19.4	17.6	0.49						
15	clino15	52	0.14	9.39		0.09		4.89	0.06				20.8	13.3	0.69						
16	clino16	52.9	0.35	7.4		0.12		5.2	0.17				23.1	11.6	0.55						
17	clino17	51.3	0.53	9.15		0.08		7.15	0.19				20.6	10.8	0.93						
18	clino18	51.5	0.49	8.97		0.08		6.53	0.18				20.09	11.1	0.74						
19	clino19	50.93	0.81	9.02		0.34		5.82					18.51	13.34	1.23						
20	clino20	51.63	0.4	8.59		0.29		6.96					21.39	9.76	0.97						
21	clino21	51.39	0.83	9.38		0.15		7.57					19.55	9.49	1.64						
22	clino22	54.68		2.65		1.76		4.39	0.12				26.41	9.15	0.09						
23	clino23	52.98	0.14	5.04		1.36		3.48	0.11				19.61	17.76	0.23						
24	clino24	53.77	0.11	4.31		1.51		3.6	0.11				20.51	16.95	0.23						
25																					





B

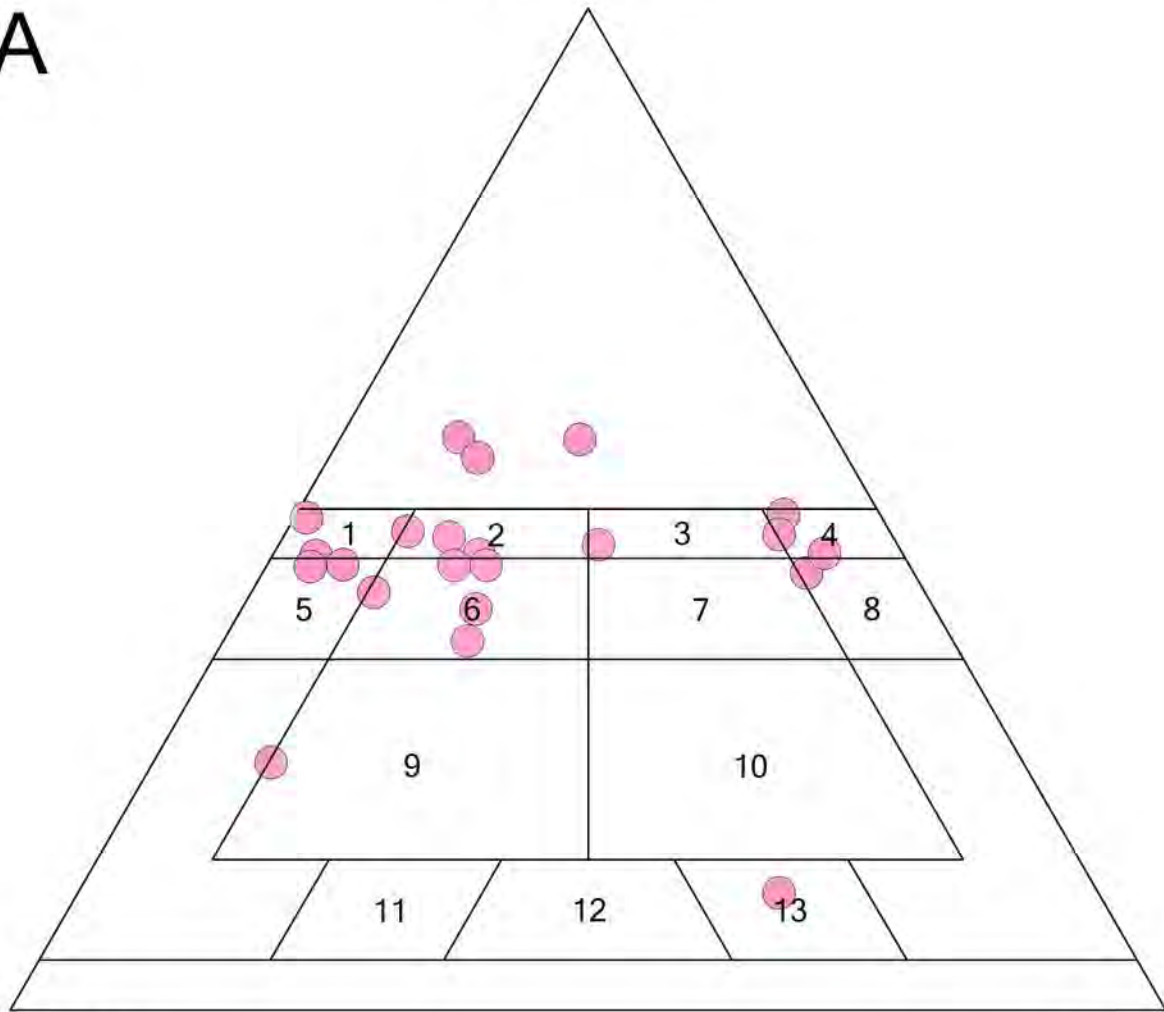
*A Windows Program for Pyroxene Calculation Classification (IMA-1988) and Thermobarometry*

*Calculation Screen*

	113	114	115	116	117	118	119	120	121	122	123	124	125	126	127
Sample	[PN95-BS]	PNU98-BA	PNU98-BH	PN99-TH	PN99-MA	PNT00	'08Eq32a](kd	[TBM85/86	TNT00	TP08Eq32d	TDN82	TMZ91](oC)	[Pyx. Group	Pyx. Name]	[Modifiers]
dino1	1.31	1.22		21.89	24.97	0.35		1156	993	1202	879	900	Ca-Mg-Fe p	AUGITE	Aluminian Chromian
dino2	15.94	17.62	11.79	18.52	22.93	14.54	15.45	1476	1357	1325	648	875	Ca-Mg-Fe p	AUGITE	Aluminian
dino3	14.81	16.25	15.24	15.57	20.10	17.28	16.18	1461	1333	1313	677	877	Ca-Mg-Fe p	AUGITE	Aluminian
dino4	1.03	0.94	12.95	11.22	15.22		4.39	1161	998	1171	873	899	Ca-Mg-Fe p	AUGITE	Aluminian
dino5	0.90	0.87	11.00	8.85	12.34	20.46	2.91	1193	1052	1179	852	895	Ca-Mg-Fe p	AUGITE	
dino6	13.41	14.51	12.47	9.46	12.10	25.19	17.48	1405	1312	1345	810	890	Ca-Mg-Fe p	AUGITE	Aluminian Chromian
dino7	13.91	14.87	13.71	9.98	12.17	22.87	16.49	1371	1255	1335	850	896	Ca-Mg-Fe p	AUGITE	Aluminian Chromian
dino8	9.23	10.20	11.02	8.09	10.40	27.61	11.77	1404	1345	1295	711	879	Ca-Mg-Fe p	AUGITE	Aluminian Chromian
dino9	9.02	10.01	9.97	7.52	9.76	28.28	12.15	1414	1337	1298	720	880	Ca-Mg-Fe p	AUGITE	Aluminian Chromian
dino10	10.14	11.28	11.07	8.63	11.03	26.71	11.73	1423	1352	1300	703	879	Ca-Mg-Fe p	AUGITE	Aluminian Chromian
dino11	10.44	12.18	13.52	11.29	14.83	29.73	11.46	1474	1397	1298	390	865	Ca-Mg-Fe p	AUGITE	Aluminian Chromian
dino12	15.07	16.34	15.48	11.99	15.16	22.72	17.36	1428	1319	1329	782	887	Ca-Mg-Fe p	AUGITE	Aluminian Chromian
dino13	10.53	11.15	14.66	10.61	13.19	18.31	9.53	1310	1185	1302	867	899	Ca-Mg-Fe p	AUGITE	Aluminian Chromian
dino14	9.88	10.61	13.39	9.53	11.84	23.82	10.35	1363	1260	1310	822	891	Ca-Mg-Fe p	AUGITE	Aluminian Chromian
dino15	17.45	19.09	16.33	12.21	14.99	19.29	21.75	1462	1376	1371	728	881	Ca-Mg-Fe p	AUGITE	Aluminian
dino16	14.98	16.77	18.81	14.58	18.35	19.24	15.15	1481	1386	1342	589	872	Ca-Mg-Fe p	AUGITE	Aluminian
dino17	18.01	19.81	22.40	17.33	21.85	14.95	16.31	1490	1342	1321	655	876	Ca-Mg-Fe p	AUGITE	Aluminian
dino18	17.94	19.69	23.43	17.87	22.82	15.61	16.60	1487	1337	1315	663	877	Ca-Mg-Fe p	AUGITE	Aluminian
dino19	17.45	18.87	23.55	17.42	22.07	18.51	17.31	1448	1280	1307	785	887	Ca-Mg-Fe p	AUGITE	Aluminian
dino20	18.34	20.35	23.32	17.58	22.66	22.82	21.31	1513	1372	1358	576	872	Ca-Mg-Fe p	AUGITE	Aluminian
dino21	20.86	22.86		20.02	25.45	18.95	21.14	1517	1317	1340	678	878	Ca-Mg-Fe p	AUGITE	Aluminian Sodian
dino22	9.76	11.81	18.08	15.39	21.29	37.04	14.12	1501	1407	1295		857	Ca-Mg-Fe p	PIGEONITE	Aluminian Calcian Chromian Ferroan Magnesian
dino23	8.41	9.06	13.01	9.89	13.91	27.00	9.73	1355	1269	1289	806	889	Ca-Mg-Fe p	AUGITE	Aluminian Chromian
dino24	8.06	8.78	9.78	7.16	10.05	30.12	11.17	1379	1295	1290	773	885	Ca-Mg-Fe p	AUGITE	Aluminian Chromian

A

$\text{CaSiO}_3$   
wollastonite



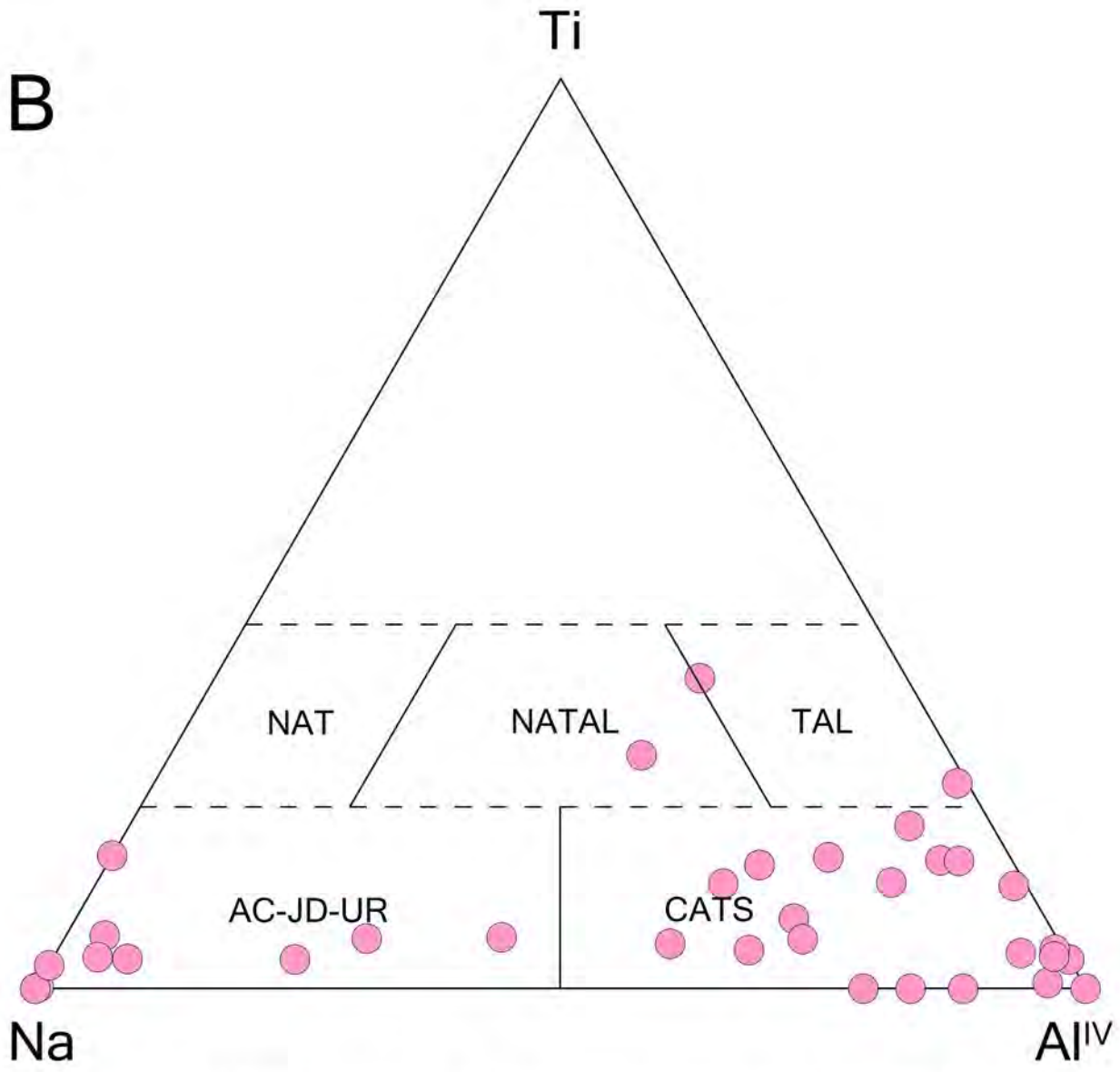
$\text{MgSiO}_3$   
clinoenstatite

$\text{FeSiO}_3$   
clinoferrosilite

- |                  |                             |
|------------------|-----------------------------|
| 1 = Diopside     | 8 = Ferrohedenbergite       |
| 2 = Salite       | 9 = Subcalcic augite        |
| 3 = Ferrosalite  | 10 = Subcalcic ferroaugite  |
| 4 = Hedenbergite | 11 = Magnesium pigeonite    |
| 5 = Endiopside   | 12 = Intermediate pigeonite |
| 6 = Augite       | 13 = Ferriferous pigeonite  |
| 7 = Ferroaugite  |                             |

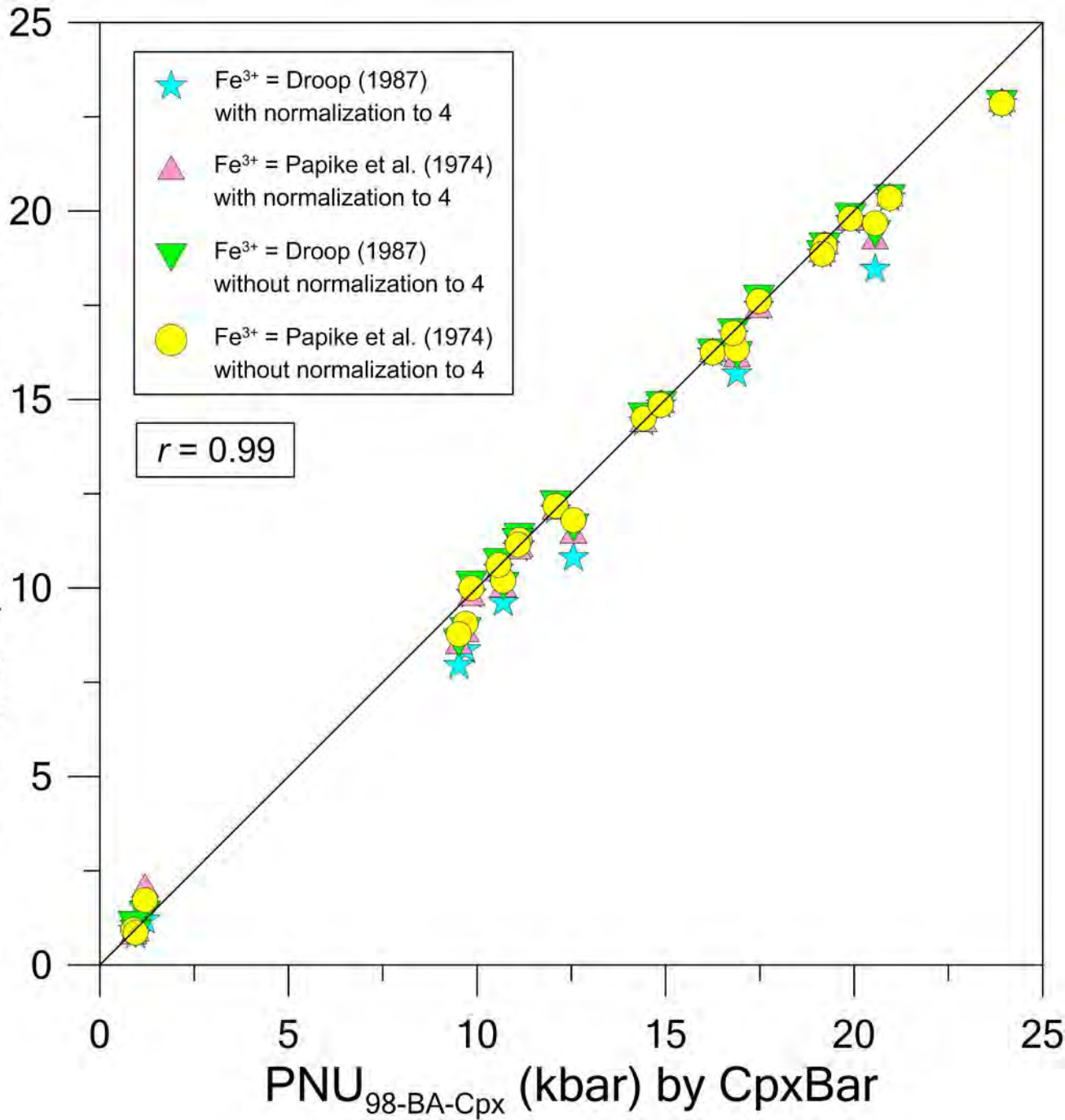


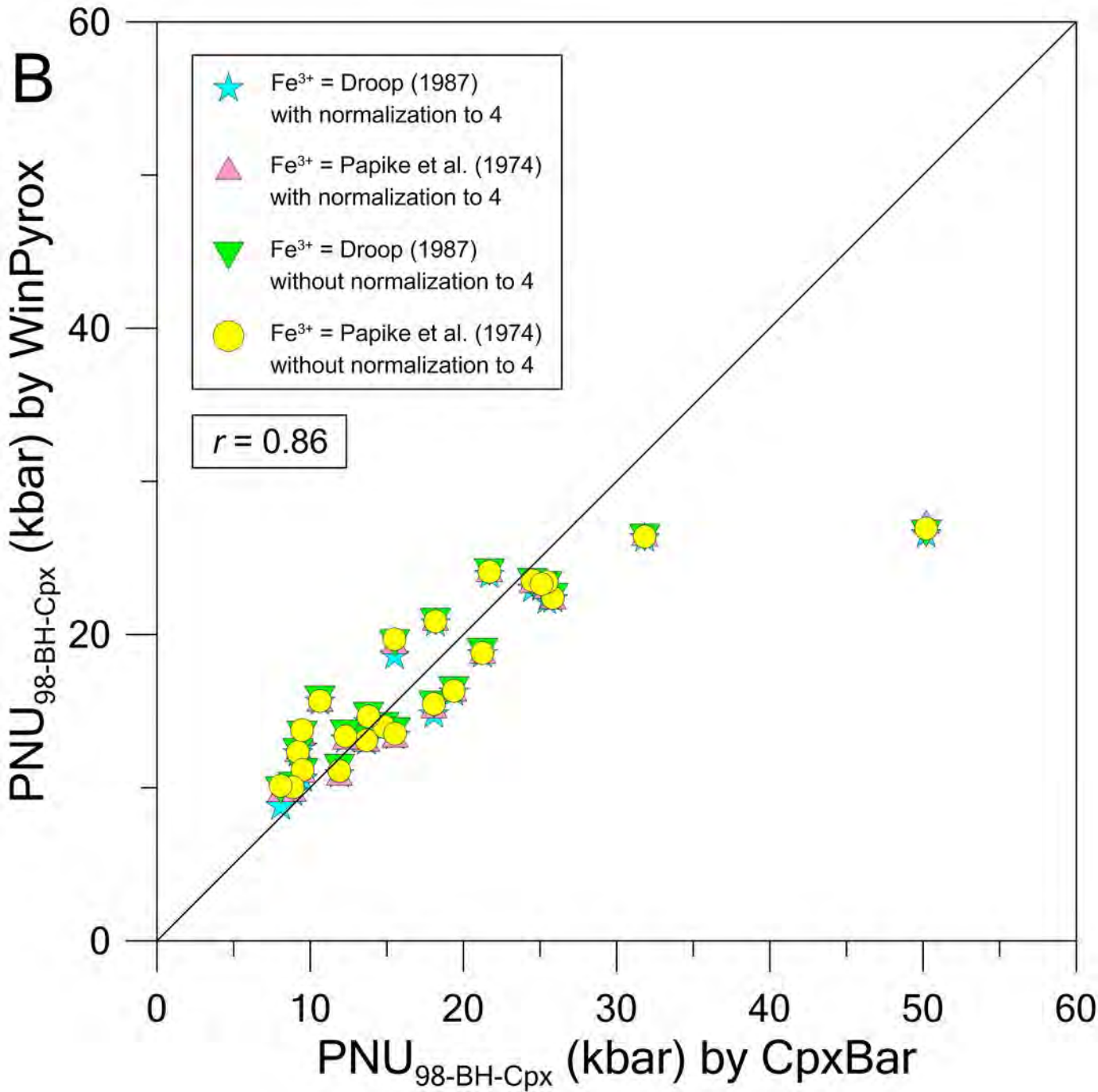
B

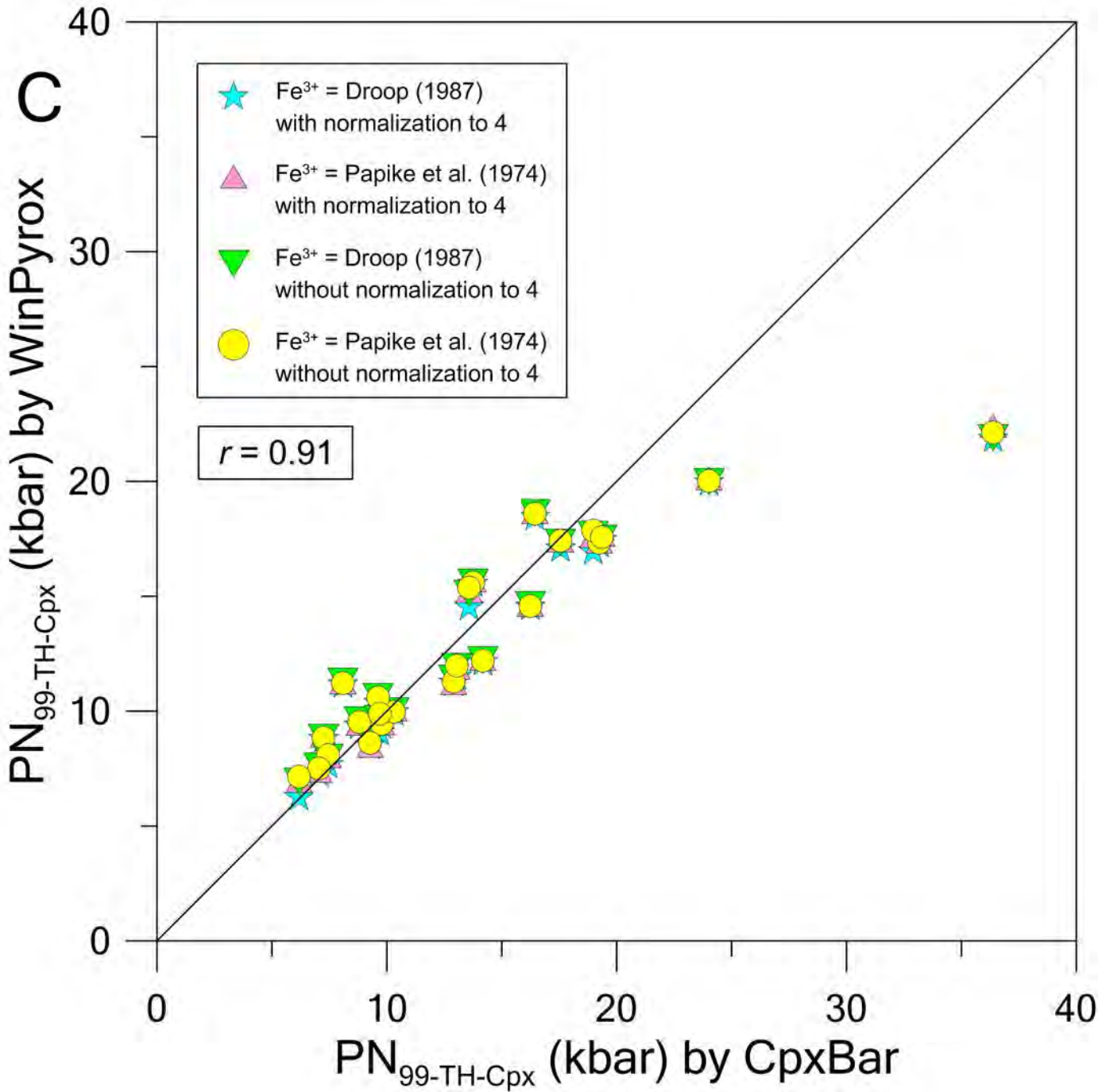


NAT	= $\text{NaTi}_{0.5}\text{R}^{2+}_{0.5}\text{Si}_2\text{O}_6$	NATAL	= $\text{NaTiSiAlO}_6$
TAL	= $\text{CaTiAl}_2\text{O}_6$	AC	= $\text{NaFeSi}_2\text{O}_6$
JD	= $\text{NaAlSi}_2\text{O}_6$	UR	= $\text{NaCrSi}_2\text{O}_6$
CATS	= $\text{CaAlAlSiO}_6$ and $\text{CaFeAlSiO}_6$		



**A****PNU<sub>98-BA-Cpx</sub> (kbar) by WinPyrox**





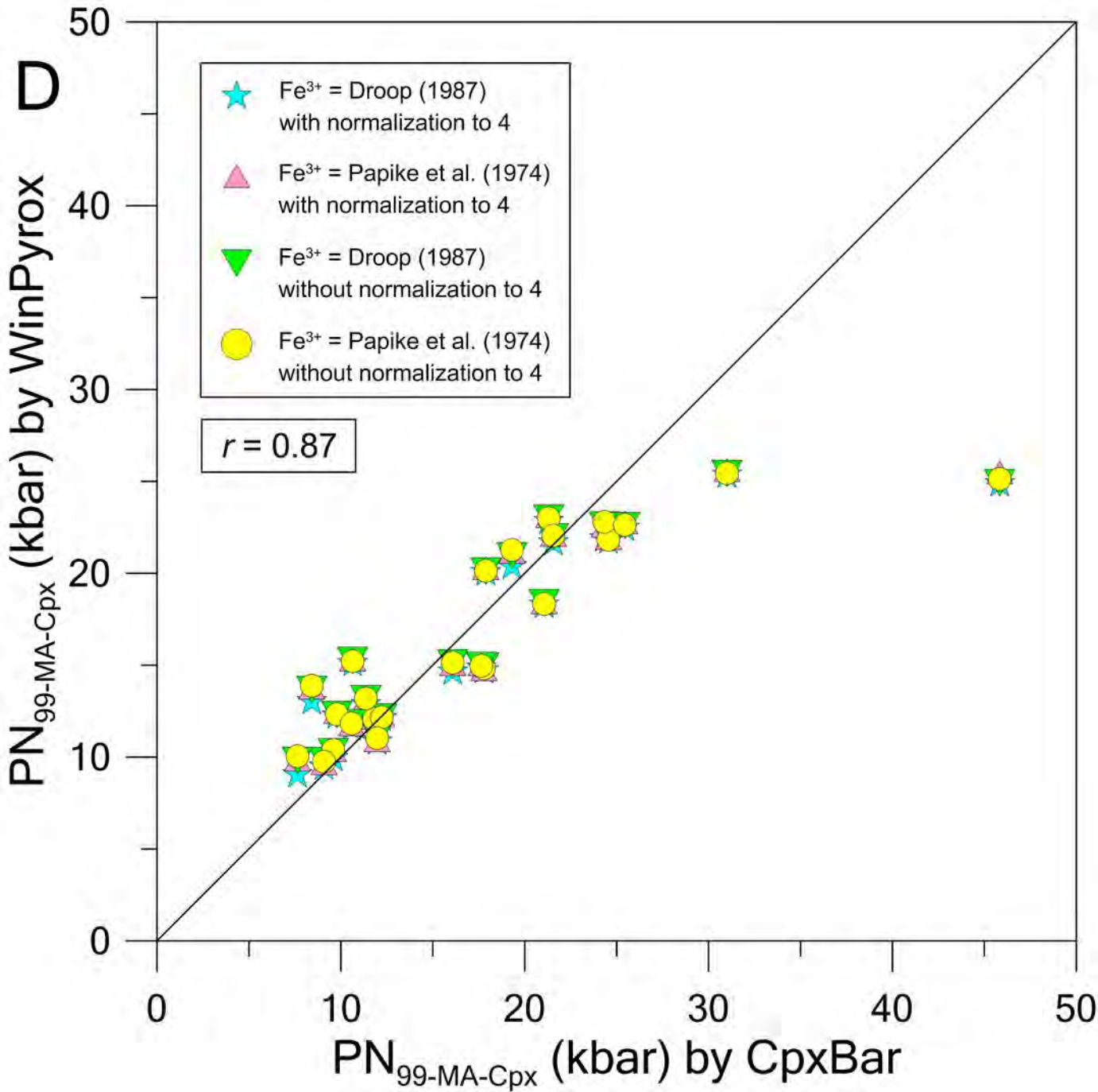


Table 1. IMA-accepted pyroxene mineral names and their chemical subdivisions (from Morimoto et al. 1988)

Mineral Names	Composition as End-member	Main Composition as Solid Solution	Space Group
<i>I. Mg-Fe Pyroxenes</i>			
1 Enstatite (En) <sup>1</sup>	Mg <sub>2</sub> Si <sub>2</sub> O <sub>6</sub>	(Mg, Fe) <sub>2</sub> Si <sub>2</sub> O <sub>6</sub>	<u>Pbca</u>
2 Ferrosilite (Fs) <sup>2</sup>	Fe <sup>2+</sup> <sub>2</sub> Si <sub>2</sub> O <sub>6</sub>		
3 Clinoenstatite		(Mg, Fe) <sub>2</sub> Si <sub>2</sub> O <sub>6</sub>	<u>P2<sub>1</sub>/c</u>
4 Clinoferrosilite			
5 Pigeonite			
<i>II. Mn-Mg Pyroxenes</i>			
6 Donpeacorite		(Mn, Mg)MgSi <sub>2</sub> O <sub>6</sub>	<u>Pbca</u>
7 Kanoite (Ka) <sup>3</sup>	MnMgSi <sub>2</sub> O <sub>6</sub>	(Mn, Mg)MgSi <sub>2</sub> O <sub>6</sub>	<u>P2<sub>1</sub>/c</u>
<i>III. Ca Pyroxenes</i>			
8 Diopside (Di) <sup>4</sup>	CaMgSi <sub>2</sub> O <sub>6</sub>	Ca(Mg, Fe)Si <sub>2</sub> O <sub>6</sub>	<u>C2/c</u>
9 Hedenbergite (Hd) <sup>5</sup>	CaFe <sup>2+</sup> Si <sub>2</sub> O <sub>6</sub>		
10 Augite		(Ca, Mg, Fe) <sub>2</sub> Si <sub>2</sub> O <sub>6</sub>	<u>C2/c</u>
11 Johannsenite (Jo) <sup>6</sup>	CaMnSi <sub>2</sub> O <sub>6</sub>		
12 Petedunnite (Pe) <sup>7</sup>	CaZnSi <sub>2</sub> O <sub>6</sub>		
13 Esseneite (Es) <sup>8</sup>	CaFe <sup>3+</sup> AlSiO <sub>6</sub>		<u>C2/c</u>
<i>IV. Ca-Na Pyroxenes</i>			
14 Omphacite		(Ca,Na) (R <sup>2+</sup> , Al)Si <sub>2</sub> O <sub>6</sub>	<u>C2/c</u> , <u>P2/n</u>
15 Aegirine-augite		(Ca,Na) (R <sup>2+</sup> , Fe <sup>3+</sup> )Si <sub>2</sub> O <sub>6</sub>	<u>C2/c</u>
<i>V. Na Pyroxenes</i>			
16 Jadeite (Jd) <sup>9</sup>	NaAlSi <sub>2</sub> O <sub>6</sub>	Na(Al, Fe <sup>3+</sup> )Si <sub>2</sub> O <sub>6</sub>	<u>C2/c</u>
17 Aegirine (Ae) <sup>10</sup>	NaFe <sup>3+</sup> Si <sub>2</sub> O <sub>6</sub>		
18 Kosmochlor (Ko) <sup>11</sup>	NaCr <sup>3+</sup> Si <sub>2</sub> O <sub>6</sub>		<u>C2/c</u>
19 Jervisite (Je) <sup>12</sup>	NaSc <sup>3+</sup> Si <sub>2</sub> O <sub>6</sub>		<u>C2/c</u>
<i>VI. Li Pyroxene</i>			
20 Spodumene (Sp) <sup>13</sup>	LiAlSi <sub>2</sub> O <sub>6</sub>		<u>C2/c</u>

Notes : Superscripts (from 1 to 13) in the column of mineral names show end-members.

Table 2. IMA-88 proposed pyroxene groups with their mineral subdivisions (from Morimoto et al. 1988)

Row	<i>I. Ca-Mg-Fe Pyroxenes (Quadrilateral or Quad)</i>	<i>II. Ca-Na Pyroxenes</i>	<i>III. Na Pyroxenes</i>	<i>IV. Other Pyroxenes</i>
1	Enstatite (En) <sup>a</sup>	Omphacite (Omp) <sup>a</sup>	Jadeite (Jd) <sup>a</sup>	Donpeacorite (Dpc) <sup>c</sup>
2	Ferrosilite (Fs) <sup>a</sup>	Aegirine-augite (Agt) <sup>b</sup>	Aegirine (Aeg) <sup>a</sup>	Kanoite (Ka) <sup>d</sup>
3	Clinoenstatite (Cen) <sup>a</sup>			Johannsenite (Jhn) <sup>a</sup>
4	Clinoferrosilite (Cfs) <sup>a</sup>			Petedunnite (Pe) <sup>d</sup>
5	Pigeonite (Pgt) <sup>a</sup>			Esseneite (Es) <sup>d</sup>
6	Diopside (Di) <sup>a</sup>			Spodumene (Spd) <sup>a</sup>
7	Hedenbergite (Hd) <sup>a</sup>			Kosmochlor (Kos) <sup>a</sup>
8	Augite (Aug) <sup>a</sup>			Jervisite (Je) <sup>d</sup>

Notes for abbreviations: (a) = from (Whitney and Evans 2010); (b) = from (Siivola and Schmid 2007); (c) = this study; (d) = from (Morimoto et al. 1988).

Table 3. Adjectival modifiers for pyroxene group minerals (revised from Morimoto et al. 1988)

Row	Cation	Content ( <i>apfu</i> )	Name	Applicable to
1	Al <sup>3+</sup>	> 0.10	Aluminian	All groups, except for jadeite and spodumene
2	Ca <sup>2+</sup>	> 0.10	Calcian	“Na” and “Other” groups, but excludes those species defined by the abundance of Ca <sup>2+</sup> (e.g., johannsenite, petedunnite, esseneite)
3	Cr <sup>3+</sup>	> 0.01	Chromian	All groups, except for kosmochlor
4	Fe <sup>2+</sup>	> 0.10	Ferroan	All groups, but excludes those species defined by the abundance of Fe <sup>2+</sup> (e.g., ferrosilite, hedenbergite, pigeonite)
5	Fe <sup>3+</sup>	> 0.10	Ferrian	All groups, but excludes those species defined by the abundance of Fe <sup>3+</sup> (e.g., esseneite, aegirine)
6	Li <sup>+</sup>	> 0.01	Lithian	All groups, but excludes those species defined by the abundance of Li <sup>+</sup> (e.g., spodumene)
7	Mg <sup>2+</sup>	> 0.10	Magnesian	All groups, but excludes those species defined by the abundance of Mg (e.g., enstatite, pigeonite, donpeacorite/kanoite, diopside, augite)
8	Mn <sup>2+</sup>	> 0.10	Manganoan	All groups, but excludes those species defined by the abundance of Mn <sup>2+</sup> (e.g., donpeacorite/kanoite, johannsenite)
9	Mn <sup>3+</sup>	> 0.01	Manganian	All groups, but excludes those species defined by the abundance of Mn <sup>3+</sup>
10	Na <sup>+</sup>	> 0.10	Sodian	“Ca-Mg-Fe” and “Other” groups, but excludes those species defined by the abundance of Na <sup>+</sup> (e.g., kosmochlor, jervisite)
11	Ni <sup>2+</sup>	> 0.01	Nickeloan	All groups
12	Si <sup>4+</sup>	< 1.75	Subsilicic	All groups, except for esseneite
13	Ti <sup>3+</sup>	> 0.01	Titanoan	All groups
14	Ti <sup>4+</sup>	> 0.10	Titanian	All groups
15	Zn <sup>2+</sup>	> 0.01	Zincian	All groups, except for petedunnite
16	Co <sup>2+</sup>	>0.01	Cobaltian <sup>(a)</sup>	All groups
17	V <sup>3+</sup>	> 0.01	Vanadoan <sup>(b)</sup>	All groups
18	Zr <sup>4+</sup>	> 0.01	Zirconian <sup>(b)</sup>	All groups
19	Sc <sup>3+</sup>	> 0.01	Scandian <sup>(b)</sup>	All groups, except for jervisite

Notes : (a) = In this study; (b) = Not given in the IMA report (Morimoto et al. 1988), but defined by Rock (1990).

Table 4. Description of column numbers in the *Calculation Screen* window of WinPyrox program

Row	Explanations	Column Numbers in the "Calculation Screen" of WinPyrox Program
1	Major oxide (wt%) clinopyroxene analyses	1-19
2	$P$ (kbar) and $T$ ( $^{\circ}\text{C}$ ) input for thermobarometry calculations	20-21
3	Recalculated cations in the $T$ , $M1$ , and $M2$ sites	22-47
4	End-member calculations	48-78
5	Fe <sup>2+</sup> -Mg partitioning	79-84
6	Molar fractions	85-91
7	Parameters used in estimating closure temperature	92-95
8	End-member activities	96-102
9	Components and activities	103-112
10	Single-clinopyroxene barometers	113-119
11	Single-clinopyroxene thermometers	120-124
12	Pyroxene classification parameters (e.g., groups, names, modifiers, and $Q$ - $J$ )	125-129
13	Checking of clinopyroxene into the quadrilateral for $P$ - $T$ estimations	130
14	Major oxide (wt%) orthopyroxene analyses	131-150
15	Recalculated cations in the $T$ , $M1$ , and $M2$ sites	151-176
16	End-member activities and components	177-186
17	Two-pyroxene barometers	187-190
18	Two-pyroxene thermometers	191-207
19	Single-orthopyroxene thermometers	208-209
20	Checking of orthopyroxene into the quadrilateral for $P$ - $T$ estimations	210



Table 5. Selected pyroxene analyses (wt%) with their structural formulae (*apfu*), end-members (%), Fe<sup>2+</sup>-Mg partitioning (*apfu*), molar fractions, and end-member activities calculated by WinPyrox program. Pyroxene analyses are taken from Rock (1990)

		S1	S2	S3	S4	S5	S6	S7	S8	S9	S10	S11	S12	S13	S14	S15	S16
1	SiO <sub>2</sub>	54.01	49.17	37.52	45.9	51.78	53.84	48.82	59.06	50.12	29.51	48.40	50.42	55.12	47.90	56.00	64.89
2	TiO <sub>2</sub>	0.03	0.68	5.72	1.4	0.38	3.71	0.43	0.08	1.14	0.99	0.00	0.55	0.00	0.00	0.00	0.00
3	Al <sub>2</sub> O <sub>3</sub>	3.95	1.42	14.29	5.9	5.14	7.91	2.60	24.62	2.57	17.95	1.20	0.42	0.23	0.00	0.00	26.74
4	V <sub>2</sub> O <sub>3</sub>	0.00	0.00	0.00	0.00	0.04	0.00	0.03	0.00	0.01	0.00	0.00	0.00	0.00	0.00	0.00	0.00
5	Cr <sub>2</sub> O <sub>3</sub>	0.57	0.00	0.11	0.00	0.95	0.00	0.00	0.00	0.00	0.00	0.00	0.00	0.00	0.00	22.6	0.00
6	Fe <sub>2</sub> O <sub>3</sub>	2.07	1.30	4.43	8.10	1.75	1.11	10.29	0.41	28.74	23.89	3.80	0.00	0.00	0.25	0.40	0.57
7	FeO	1.57	32.93	7.12	7.60	2.14	11.45	9.91	0.18	1.57	0.69	5.70	8.59	0.14	0.98	0.00	0.04
8	MnO	0.00	0.59	0.14	0.35	0.12	0.37	2.93	0.03	0.60	0.11	0.00	0.44	18.48	26.81	0.00	0.01
9	NiO	0.09	0.00	0.00	0.00	0.04	0.00	0.00	0.00	0.00	0.00	0.00	0.00	0.00	0.00	0.00	0.00
10	ZnO	0.00	0.00	0.00	0.00	0.00	0.00	0.00	0.00	0.00	0.00	12.60	0.00	0.00	0.00	0.00	0.00
11	MgO	35.65	8.87	6.72	8.00	16.04	3.01	4.08	0.17	0.59	2.68	2.40	2.80	26.31	0.96	5.40	0.00
12	CaO	0.99	5.25	24.06	20.00	20.32	9.05	16.48	0.35	1.30	23.4	21.30	7.25	0.69	21.62	3.70	0.00
13	Na <sub>2</sub> O	0.08	0.30	0.09	1.35	1.06	8.42	3.92	14.95	12.24	0.14	0.70	5.55	0.03	0.00	11.60	0.05
14	K <sub>2</sub> O	0.00	0.21	0.00	0.04	0.08	0.14	0.16	0.01	0.19	0.00	0.00	0.00	0.00	0.00	0.00	0.16
15	ZrO <sub>2</sub>	0.00	0.00	0.00	0.00	0.00	0.00	0.19	0.00	0.65	0.00	0.00	0.00	0.00	0.00	0.00	0.00
16	Sc <sub>2</sub> O <sub>3</sub>	0.00	0.00	0.00	0.00	0.00	0.00	0.00	0.00	0.00	0.00	0.00	18.48	0.00	0.00	0.00	0.00
17	Li <sub>2</sub> O	0.00	0.00	0.00	0.00	0.00	0.00	0.00	0.00	0.00	0.00	0.00	0.00	0.00	0.00	0.00	7.12
18	Total (wt%)	99.01	100.72	100.20	98.64	99.84	99.01	99.84	99.86	99.72	99.36	96.10	94.50	101.00	98.52	99.70	99.58
Cations based on 6 oxygen																	
19	Si	1.855	1.965	1.441	1.788	1.883	2.006	1.907	1.998	1.927	1.188	2.049	1.870	1.972	1.991	2.061	2.063
20	Ti	0.001	0.020	0.165	0.041	0.010	0.104	0.013	0.002	0.033	0.030	0.000	0.015	0.000	0.000	0.000	0.000
21	Al	0.160	0.067	0.647	0.271	0.220	0.347	0.120	0.981	0.117	0.851	0.060	0.018	0.010	0.000	0.000	1.002
22	V	0.000	0.000	0.000	0.000	0.001	0.000	0.001	0.000	0.000	0.000	0.000	0.000	0.000	0.000	0.000	0.000
23	Cr	0.015	0.000	0.003	0.000	0.027	0.000	0.000	0.000	0.000	0.000	0.000	0.000	0.000	0.000	0.658	0.000
24	Fe <sup>3+</sup>	0.054	0.039	0.128	0.237	0.048	0.031	0.303	0.010	0.832	0.723	0.121	0.000	0.026	0.008	0.011	0.014
25	Fe <sup>2+</sup>	0.045	1.101	0.229	0.248	0.065	0.356	0.324	0.005	0.050	0.023	0.202	0.643	0.000	0.034	0.000	0.001
26	Mn	0.000	0.020	0.005	0.012	0.004	0.012	0.097	0.001	0.020	0.004	0.000	0.014	0.560	0.944	0.000	0.000
27	Ni	0.002	0.000	0.000	0.000	0.001	0.000	0.000	0.000	0.000	0.000	0.000	0.000	0.000	0.000	0.000	0.000
28	Zn	0.000	0.000	0.000	0.000	0.000	0.000	0.000	0.000	0.000	0.000	0.394	0.000	0.000	0.000	0.000	0.000
29	Mg	1.826	0.529	0.385	0.465	0.870	0.167	0.238	0.008	0.034	0.161	0.151	0.155	1.403	0.059	0.296	0.000
30	Ca	0.036	0.225	0.990	0.835	0.792	0.361	0.690	0.013	0.054	1.009	0.966	0.288	0.026	0.963	0.146	0.000
31	Na	0.005	0.023	0.007	0.102	0.075	0.608	0.297	0.981	0.913	0.011	0.057	0.399	0.002	0.000	0.828	0.003
32	K	0.000	0.011	0.000	0.002	0.004	0.007	0.008	0.000	0.009	0.000	0.000	0.000	0.000	0.000	0.000	0.006
33	Zr	0.000	0.000	0.000	0.000	0.000	0.000	0.004	0.000	0.012	0.000	0.000	0.000	0.000	0.000	0.000	0.000
34	Sc	0.000	0.000	0.000	0.000	0.000	0.000	0.000	0.000	0.000	0.000	0.000	0.597	0.000	0.000	0.000	0.000
35	Li	0.000	0.000	0.000	0.000	0.000	0.000	0.000	0.000	0.000	0.000	0.000	0.000	0.000	0.000	0.000	0.910
36	Total ( <i>apfu</i> )	3.999	4.000	4.000	4.001	4.000	3.999	4.002	3.999	4.001	4.000	4.000	3.999	3.999	3.999	4.000	3.999
37	<i>Q</i> ( <i>apfu</i> )	1.907	1.854	1.604	1.547	1.726	0.885	1.251	0.026	0.138	1.193	1.319	1.086	1.430	1.057	0.442	0.001
38	<i>J</i> ( <i>apfu</i> )	0.011	0.047	0.013	0.204	0.149	1.216	0.594	1.961	1.825	0.022	0.115	0.798	0.004	0.000	1.656	0.006
39	Group	Ca-Mg-Fe	Ca-Mg-Fe	Ca-Mg-Fe	Ca-Mg-Fe	Ca-Mg-Fe	Ca-Na	Ca-Na	Na	Na	Rare Ca	Rare Ca	Rare Na	Rare Mn-Mg	Rare Ca	Rare Na-Cr <sup>3+</sup>	Rare Li-Al
40	Name	En or Cen	Pgt	Di	Hd	Aug	Omp	Agt	Jd	Aeg	Es	Pe	Je	Dpc/Ka	Jhn	Kos	Spd
41	Modifiers	Aluminian, chromian	Calcian, ferroan, magnesian	Aluminian, ferroan, ferrian, subsilicic, titanian	Aluminian, ferrian, magnesian, sodian	Aluminian, chromian	Ferroan, magnesian, titanian	Aluminian, ferroan, magnesian		Aluminian, zirconian		Ferroan, ferrian, magnesian	Calcian, ferroan, magnesian			Calcian, magnesian	

42	Wo	1.91	12.13	61.74	53.96	45.86	40.81	55.13	48.14	38.85	84.57	73.22	26.54	1.85	91.14	33.00	0.00
43	En	95.73	28.51	23.99	30.03	50.37	18.89	18.99	32.54	24.53	13.48	11.48	14.26	98.15	5.64	67.00	0.00
44	Fs	2.36	59.36	14.27	16.01	3.77	40.30	25.88	19.32	36.62	1.95	15.30	59.20	0.00	3.22	0.00	100.00
45	Total (%)	100	100	100	100	100	100	100	100	100	100	100	100	100	100	100	100
46	Q	99.45	97.55	99.17	88.35	92.03	42.12	67.81	1.33	7.02	98.20	91.99	57.63	99.71	100.00	21.08	14.71
47	Jd	0.12	1.11	0.34	2.32	5.45	53.12	2.65	97.63	4.64	0.09	2.65	0.00	0.00	0.00	0.00	84.14
48	Aeg	0.43	1.34	0.49	9.33	2.52	4.76	29.54	1.04	88.34	1.71	5.36	0.00	0.29	0.00	78.92	1.15
49	Total (%)	100	100	100	100	100	100	100	100	100	100	100	57.63	100	100	100	100
50	Wo	1.88	11.65	58.02	48.55	40.90	19.50	41.25	0.64	4.81	80.94	67.24	19.23	1.33	48.14	7.57	0.00
51	Hyp	96.26	85.47	36.22	42.09	48.48	28.92	39.37	0.73	9.33	15.06	24.59	54.14	98.57	51.86	15.37	0.13
52	Jd	1.86	2.88	5.76	9.36	10.62	51.58	19.38	98.63	85.86	4.00	8.17	26.63	0.10	0.00	77.06	99.87
53	Total (%)	100	100	100	100	100	100	100	100	100	100	100	100	100	100	100	100
54	Aug	93.28	92.84	78.75	72.29	85.08	53.91	65.49	1.31	7.30	43.89	78.48	100.00	96.50	98.54	95.23	0.05
55	Jd	1.49	3.24	8.67	5.52	10.2	42.30	2.84	97.65	4.63	2.87	7.12	0.00	0.00	0.00	0.00	98.61
56	Aeg	5.23	3.92	12.58	22.19	4.72	3.79	31.67	1.04	88.07	53.24	14.40	0.00	3.50	1.46	4.77	1.34
57	Total (%)	100	100	100	100	100	100	100	100	100	100	100	100	100	100	100	100
58	Acm+Jd	0.55	2.32	0.56	8.98	6.81	45.91	23.38	57.6	87.92	1.21	4.85	30.95	0.18	0.00	66.72	0.93
59	Ts	27.92	21.11	77.34	55.88	52.2	25.85	40.15	41.88	5.4	90.38	64.25	18.13	22.64	42.34	8.82	49.57
60	Hd	4.67	76.57	19.37	22.4	5.97	27.51	32.26	0.35	6.68	3.00	17.05	50.92	49.49	57.33	0.00	0.13
61	Di	66.86	0.00	2.73	12.74	35.02	0.73	4.21	0.17	0.00	5.41	13.85	0.00	27.69	0.33	24.46	49.37
62	Total (%)	100	100	100	100	100	100	100	100	100	100	100	100	100	100	100	100
63	Jd	0.51	3.46	0.67	10.62	7.87	44.4	25.46	98.32	41.55	1.09	7.68	30.01	0.29	0.00	38.72	1.87
64	Acm	0.00	0.00	0.00	0.00	0.00	19.32	15.46	0.00	36.31	0.00	0.00	28.62	0.00	0.00	38.72	0.00
65	Ca-ferriTs	3.27	1.99	6.56	12.13	3.77	1.12	12.63	0.52	18.75	36.24	8.09	0.00	1.79	0.74	15.65	1.33
66	Ca-Ti-Ts	0.07	2.08	16.5	4.19	1.04	7.51	1.05	0.20	1.49	3.00	0.00	1.15	0.00	0.00	0.00	0.00
67	Ca-Ts	7.26	0.00	15.47	4.34	6.07	0.00	0.00	0.00	0.00	39.09	0.16	0.00	0.53	0.00	0.00	96.70
68	Wo	0.00	9.42	30.17	32.33	34.29	8.73	21.96	0.27	0.00	11.37	60.46	10.25	0.67	90.44	0.00	0.00
69	En	86.63	26.95	19.21	23.74	43.64	6.04	9.92	0.43	0.76	8.05	10.12	5.82	96.74	5.61	6.93	0.00
70	Fs	2.26	56.1	11.42	12.65	3.32	12.88	13.52	0.26	1.14	1.16	13.49	24.15	0.00	3.21	0.00	0.10
71	Total (%)	100	100	100	100	100	100	100	100	100	100	100	100	100	100	100	100
72	CaTs	7.16	1.81	33.62	11.64	6.46	0.00	4.60	0.21	6.63	65.34	0.00	1.14	0.49	0.00	0.00	0.00
73	Jd	0.26	1.22	0.40	5.60	4.13	35.65	14.75	97.09	83.07	0.88	2.62	24.74	0.10	0.00	65.18	0.61
74	KJd	0.00	0.56	0.00	0.11	0.21	0.39	0.40	0.04	0.85	0.00	0.00	0.00	0.00	0.00	0.00	1.28
75	CaEs	0.00	0.00	0.00	0.00	0.00	0.00	0.00	0.00	0.00	0.00	0.06	0.00	0.00	0.00	0.00	97.85
76	Di	0.00	19.94	51.94	68.42	74.63	42.36	59.35	2.08	0.00	31.61	88.11	33.44	1.68	66.32	22.98	0.00
77	En	90.35	17.73	0.00	0.00	10.77	0.00	0.00	0.00	3.08	0.00	0.00	0.00	69.61	0.00	11.84	0.00
78	Fs	2.23	58.74	14.04	14.23	3.80	21.6	20.9	0.59	6.37	2.17	9.21	40.68	28.12	33.68	0.00	0.26
79	Total (%)	100	100	100	100	100	100	100	100	100	100	100	100	100	100	100	100
80	Fe <sub>M1</sub>	0.004	0.451	0.000	0.210	0.034	0.345	0.313	0.002	0.046	0.018	0.197	0.358	0.000	0.000	0.000	0.000
81	Mg <sub>M1</sub>	0.908	0.457	0.313	0.453	0.775	0.166	0.237	0.006	0.033	0.160	0.150	0.141	0.992	0.000	0.270	0.000
82	Fe <sub>M2</sub>	0.041	0.649	0.649	0.038	0.031	0.011	0.011	0.003	0.005	0.005	0.005	0.285	0.285	0.285	0.285	0.990
83	Mg <sub>M2</sub>	0.917	0.072	0.072	0.012	0.095	0.001	0.001	0.002	0.001	0.001	0.001	0.014	0.411	0.411	0.026	0.026
84	Ca <sub>M2</sub>	0.036	0.225	0.011	0.835	0.792	0.361	0.402	0.013	0.054	0.015	0.057	0.288	0.026	0.944	0.146	0.000
85	Na <sub>M2</sub>	0.005	0.034	0.007	0.104	0.078	0.615	0.305	0.981	0.922	0.011	0.057	0.399	0.002	0.000	0.828	1.000
86	X <sup>3+</sup> <sub>M1</sub>	0.085	0.471	0.615	0.535	0.189	0.833	0.737	0.992	0.966	0.835	0.716	0.615	0.026	0.413	0.693	1.000
87	X <sup>Fe2+</sup> <sub>M1</sub>	0.004	0.451	0.000	0.210	0.034	0.347	0.351	0.002	0.047	0.019	0.373	0.696	0.000	0.000	0.000	0.000
88	X <sup>Mg</sup> <sub>M1</sub>	0.911	0.457	0.448	0.453	0.777	0.167	0.265	0.006	0.034	0.165	0.285	0.275	0.974	0.000	0.288	0.000
89	X <sup>Fe2+</sup> <sub>M2</sub>	0.041	0.649	0.649	0.038	0.031	0.011	0.011	0.003	0.005	0.005	0.005	0.285	0.222	0.222	0.222	0.491

90	$X_{M1}^{Mg}$	0.917	0.072	0.072	0.012	0.095	0.001	0.001	0.002	0.001	0.001	0.001	0.014	0.320	0.320	0.020	0.013
91	$X_{M2}^{Ca}$	0.036	0.225	0.011	0.835	0.792	0.361	0.402	0.013	0.054	0.015	0.057	0.288	0.021	0.735	0.114	0.000
92	$X_{M2}^{Na}$	0.005	0.034	0.007	0.104	0.078	0.615	0.305	0.981	0.922	0.011	0.057	0.399	0.002	0.000	0.644	0.496
93	$a_{En}$	0.835	0.033	0.032	0.005	0.074	0.000	0.000	0.000	0.000	0.000	0.000	0.004	0.312	0.000	0.006	0.000
94	$a_{Di}$	0.033	0.104	0.443	0.379	0.617	0.061	0.169	0.000	0.002	0.162	0.269	0.071	0.026	0.000	0.043	0.000
95	$a_{Fs}$	0.000	0.293	0.000	0.008	0.001	0.004	0.004	0.000	0.000	0.000	0.002	0.198	0.000	0.000	0.000	0.000
96	$a_{Ca-Ts}$	0.001	0.007	0.001	0.049	0.082	0.125	0.011	0.012	0.002	0.001	0.003	0.000	0.000	0.000	0.000	0.000
97	$a_{Mg-Ts}$	0.014	0.002	0.006	0.001	0.010	0.000	0.000	0.002	0.000	0.000	0.000	0.000	0.000	0.000	0.000	0.013
98	$a_{Hd}$	0.000	0.102	0.000	0.175	0.027	0.125	0.141	0.000	0.002	0.000	0.021	0.200	0.000	0.000	0.000	0.000
99	$a_{Jd}$	0.000	0.001	0.001	0.006	0.008	0.214	0.008	0.961	0.040	0.000	0.003	0.000	0.000	0.000	0.000	0.497

Notes :  $apfu$  = atomic per formula unit;  $Q$  = Ca+Mg+Fe<sup>2+</sup> (row 37);  $J$  = 2Na (row 38); Abbreviation of pyroxene names: En = Enstatite, Cen = Clinoenstatite, Pgt = Pigeonite, Di = Diopside, Hd = Hedenbergite, Aug = Augite, Omp = Omphacite, Agt = Aegirine-Augite, Jd = Jadeite, Aeg = Aegirine, Es = Esseneite, Pe = Petedunnite, Je = Jervisite, Dpc/Ka = Donpeacorite/Kanoite, Jhn = Johannsenite, Kos = Kosmochlor, Spd = Spodumene ; Abbreviation of end-member components : Wo = Wollastonite (rows 42 and 50), En = Enstatite (rows 43 and 68), Fs = Ferrosilite (rows 44 and 69), Q = Quad (row 46), Jd = Jadeite (rows 47, 52, 55 and 64), Aeg = Aegirine (rows 48 and 56), Hyp = Hyperstene, Aug = Augite, Acm = Acmite, Ts = Tschermakite, Hd = Hederbergite; Di = Diopside, CaTs = Ca tschermakite, KJd = K-jadeite, CaEs = Ca-Eskola, Ca-ferrits = Ca-ferritschermakite, Ca-Ti-Ts = Ca-Ti-tschermakite, Ca-Ts = Ca-tschermakite; Formulations for end-members (rows 42-57) from Soto and Soto (1995); End-members (rows 58-62) from Yoder and Tilley (1962); End-members (rows 63-71) from Cawthorn and Collerson (1974); End-members (rows 72-79) from Harlow (1997); Fe<sup>2+</sup>-Mg partitioning as:  $Fe_{M1} = Fe^{2+}$  in M2 site,  $Mg_{M1} = Mg$  in M1 site,  $Fe_{M2} = Fe^{2+}$  in M2 site,  $Mg_{M2} = Mg$  in M2 site,  $Ca_{M2} = Ca$  in M2 site, and  $Na_{M2} = Na$  in M2 site from Nimis (2000); Molar fractions (rows 86-92) from Soto and Soto (1995; see references therein),  $X_{M1}^{3+} = (Al^{VI} + Ti + Cr + Fe^{3+} + Fe^{2+}_{M1}) / (Fe^{2+}_{M1} + Mg_{M1} + Al^{VI} + Fe^{3+} + Cr + Ti)$ ,  $X_{M1}^{Fe^{2+}} = Fe^{2+}_{M1} / (Fe^{2+}_{M1} + Mg_{M1} + Al^{VI} + Fe^{3+} + Cr + Ti)$ ,  $X_{M1}^{Mg} = Mg_{M1} / (Fe^{2+}_{M1} + Mg_{M1} + Al^{VI} + Fe^{3+} + Cr + Ti)$ ,  $X_{M2}^{Fe^{2+}} = Fe^{2+}_{M2} / (Fe^{2+}_{M2} + Mg_{M2} + Ca + Mn + Na)$ ,  $X_{M2}^{Ca} = Ca_{M2} / (Fe^{2+}_{M2} + Mg_{M2} + Ca + Mn + Na)$ ,  $X_{M2}^{Na} = Na_{M2} / (Fe^{2+}_{M2} + Mg_{M2} + Ca + Mn + Na)$ ; End-member activities (rows 93-99) from Soto and Soto (1995; see references therein),  $a_{En} = X_{M2}^{Mg} * X_{M1}^{Mg}$ ,  $a_{Di} = X_{M2}^{Ca} * X_{M1}^{Mg}$ ,  $a_{Fs} = X_{M2}^{Fe^{2+}} * X_{M1}^{Fe^{2+}}$ ,  $a_{Ca-Ts} = X_{M2}^{Ca} * X_{M1}^{Al^{VI}}$ ,  $a_{Mg-Ts} = X_{M2}^{Mg} * X_{M1}^{Al^{VI}}$ ,  $a_{Hd} = X_{M2}^{Ca} * X_{M1}^{Fe^{2+}}$ ,  $a_{Jd} = X_{M2}^{Na} * X_{M1}^{Al^{VI}}$ .

Table 6. Calculation (total cation fractions without normalization to 4) and classification of clinopyroxenes by WinPyrox program with their calculated components and thermobarometers. Analyses are taken from an Excel spreadsheet (i.e., Two-pyroxene *P-T*) developed by (Putirka 2008)

Row		Cpx1 (-)	Cpx4 (Z-342-02)	Cpx7 (A-12)	Cpx13 (B 304)	Cpx19 (1KH-39)	Cpx23 (INT-D5)	Cpx24 (INT-D2)
1	SiO <sub>2</sub>	52.30	51.06	51.12	51.3	50.93	52.98	53.77
2	TiO <sub>2</sub>	0.70	0.62	0.10	0.19	0.81	0.14	0.11
3	Al <sub>2</sub> O <sub>3</sub>	3.00	3.16	8.07	7.20	9.02	5.04	4.31
4	Cr <sub>2</sub> O <sub>3</sub>	0.58	0.01	1.16	0.50	0.34	1.36	1.51
5	FeO <sub>tot</sub>	5.10	6.18	3.57	3.90	5.82	3.48	3.60
6	MnO	0.11	0.12	0.00	0.09	0.00	0.11	0.11
7	MgO	16.60	15.78	17.95	17.60	18.51	19.61	20.51
8	CaO	21.50	20.82	17.26	19.10	13.34	17.76	16.95
9	Na <sub>2</sub> O	0.33	0.27	0.77	0.50	1.23	0.23	0.23
10	Total (wt%)	100.22	98.02	100.00	100.38	100.00	100.71	101.10
<i>T-site</i>								
11	Si	1.912	1.915	1.836	1.846	1.826	1.890	1.907
12	Al <sup>IV</sup>	0.088	0.085	0.164	0.154	0.174	0.110	0.093
13	Total (apfu)	2.000	2.000	2.000	2.000	2.000	2.000	2.000
<i>M1-site</i>								
14	Al <sup>VI</sup>	0.041	0.054	0.178	0.151	0.207	0.102	0.087
15	Fe <sup>3+</sup>	0.014	0.016	0.001	0.013	0.000	0.000	0.000
16	Ti	0.019	0.017	0.003	0.005	0.022	0.004	0.003
17	Cr	0.017	0.000	0.033	0.014	0.010	0.038	0.042
18	Mg	0.905	0.882	0.786	0.816	0.762	0.856	0.868
19	Fe <sup>2+</sup>	0.003	0.030	0.000	0.000	0.000	0.000	0.000
20	Total (apfu)	1.000	1.000	1.000	1.000	1.000	1.000	1.000
<i>M2-site</i>								
21	Mg	0.000	0.000	0.176	0.128	0.227	0.187	0.217
22	Fe <sup>2+</sup>	0.117	0.148	0.107	0.105	0.175	0.126	0.133
23	Mn	0.003	0.004	0.000	0.003	0.000	0.003	0.003
24	Ca	0.842	0.836	0.664	0.736	0.512	0.679	0.679
25	Na	0.023	0.020	0.054	0.035	0.085	0.016	0.016
26	Total (apfu)	0.986	1.008	1.000	1.006	1.000	1.011	1.013
27	<i>Q</i> (apfu)	1.867	1.897	1.732	1.785	1.676	1.848	1.862
28	<i>J</i> (apfu)	0.047	0.039	0.107	0.070	0.171	0.032	0.032
29	Group	Ca-Mg-Fe	Ca-Mg-Fe	Ca-Mg-Fe	Ca-Mg-Fe	Ca-Mg-Fe	Ca-Mg-Fe	Ca-Mg-Fe
30	Name	Aug	Aug	Aug	Aug	Aug	Aug	Aug
Clinopyroxene components								
31	Jd	0.023	0.020	0.054	0.035	0.085	0.016	0.016
32	CaTs	0.018	0.035	0.125	0.117	0.121	0.086	0.071
33	CaTi	0.035	0.025	0.020	0.019	0.026	0.012	0.011
34	CrCaTs	0.008	0.000	0.016	0.007	0.005	0.019	0.021
35	DiHd	0.781	0.776	0.504	0.594	0.360	0.562	0.541
36	EnFs	0.129	0.150	0.282	0.234	0.402	0.304	0.338
37	Total	0.994	1.006	1.001	1.006	0.999	0.999	0.998
38	En	0.112	0.122	0.254	0.207	0.342	0.270	0.301
39	Di	0.678	0.634	0.453	0.527	0.306	0.500	0.480
40	$a_{En}$	0.245	0.227	0.247	0.242	0.253	0.291	0.312
41	$a_{Di}$	0.610	0.602	0.531	0.567	0.434	0.529	0.506
Single-clinopyroxene barometers (kbar)								
42	$PN_{95-BS-Cpx}$ (Eq. 1)	1.77	1.03	13.91	10.53	17.45	8.41	8.06
43	$PNU_{98-BA-Cpx}$ (Eq. 5)	1.72	0.94	14.87	11.15	18.87	9.06	8.78
44	$PN_{98cor-BH-Cpx}$ (Eq. 7)	26.94	15.69	14.00	14.66	23.55	13.77	10.14
45	$PN_{99-TH-Cpx}$ (Eq. 8)	22.13	11.23	9.98	10.61	17.42	9.89	7.16
46	$PN_{99-MA-Cpx}$ (Eq. 9)	25.15	15.24	12.17	13.19	22.07	13.91	10.05
47	$PNT_{00-Cpx}$ (Eq. 10)	0.35	n.d.	22.87	18.31	18.51	27.00	n.d.
48	$PP_{08-Cpx}$ (Eq. 11)	n.d.	4.39	16.49	9.53	17.31	9.73	11.17

Single-clinopyroxene thermometers ( $^{\circ}\text{C}$ )

49	$TBM_{85/86-Cpx}$	(Eq. 12)	1120	1161	1371	1310	1448	1355	1379
50	$TNT_{00-Cpx}$	(Eq. 13)	1000	998	1255	1185	1280	1269	1295
51	$TP_{08-Cpx}$	(Eq. 14)	1207	1171	1335	1302	1307	1289	1290
52	$TDN_{82-Cpx}$	(Eq. 15)	879	873	850	867	785	806	773
53	$TMZ_{91-Cpx}$	(Eq. 16)	900	899	896	899	887	889	885

Notes :  $apfu$  = atomic per formula unit;  $Fe^{3+}$  estimation by Papike et al. (1974);  $Q = Ca+Mg+Fe^{2+}$  (row 27);  $J = 2Na$  (row 28); Aug = Augite (row 30); Estimation method of clinopyroxene components (rows 31-37) from Putirka (2008);  $En$  (row 38) =  $Fm_2Si_2O_6*(Mg/(Mg+Fe_{tot}+Mn))$ ;  $Di$  (row 39) =  $CaFmSi_2O_6*(Mg/(Mg+Fe_{tot}+Mn))$ ;  $a_{En}$  (row 40) =  $(0.5*Mg/(Ca+0.5*Fe^{2+}+Mn+Na))*(0.5*Mg/(Fe^{3+}+0.5*Fe^{2+}+Al^{VI}+Ti+Cr+0.5*Mg))$ ;  $a_{Di}$  (row 41) =  $Ca/(Ca+0.5*Mg+0.5*Fe^{2+}+Mn+Na)$ ; Single-clinopyroxene barometers of  $PN_{95-B5-Cpx}$  (row 42) from Nimis (1995; see Eq. 1 in text),  $PN_{98-BA-Cpx}$  (row 43) from Nimis and Ulmer (1998; see Eq. 5 in text),  $PN_{98cor-BH-Cpx}$  (row 44) from Nimis and Ulmer (1998; see Eq. 7 in text),  $PN_{99-TH-Cpx}$  (row 45) from Nimis (1999; see Eq. 8 in text),  $PN_{99-MA-Cpx}$  (row 46) from Nimis (1999; see Eq. 9 in text),  $PNT_{00-Cpx}$  (row 47) from Nimis and Taylor (2000; see Eq. 10 in text),  $PP_{08-Cpx}$  (row 48) from Putirka (2008; see Eq. 11 in text); Single-clinopyroxene thermometers of  $TBM_{85/86-Cpx}$  (row 49) from Bertrand and Mercier (1985/1986; see Eq. 12 in text),  $TNT_{00-Cpx}$  (row 50) from Nimis and Taylor (2000; see Eq. 13 in text),  $TP_{08-Cpx}$  (row 51) from Putirka (2008; see Eq. 14 in text),  $TDN_{82-Cpx}$  (row 52) from Dal Negro et al. (1982; see Eq. 15 in text),  $TMZ_{91-Cpx}$  (row 53) from Molin and Zanazzi (1991; see Eq. 16 in text); n.d. = not determined.

Table 7. Calculation (total cation fractions without normalization to 4) and classification of orthopyroxenes by WinPyrox program with their calculated components and thermobarometers. Analyses are taken from an Excel spreadsheet (i.e., Two-pyroxene *P-T*) developed by (Putirka 2008)

Row		Opx1 (-)	Opx4 (Z-342-02)	Opx7 (A-12)	Opx13 (B 304)	Opx19 (1KH-39)	Opx23 (INT-D5)	Opx24 (INT-D2)
1	SiO <sub>2</sub>	55.00	55.15	54.10	52.90	52.95	58.89	56.66
2	TiO <sub>2</sub>	0.34	0.17	0.00	0.09	0.52	0.04	0.05
3	Al <sub>2</sub> O <sub>3</sub>	1.50	1.19	5.70	6.90	7.43	3.19	3.47
4	Cr <sub>2</sub> O <sub>3</sub>	0.19	0.15	0.50	0.50	0.16	0.84	0.94
5	FeO <sub>tot</sub>	11.30	10.21	6.30	6.72	8.01	5.48	5.40
6	MnO	0.24	0.22	0.00	0.12	0.00	0.10	0.12
7	MgO	30.70	29.90	31.50	30.60	28.72	33.72	32.82
8	CaO	0.90	1.66	1.65	1.63	1.93	1.05	1.56
9	Na <sub>2</sub> O	0.01	0.03	0.25	0.07	0.27	0.00	0.04
10	Total (wt%)	101.18	98.77	100.00	99.53	99.99	101.31	101.06
<i>T</i> -site								
11	Si	1.944	1.969	1.875	1.847	1.849	1.934	1.933
12	Al <sup>IV</sup>	0.056	0.031	0.125	0.153	0.151	0.066	0.067
13	Total (apfu)	2.000	2.000	2.000	2.000	2.000	2.000	2.000
<i>M1</i> -site								
14	Al <sup>VI</sup>	0.006	0.019	0.108	0.131	0.154	0.061	0.072
15	Fe <sup>3+</sup>	0.027	0.001	0.020	0.009	0.000	0.000	0.000
16	Ti	0.009	0.005	0.000	0.002	0.014	0.001	0.001
17	Cr	0.005	0.004	0.014	0.014	0.004	0.023	0.025
18	Mg	0.952	0.971	0.858	0.844	0.827	0.915	0.901
19	Fe <sup>2+</sup>	0.000	0.000	0.000	0.000	0.000	0.000	0.000
20	Total (apfu)	1.000	1.000	1.000	1.000	1.000	1.000	1.000
<i>M2</i> -site								
21	Mg	0.665	0.625	0.769	0.748	0.667	0.793	0.768
22	Fe <sup>2+</sup>	0.306	0.304	0.163	0.187	0.250	0.175	0.184
23	Mn	0.007	0.007	0.000	0.004	0.000	0.003	0.003
24	Ca	0.034	0.063	0.061	0.061	0.072	0.038	0.057
25	Na	0.001	0.002	0.017	0.005	0.018	0.000	0.003
26	Total (apfu)	1.014	1.001	1.010	1.005	1.008	1.010	1.015
27	<i>Q</i> (apfu)	1.958	1.963	1.852	1.841	1.818	1.922	1.910
28	<i>J</i> (apfu)	0.004	0.004	0.034	0.009	0.037	0.000	0.005
29	Group	Ca-Mg-Fe	Ca-Mg-Fe	Ca-Mg-Fe	Ca-Mg-Fe	Ca-Mg-Fe	Ca-Mg-Fe	Ca-Mg-Fe
30	Name	En	En	En	En	En	En	En
Orthopyroxene components								
31	NaAlSi <sub>2</sub> O <sub>6</sub>	0.001	0.002	0.017	0.005	0.018	0.000	0.003
32	FmTiAlSiO <sub>6</sub>	0.009	0.005	0.000	0.002	0.014	0.001	0.001
33	CrAl <sub>2</sub> SiO <sub>6</sub>	0.005	0.004	0.014	0.014	0.004	0.023	0.025
34	FmAl <sub>2</sub> SiO <sub>6</sub>	0.000	0.013	0.078	0.112	0.132	0.039	0.044
35	CaFmSi <sub>2</sub> O <sub>6</sub>	0.034	0.064	0.061	0.061	0.072	0.038	0.057
36	Fm <sub>2</sub> Si <sub>2</sub> O <sub>6</sub>	0.958	0.913	0.836	0.808	0.764	0.904	0.877
37	Total	1.003	1.000	1.000	1.000	1.000	1.000	1.000
38	En	0.791	0.764	0.751	0.718	0.654	0.819	0.788
39	Di	0.028	0.053	0.055	0.054	0.062	0.035	0.051
40	$\alpha_{En}$	0.645	0.637	0.656	0.632	0.555	0.723	0.686
41	$\alpha_{Di}$	0.034	0.062	0.063	0.064	0.075	0.039	0.058
Two-pyroxene barometers (kbar)								
42	<i>PM</i> (1) <sub>84-Opx-Cpx</sub> (Eq. 35)	27.49	6.21	36.55	25.46	50.93	n.d.	51.71
43	<i>PM</i> (2) <sub>84-Opx-Cpx</sub> (Eq. 36)	22.40	6.76	28.75	20.95	38.46	54.43	38.98
44	<i>PP</i> (1) <sub>08-Opx-Cpx</sub> (Eq. 37)	2.19	2.38	14.91	10.90	15.34	10.88	10.50
45	<i>PP</i> (2) <sub>08-Opx-Cpx</sub> (Eq. 38)	2.57	3.24	16.18	11.12	17.18	7.83	11.34
Two-pyroxene and single-orthopyroxene thermometers (°C) by WinPyrox								
46	<i>TWB</i> <sub>73-Opx-Cpx</sub> (Eq. 18)	1252	1237	1361	1341	1320	1376	1396
47	<i>TW</i> <sub>77-Opx-Cpx</sub> (Eq. 19)	1285	1263	1338	1333	1361	1361	1400
48	<i>TNB</i> (A1) <sub>84-Opx-Cpx</sub> (Eq. 20)	1133	1232	1109	1189	1201	1229	1299

49	TNB(A2) <sub>84-Opx-Cpx</sub>	(Eq. 20)	937	907	1007	1037	1091	1069	1136
50	TNB(B1) <sub>84-Opx-Cpx</sub>	(Eq. 21)	1264	1399	1423	1301	1421	1296	1385
51	TNB(B2) <sub>84-Opx-Cpx</sub>	(Eq. 21)	968	1123	1262	1141	1230	1154	1227
52	TN <sub>85-Opx-Cpx</sub>	(Eq. 22)	1085	1106	1346	1282	1462	1317	1359
53	TBM <sub>85/86-Opx-Cpx</sub>	(Eq. 23)	962	986	1285	1217	1375	1280	1320
54	TCL(A) <sub>88-Opx-Cpx</sub>	(Eq. 24)	1131	1031	938	1049	862	993	1060
55	TCL(B) <sub>88-Opx-Cpx</sub>	(Eq. 25)	757	938	1321	1221	1448	1064	1165
56	TSJ(1) <sub>89-Opx-Cpx</sub>	(Eq. 26)	1493	1452	1486	1499	1616	1530	1615
57	TSJ(2) <sub>89-Opx-Cpx</sub>	(Eq. 27)	1042	1213	1258	1239	1394	1113	1244
58	TBK <sub>90-Ca-in-Opx-Cpx</sub>	(Eq. 28)	971	999	1265	1189	1286	1255	1275
59	TBK <sub>90-Na-in-Opx-Cpx</sub>	(Eq. 29)	812	1140	1426	1229	1346	1526	1275
60	TBK <sub>90-Ca-in-Opx</sub>	(Eq. 30)	1230	1408	1472	1453	1525	1310	1421
61	TT <sub>98-Opx-Cpx</sub>	(Eq. 31)	960	976	1291	1229	1346	1233	1261
62	TP(1) <sub>08-Opx-Cpx</sub>	(Eq. 32)	965	1000	1325	1172	1321	1225	1273
63	TP(2) <sub>08-Opx-Cpx</sub>	(Eq. 33)	957	975	1295	1170	1334	1228	1247
64	TNT <sub>10-Ca-in-Opx</sub>	(Eq. 34)	953	987	1264	1191	1283	1254	1272
Input <i>T-P</i> values for thermobarometric estimations (from Putirka 2008)									
65	<i>T</i> (°C)		0	950	1325	1215	1300	1270	1300
66	<i>P</i> (kbar)		0.00	1.94	15.00	12.00	15.00	10.00	10.00
Two-pyroxene and single-orthopyroxene thermometers (°C) with an Excel spreadsheet by Putirka (2008)									
67	TWB <sub>73-Opx-Cpx</sub>		1247	1237	1361	1341	1329	1394	1425
68	TW <sub>77-Opx-Cpx</sub>		1277	1263	1338	1333	1363	1371	1414
69	TNB(A1) <sub>84-Opx-Cpx</sub>		1177	1232	1109	1189	1213	1206	1277
70	TNB(A2) <sub>84-Opx-Cpx</sub>		936	907	1007	1037	1092	1077	1146
71	TNB(B1) <sub>84-Opx-Cpx</sub>		1261	1397	1419	1298	1389	1279	1357
72	TNB(B2) <sub>84-Opx-Cpx</sub>		972	1123	1262	1141	1233	1153	1226
73	TN <sub>85-Opx-Cpx</sub>		1085	1106	1346	1282	1462	1317	1359
74	TCL(A) <sub>88-Opx-Cpx</sub>		1086	1031	938	1049	846	1014	1078
75	TCL(B) <sub>88-Opx-Cpx</sub>		760	938	1321	1221	1452	1068	1172
76	TSJ(1) <sub>89-Opx-Cpx</sub>		1477	1452	1486	1499	1604	1533	1613
77	TSJ(2) <sub>89-Opx-Cpx</sub>		1044	1213	1258	1239	1397	1114	1246
78	TBK <sub>90-Ca-in-Opx-Cpx</sub>		967	1003	1254	1183	1295	1266	1291
79	TBK <sub>90-Na-in-Opx-Cpx</sub>		812	1140	1426	1229	1346	n.d.	1275
80	TBK <sub>90-Ca-in-Opx</sub>		957	1135	1198	1180	1252	1037	1148
81	TP(1) <sub>08-Opx-Cpx</sub>		980	1000	1325	1172	1321	1217	1265
82	TP(2) <sub>08-Opx-Cpx</sub>		964	975	1295	1170	1337	1240	1265
83	PM(1) <sub>84-Opx-Cpx</sub>		34.71	9.54	44.93	30.99	60.12	79.36	54.06
84	PM(2) <sub>84-Opx-Cpx</sub>		27.47	9.28	34.46	24.88	44.44	56.46	40.52
85	PP(1) <sub>08-Opx-Cpx</sub>		2.2	2.4	14.9	10.9	14.8	10.8	10.3
86	PP(2) <sub>08-Opx-Cpx</sub>		3.1	3.2	16.2	11.1	16.5	7.1	10.3

Notes : *apfu* = atomic per formula unit; Fe<sup>3+</sup> estimation by Papike et al. (1974); *Q* = Ca+Mg+Fe<sup>2+</sup> (row 27); *J* = 2Na (row 28); En = Enstatite (row 30); Estimation method of orthopyroxene components (rows 31-37) from Putirka (2008); En (row 38) =  $Fm_2Si_2O_6^*(Mg/(Mg+Fet_{ot}+Mn))$ ; Di (row 39) =  $CaFmSi_2O_6^*(Mg/(Mg+Fe_{tot}+Mn))$ ;  $a_{En}$  (row 40) =  $(0.5*Mg/(Ca+0.5*Fe^{2+}+Mn+Na))*(0.5*Mg/(Fe^{3+}+0.5*Fe^{2+}+Al^VI+Ti+Cr+0.5*Mg))$ ;  $a_{Di}$  (row 41) =  $Ca/(Ca+0.5*Mg+0.5*Fe^{2+}+Mn+Na)$ ; Two-clinopyroxene barometers of PM(1)<sub>84-Opx-Cpx</sub> (row 42) from Mercier et al. (1984; see Eq. 35 in text), PM(2)<sub>84-Opx-Cpx</sub> (row 43) from Mercier et al. (1984; see Eq. 36 in text), PP(1)<sub>08-Opx-Cpx</sub> (row 44) from Putirka (2008; see Eq. 37 in text), PP(2)<sub>08-Opx-Cpx</sub> (row 45) from Putirka (2008; see Eq. 38 in text); Two-pyroxene thermometers of TWB<sub>73-Opx-Cpx</sub> (row 46) from Wood and Banno (1973; see Eq. 18 in text), TW<sub>77-Opx-Cpx</sub> (row 47) from Wells (1977; see Eq. 19 in text), TNB(A1)<sub>84-Opx-Cpx</sub> (row 48) from Nickel and Brey (1984; using FmO as in Putirka 2008 ; see Eq. 20 in text), TNB(A2)<sub>84-Opx-Cpx</sub> (row 49) from Nickel and Brey (1984; using Mg as in Putirka 2008 ; see Eq. 20 in text), TNB(B1)<sub>84-Opx-Cpx</sub> (row 50) from Nickel and Brey (1984; using FmO as in Putirka 2008 ; see Eq. 21 in text), TNB(B2)<sub>84-Opx-Cpx</sub> (row 51) from Nickel and Brey (1984; using Mg as in Putirka 2008 ; see Eq. 21 in text), TN<sub>85-Opx-Cpx</sub> (row 52), from Nickel et al. (1985; see Eq. 22 in text), TBM<sub>85/86-Opx-Cpx</sub> (row 53) from Bertrand and Mercier (1985/1986; see Eq. 23 in text), TCL(A)<sub>88-Opx-Cpx</sub> (row 54) from Carlson and Lindsley (1988; see Eq. 24 in text), TCL(B)<sub>88-Opx-Cpx</sub> (row 55) from Carlson and Lindsley (1988; see Eq. 25 in text), TSJ(1)<sub>89-Opx-Cpx</sub> (row 56) from Sen and Jones (1989; see Eq. 26 in text), TSJ(2)<sub>89-Opx-Cpx</sub> (row 57) from Sen and Jones (1989; see Eq. 27 in text), TBK<sub>90-Ca-in-Opx-Cpx</sub> (row 58) from Brey and Köhler (1990; see Eq. 28 in text), TBK<sub>90-Na-in-Opx-Cpx</sub> (row 59) from Brey and Köhler (1990; see Eq. 29 in text), TBK<sub>90-Ca-in-Opx</sub> (row 60) from Brey and Köhler (1990; see Eq. 30 in text), TT<sub>98-Opx-Cpx</sub> (row 61) from Taylor (1998; see Eq. 31 in text), TP(1)<sub>08-Opx-Cpx</sub> (row 62) from Putirka (1998; see Eq. 32 in text), TP(2)<sub>08-Opx-Cpx</sub> (row 63) from Putirka (1998; see Eq. 33 in text), TNT<sub>10-Ca-in-Opx</sub> (row 64) from Nimis and Grütter (2010; see Eq. 34 in text); Calculation inputs of *T* (°C) and *P* (kbar) (rows 65-66) for pyroxene thermobarometry are taken from Putirka (2008); *P-T* values in rows 67-86 are taken from Putirka (2008) for comparison of outputs by WinPyrox (see rows 42-64); n.d. = not determined.

Table 8. Comparison of single-clinopyroxene barometers based on ferric iron estimation methods and normalizations

Row		Cpx1	Cpx4	Cpx7	Cpx13	Cpx19	Cpx23	Cpx24
Input <i>T</i> values for barometric estimations (from Putirka 2008)								
1	<i>T</i> (°C)	0	950	1325	1215	1300	1270	1300
Single-clinopyroxene barometers (kbar) by CpxBar (Nimis 2000) <sup>(a)</sup>								
2	<i>PNU</i> <sub>98-BA-Cpx</sub>	1.20	0.89	14.87	11.08	19.15	9.69	9.52
3	<i>PNU</i> <sub>98cor-BH-Cpx</sub>	50.21	10.64	14.79	13.82	24.52	9.48	8.08
4	<i>PN</i> <sub>99-TH-Cpx</sub>	36.39	8.09	10.32	9.62	17.55	9.69	6.17
5	<i>PN</i> <sub>99-MA-Cpx</sub>	45.85	10.65	12.23	11.37	21.56	8.43	7.65
Single-clinopyroxene barometers (kbar) by WinPyrox <sup>(b)</sup>								
6	<i>PNU</i> <sub>98-BA-Cpx</sub>	1.20	0.92	14.86	11.07	18.86	8.36	7.95
7	<i>PNU</i> <sub>98cor-BH-Cpx</sub>	26.54	15.61	13.95	14.27	22.99	12.60	8.78
8	<i>PN</i> <sub>99-TH-Cpx</sub>	21.84	11.17	9.95	10.36	17.07	9.08	6.25
9	<i>PN</i> <sub>99-MA-Cpx</sub>	24.89	15.13	12.12	12.88	21.67	13.04	9.07
Single-clinopyroxene barometers (kbar) by WinPyrox <sup>(c)</sup>								
10	<i>PNU</i> <sub>98-BA-Cpx</sub>	2.02	0.78	14.86	10.99	18.87	8.80	8.47
11	<i>PNU</i> <sub>98cor-BH-Cpx</sub>	27.15	15.51	13.90	14.31	23.29	13.31	9.60
12	<i>PN</i> <sub>99-TH-Cpx</sub>	22.28	11.10	9.92	10.39	17.27	9.58	6.80
13	<i>PN</i> <sub>99-MA-Cpx</sub>	25.30	15.11	12.10	12.94	21.89	13.59	9.67
Single-clinopyroxene barometers (kbar) by WinPyrox <sup>(d)</sup>								
14	<i>PNU</i> <sub>98-BA-Cpx</sub>	1.35	1.08	14.87	11.23	18.87	8.87	8.56
15	<i>PNU</i> <sub>98cor-BH-Cpx</sub>	26.64	15.82	14.06	14.75	23.47	13.52	9.86
16	<i>PN</i> <sub>99-TH-Cpx</sub>	21.91	11.31	10.02	10.66	17.36	9.70	6.96
17	<i>PN</i> <sub>99-MA-Cpx</sub>	24.96	15.28	12.20	13.21	22.00	13.69	9.83
Single-clinopyroxene barometers (kbar) by WinPyrox <sup>(e)</sup>								
18	<i>PNU</i> <sub>98-BA-Cpx</sub>	1.72	0.94	14.87	11.15	18.87	9.06	8.78
19	<i>PNU</i> <sub>98cor-BH-Cpx</sub>	26.94	15.69	14.00	14.66	23.55	13.77	10.14
20	<i>PN</i> <sub>99-TH-Cpx</sub>	22.13	11.23	9.98	10.61	17.42	9.89	7.16
21	<i>PN</i> <sub>99-MA-Cpx</sub>	25.15	15.24	12.17	13.19	22.07	13.91	10.05

Notes : (a) = Fe<sup>3+</sup> estimation by Papike et al. (1974) and cation fractions with normalization to 4 using CpxBar (Nimis 2000); (b) = Fe<sup>3+</sup> estimation by Droop (1987) and cation fractions with normalization to 4 using WinPyrox; (c) = Fe<sup>3+</sup> estimation by Papike et al. (1974) and cation fractions with normalization to 4 using WinPyrox; (d) = Fe<sup>3+</sup> estimation by Droop (1987) and cation fractions without normalization to 4 using WinPyrox; (e) = Fe<sup>3+</sup> estimation by Papike et al. (1974) and cation fractions without normalization to 4 using WinPyrox.